arXiv:cond-mat/0406731v2 [cond-mat.stat-mech] 27 Jul 2004

Charge renormalization and other exact coupling corrections in the dipolar effective interaction in an electrolyte near a dielectric wall

J.-N. Aqua

Laboratoire de Physique

École Normale Supérieure de Lyon

46 allée d'Italie, 69364 Lyon, FRANCE*

F. Cornu

Laboratoire de Physique Théorique

Université Paris-Sud, Bâtiment 210

91405 Orsay, FRANCE†

(Dated: February 2, 2008)

The aim of the paper is to study the renormalizations of the charge and of the screening length that appear in the large-distance behavior of the effective pairwise interaction $w_{\alpha\alpha'}$ between two charges e_α and $e_{\alpha'}$ in a dilute electrolyte solution, both along a dielectric wall and in the bulk. The electrolyte is described by the primitive model in the framework of classical statistical mechanics and the electrostatic response of the wall is characterized by its dielectric constant. In Ref.[1] a graphic reorganization of resummed Mayer diagrammatics has been devised in order to exhibit the general structure of the $1/y^3$ leading tail of $w_{\alpha\alpha'}(x, x', y)$ for two charges located at distances x and x' from the wall and separated by a distance y along the wall. When all species have the same closest approach distance b to the wall, the coefficient of the $1/y^3$ tail is the product $D_\alpha(x)D_{\alpha'}(x')$ of two effective dipoles. Here we use the same graphic reorganization in order to systematically investigate the exponential large-distance behavior of $w_{\alpha\alpha'}$ in the bulk. (We show that the reorganization also enables one to derive the basic screening rules in both cases.) Then, in a regime of high dilution and weak coupling, the exact analytical corrections to the leading tail of $w_{\alpha\alpha'}$, both in the bulk or along the wall, are calculated at first order in the coupling parameter ε and in the limit where b becomes negligible with respect to the Debye screening length. (ε is proportional to the so-called plasma parameter.) The structure of corrections to the terms of order ε is exhibited, and the scaling regime for the validity of the Debye limit is specified. In the vicinity of the wall, we use the density profiles calculated in Ref.[2] up to order ε and the method devised in Ref.[3] for the determination of the corresponding correction in the auxiliary screened potential, which also appears in the linear-response theory. The first coupling correction to the effective dipole $D_\alpha(x)$ is a function (not a mere exponential decay) determined by the nonuniformity of the density profiles as well as by three- and four-body screened interactions in $w_{\alpha\alpha'}$. Though the effective screening length (beyond the Debye value) in the direction perpendicular to the wall is the same as in the bulk, the bare solvated charges are not renormalized by the same quantity as in the bulk, because of combined steric and electrostatic effects induced by the wall.

PACS numbers: 05.20.Jj, 05.70.Np.

Corresponding author : cornu@th.u-psud.fr.

I. INTRODUCTION

A. Issue at stake

The paper is devoted to the large-distance behavior of the pairwise effective interaction between two charges in an electrolyte solution, which is confined to the region $x > 0$ by a plane impenetrable dielectric wall. The electrolyte solution is described by the usual *primitive model* [4] with n_s species of charges which interact via the Coulomb interaction. Every charged particle of species α is represented as a hard sphere – with diameter σ_α – where the net bare solvated charge $e_\alpha \equiv Z_\alpha e$ is concentrated at the center of the sphere. (e is the abolute value of the electron charge and Z_α may be positive or negative.) The solvent is handled with as a continuous medium of uniform dielectric constant $\epsilon_{\rm solv}$. The wall matter is characterized by a dielectric constant $\epsilon_W \neq \epsilon_{\rm solv}$, and the latter difference results into an electrostatic response of the wall to the moving charges in the electrolyte. Moreover, the excluded-volume sphere of every particle is assumed to be made of a material with the same dielectric constant as that of the solvent. (Therefore $\epsilon = \epsilon_{\rm solv}$ when $x > 0$ and $\epsilon = \epsilon_{\rm W}$ when $x < 0$). In the framework of statistical mechanics, the effective pairwise interaction $w_{\alpha\alpha'}(\mathbf{r}, \mathbf{r}')$ between two charges e_α and $e_{\alpha'}$ located at positions $\mathbf{r}$ and $\mathbf{r}'$, respectively, is defined from the pair correlation function $h_{\alpha\alpha'}$ by (see e.g. Ref.[5])

$$1 + h_{\alpha\alpha'} \equiv \exp(-\beta w_{\alpha\alpha'}), \tag{1}$$

---

[*] Laboratoire associé au Centre National de la Recherche Scientifique UMR 5672; Present address : Institute for Physical Science and Technology, University of Maryland, College Park, Maryland 20910, USA

[†] Laboratoire associé au Centre National de la Recherche Scientifique - UMR 8627

where $\beta = 1/k_B T$ is the inverse temperature, in which k_B is Boltzmann constant and T is the absolute temperature. ($w_{\alpha\alpha'}$ is also called potential of mean force, while $h_{\alpha\alpha'}$ is known as the Ursell function.) In the vicinity of the wall, symmetries enforce that $w_{\alpha\alpha'}(\mathbf{r},\mathbf{r}') = w_{\alpha\alpha'}(x,x',y)$, where x and x' are the distances of $\mathbf{r}$ and $\mathbf{r}'$ from the wall and y is the norm of the projection $\mathbf{y}$ of $\mathbf{r}-\mathbf{r}'$ onto the wall plane. Along the wall, contrary to the bulk case, $w_{\alpha\alpha'}(x,x',y)$ does not decay exponentially fast: its leading behavior at large distances y takes a dipolar form $f_{\alpha\alpha'}(x,x')/y^3$, as a result of the deformation of screening clouds enforced by the presence of the wall (see Ref[6] for a review or e.g. Ref.[1]).

An electrolyte solution can be considered as a dilute charge fluid where the closest approach distance between the center of a charge with species α and the dielectric wall takes the same value b for all species. The reason is that the differences in the various ion diameters are negligible with respect to all other characteristic lengths. ($b_\alpha = b$ for all α's, whether b_α is only determined by the radius of the excluded-volume sphere of species α or b_α involves some other more complicated microscopic mechanism for the short-distance repulsion from the wall. For instance, a layer of water molecules, with a thickness of molecular dimensions, may lie between the wall and the electrolyte solution, as it has been suggested for instance for another situation, the mercury-aqueous solution interface [7].) As a consequence, as shown in Ref.[1], called Paper I in the following, the coefficient $f_{\alpha\alpha'}(x,x')$ of the $1/y^3$ tail of $w_{\alpha\alpha'}(x,x',y)$ is a product of effective dipoles $D_\alpha(x)$ and $D_{\alpha'}(x')$,

$$w_{\alpha\alpha'}(x,x',y) \underset{y\to+\infty}{\sim} \frac{D_\alpha(x)D_{\alpha'}(x')}{y^3}. \tag{2}$$

(Therefore the tail of $w_{\alpha\alpha}(x,x',y)$ between two particles of the same species α is repulsive when $x = x'$, as it is the case for identical point dipoles with the same direction.)

The general result (2) arises from a property about the screened potential ϕ defined as follows. $(\delta q\delta q'/\epsilon_{\text{solv}})\phi$ is the immersion free energy between two *infinitesimal external point* charges δq and $\delta q'$ calculated in the framework of the linear-response theory as if the radii of the excluded-volume spheres of the fluid charges were equal to zero [8]. (The effect of hard cores is briefly discussed after (65).) As shown in Paper I, when all particles have the same closest approach distance b to the wall,

$$\phi(x,x',y) \underset{y\to+\infty}{\sim} \frac{\overline{D}_\phi(x)\overline{D}_\phi(x')}{y^3}. \tag{3}$$

(In (3) $\overline{D}_\phi(x)$ vanishes for $x < b$.) In the following, a quantity that is independent of charge species α is denoted by an overlined letter when it is analogous to another one that depends on α, as it is the case for $D_\alpha(x)$ and $\overline{D}_\phi(x)$. Since ϕ obeys an "inhomogeneous" Debye equation where the effective screening length depends on the distance x

from the wall through the density profiles, $\overline{D}_\phi(x)$ has the same sign at any distance x from the wall, contrarily to the effective dipole $D_\alpha(x)$, the sign of which may *a priori* vary with the distance x. Thus, the $1/y^3$ tail of $\phi(x,x',y)$ is repulsive at all distances x and x' from the wall. Moreover, the x-dependent screening length tends to the Debye length ξ_D at large distances, and $\overline{D}_\phi(x)$ can be rewritten, for $x>b$, as

$$\overline{D}_\phi(x) = -\sqrt{\frac{2\epsilon_W}{\epsilon_{\mathrm{solv}}}}\frac{e^{-\kappa_{\mathrm{D}}(x-b)}}{\kappa_{\mathrm{D}}}\left[1+C_\phi+\overline{G}_\phi^{\mathrm{exp}}(x)\right], \tag{4}$$

where $\overline{G}_\phi^{\mathrm{exp}}(x)$ tends to zero exponentially fast over a scale of order $1/\kappa_{\mathrm{D}}$. In Gauss units, the Debye length ξ_D reads

$$\xi_D^{-1} \equiv \kappa_{\mathrm{D}} = \sqrt{\frac{4\pi\beta e^2}{\epsilon_{\mathrm{solv}}}\sum_\alpha Z_\alpha^2 \rho_\alpha^{\mathrm{B}}}, \tag{5}$$

where ρ_α^{B} is the bulk density of species α. C_ϕ is a constant which vanishes, as well as $\overline{G}_\phi^{\mathrm{exp}}(x)$, in the infinite-dilution and vanishing-coupling limit considered hereafter. The global minus sign in (4) has been introduced, because, in the latter limit and in the case of a plain wall ($\epsilon_W = \epsilon_{\mathrm{solv}}$), $\overline{D}_\phi(x)$ is expected to have the same sign as the dipole $d(x)$ carried by the set made of a positive unit charge and its screening cloud repelled from the wall. The sign of $1+C_\phi$ depends on the temperature, on the composition of the electrolyte, on the value of the closest approach distance b to the wall, and on the dielectric constants ϵ_W and ϵ_{solv}.

In an electrolyte solution, the Z_α's of all species α's are of unit order and the diameters σ_α's of excluded-volume spheres also have the same typical value, denoted by σ. Moreover, all densities ρ_α^{B}'s are of the same magnitude order. Thus, if the solution is highly diluted, the Coulomb coupling between charges of any species separated by the mean interparticle distance a is weak: the condition of low densities, $\sigma/a \ll 1$, implies that $(\beta e^2/(\epsilon_{\mathrm{solv}}a)) \ll 1$, if the temperature is high enough for $\beta e^2/(\epsilon_{\mathrm{solv}}\sigma)$ to be far smaller than 1 or of unit order. Detailed scaling regimes are given in Section I B. In the corresponding limit, denoted by the superscript (0) hereafter, where the fluid is infinitely diluted and extremely weakly-coupled, the large-distance behavior $w_{\alpha\alpha'}^{\mathrm{as}}(\mathbf{r},\mathbf{r}')$ of the effective pairwise interaction $w_{\alpha\alpha'}(\mathbf{r},\mathbf{r}')$ is the same as if the charges e_α and $e_{\alpha'}$ were infinitesimal external point charges embedded in the infinitely-diluted and vanishingly-coupled fluid,

$$w_{\alpha\alpha'}^{\mathrm{as}\,(0)} = \frac{e^2}{\epsilon_{\mathrm{solv}}} Z_\alpha Z_{\alpha'} \phi^{\mathrm{as}\,(0)}. \tag{6}$$

Moreover, in this limit, the density profiles are uniform at leading order and $\overline{D}_\phi^{(0)}(x)$ is given by (4) where the constant C_ϕ and the function $\overline{G}_\phi^{\mathrm{exp}}(x)$ vanish: $C_\phi^{(0)}=0$ and $\overline{G}_\phi^{\mathrm{exp}\,(0)}(x)=0$ [9, 10]. Then, by virtue of (2) and (6),

$$D_\alpha^{(0)}(x) = \frac{e}{\sqrt{\epsilon_{\mathrm{solv}}}} Z_\alpha \overline{D}_\phi^{(0)}(x) \quad \text{with} \quad \overline{D}_\phi^{(0)}(x) = -\sqrt{\frac{2\epsilon_W}{\epsilon_{\mathrm{solv}}}}\frac{e^{-\kappa_{\mathrm{D}}(x-b)}}{\kappa_{\mathrm{D}}}. \tag{7}$$

As long as the dilution is high enough, the large-distance behavior $w^{\text{as}}_{\alpha\alpha'}(\mathbf{r},\mathbf{r}')$ of the effective pairwise interaction $w_{\alpha\alpha'}(\mathbf{r},\mathbf{r}')$ is expected to have the same functional form as its expression $w^{\text{as}\,(0)}_{\alpha\alpha'}(\mathbf{r},\mathbf{r}')$ in the infinite-dilution and vanishing-coupling limit. This assuption is supported by two reasons. First, since densities are low, the functional form of the large-distance behavior $w^{\text{as}}_{\alpha\alpha'}(\mathbf{r},\mathbf{r}')$ is ruled by the effect of long-range Coulomb interactions, whereas short-ranged hard-core repulsions are only involved in the values of the coefficients of this leading tail. Second, the leading Coulomb effects are due to the large-distance nonintegrability of Coulomb interaction, and the leading-order contribution from any integral involving the Boltzman factor of either the effective interaction $w_{\alpha\alpha'}$ or the bare Coulomb interaction $e_\alpha e_{\alpha'} v$ is obtained by linearizing the latter exponential factors. This is the procedure that underlies the Debye-Hückel approximation for bulk correlations, which was initially derived as a linearized Poisson-Boltzmann theory, where $w_{\alpha\alpha'}$ is dealt with in a linear-response framework as if charges e_α and $e_{\alpha'}$ were infinitesimal external charges [4, 11]. (In the Mayer diagrammatic approach of Debye-Hückel theory, the linearized Boltzmann factor is that of the bare potential and one must also resum the infinite series of the most divergent integrals that arise from this linearization (see e.g. Ref.[5]).) The second reason amounts to state that leading Coulomb effects are properly described in a linearized mean-field scheme.

In other words, as long as the dilution and the temperature are high enough, in $w^{\text{as}}_{\alpha\alpha'}$ the many-body effects beyond the linearized mean-field structure only result into the renormalization of charges and of the screening length with respect to their values in the infinite-dilution and vanishing-coupling limit, namely with respect to the bare solvated charges Z_α's and the Debye screening length ξ_D. For instance, in the bulk, $w^{\text{B}\,\text{as}}_{\alpha\alpha'}(\mathbf{r},\mathbf{r}')$ behaves as the leading-order function $w^{\text{B}\,\text{as}\,(0)}_{\alpha\alpha'}(\mathbf{r},\mathbf{r}')$ given by the Debye-Hückel theory for point charges, but bare charges Z_α's and the Debye length κ_{D}^{-1} are replaced by effective charges $Z_\alpha^{\text{B}\,\text{eff}}$'s and the screening length κ_{B}^{-1}, respectively:

$$w^{\text{B}}_{\alpha\alpha'}(|\mathbf{r}-\mathbf{r}'|) \underset{|\mathbf{r}-\mathbf{r}'|\to+\infty}{\sim} \frac{e^2}{\epsilon_{\text{solv}}} Z_\alpha^{\text{eff B}} Z_{\alpha'}^{\text{eff B}} \frac{e^{-\kappa_{\text{B}}|\mathbf{r}-\mathbf{r}'|}}{|\mathbf{r}-\mathbf{r}'|}, \tag{8}$$

where

$$Z_\alpha^{\text{eff B}\,(0)} = Z_\alpha \quad \text{and} \quad \kappa_{\text{B}}^{(0)} = \kappa_{\text{D}}. \tag{9}$$

(In the following, the superscript B signals all bulk quantities.) In the present paper we show that the effective dipole $D_\alpha(x)$ in the large-distance pairwise interaction along a dielectric wall takes the form

$$D_\alpha(x) = -\sqrt{\frac{2\epsilon_W}{\epsilon_{\text{solv}}}} \frac{e}{\sqrt{\epsilon_{\text{solv}}}} Z_\alpha^{\text{eff W}} \frac{e^{-\kappa(x-b)}}{\kappa} \left[1 + G_\alpha^{\text{exp}}(x)\right], \tag{10}$$

where $G_\alpha^{\text{exp}}(x)$ is an exponentially decaying function which tends to 0 when x goes to infinity. At distances from the wall larger than a few screening lengths, $D_\alpha(x)$ takes the same functional form as $D_\alpha^{(0)}(x)$, and many-body effects reduce to the introduction of effective charges $Z_\alpha^{\text{eff W}}$ and of a screening length κ^{-1}.

On the other hand, in the bulk many-body effects upon effective charges and the screening length arise only from pair interactions between ions, whereas along the wall they involve also the electrostatic potential and the geometric constraint created by the wall. In order to investigate these differences, we also determine the bulk pairwise interaction $w^{\text{B}}_{\alpha\alpha'}$ up to the same order in the coupling parameter as for the pairwise interaction along the wall.

B. Main results

In the present paper we determine $w^{\text{B}}_{\alpha\alpha'}(|\mathbf{r}-\mathbf{r}'|)$, $\overline{D}_\phi(x)$, and $D_\alpha(x)$ up to first-order in the dimensionless coupling parameter

$$\varepsilon \equiv \frac{1}{2}\kappa_{\text{D}}\frac{\beta e^2}{\epsilon_{\text{solv}}} \ll 1. \tag{11}$$

in regimes where $\varepsilon \ll 1$, $(\sigma/a)^3 \ll 1$ and $\kappa_{\text{D}} b \ll 1$. $\varepsilon \propto \left(\beta e^2/\epsilon_{\text{solv}} a\right)^{3/2}$ and (11) implies that $\beta e^2/\epsilon_{\text{solv}} \ll a \ll \xi_D$. (Up to the factor 1/2, ε coincides with the so-called plasma parameter of an electron gas.) As shown in Section III, contributions from steric effects involving σ/a are corrections of higher order with respect to the terms of order ε in some scaling regimes of high dilution where $(\sigma/a)^3 \ll \varepsilon$. Moreover, as shown in Section V C 3, the first corrections involving $\kappa_{\text{D}} b$ appear only at order $\varepsilon \ln(\kappa_{\text{D}} b)$. In the first scaling regime, the density vanishes while the temperature is fixed; then $\beta e^2/(\epsilon_{\text{solv}}\sigma)$ and $\beta e^2/(\epsilon_{\text{solv}} b)$ are fixed, namely

$$\left(\frac{\sigma}{a}\right)^3 \propto \varepsilon^2 \quad \text{and} \quad \kappa_{\text{D}} b \propto \varepsilon \ll 1 \quad \text{regime (1)}. \tag{12}$$

In the second case, the density vanishes while the temperature goes to infinity, but not too fast in order to ensure that $(\sigma/a)^3 \ll \varepsilon$; then both $\beta e^2/(\epsilon_{\text{solv}}\sigma)$ and $\beta e^2/(\epsilon_{\text{solv}} b)$ vanish. These conditions can be summarized in the following way,

$$\varepsilon^2 \ll \left(\frac{\sigma}{a}\right)^3 \ll \varepsilon \ll \kappa_{\text{D}} b \ll 1 \quad \text{regime (2)}. \tag{13}$$

The expressions at leading order in ε and $\kappa_{\text{D}} b$ in regime (2) can be obtained from those derived in regime (1) for a fixed ratio $(\varepsilon/\kappa_{\text{D}} b) \propto \beta e^2/(\epsilon_{\text{solv}} b)$ by taking the limit where $\beta e^2/(\epsilon_{\text{solv}} b)$ goes to zero while $\kappa_{\text{D}} b$ is kept fixed. We notice that, when the solvent is water, the Bjerrum length $\beta e^2/\epsilon_{\text{solv}}$ at room temperature is about 7 Angstrœm and, for concentrations around 10^{-4} mol/liter, ε is of order 10^{-2} and $(\sigma/a)^3$ is of order ε^2 for $\sigma \sim 5$ Angstrœm. For the sake of conciseness, both regimes (1) and (2) will be referred to as the "weak-coupling " regime and we shall speak only in terms of ε-expansions.

Our exact analytical calculations are performed in the framework of resummed Mayer diagrammatics introduced in Paper I. For the inverse screening length in the bulk we retrieve [12]-[13] that, up to order ε,

$$\kappa_{\mathrm{B}} = \kappa_{\mathrm{D}} \left[1 + \varepsilon \left(\frac{\Sigma_3}{\Sigma_2} \right)^2 \frac{\ln 3}{4} + o(\varepsilon) \right] \tag{14}$$

where

$$\Sigma_m \equiv \sum_{\alpha=1}^{n_s} \rho_\alpha^{\mathrm{B}} Z_\alpha^m . \tag{15}$$

The leading corrections involved in the notation $o(\varepsilon)$ are given in (64). As announced above, only screening effects of the non-integrable long-range Coulomb interaction are involved up to order ε; the diameters σ_α's of charges appear only in higher-order terms. This property holds in the bulk as well as in the vicinity of a wall (see e.g. Ref.[3]). More generally, the specific form of the short-distance steric repulsion between charges does not appear in the leading correction of order ε. The correction of order ε in the bulk screening length κ_{B}^{-1} vanishes in a charge symmetric electrolyte, where species with charge $-Z_\alpha e$ has the same density as species with charge $Z_\alpha e$ ($\Sigma_3 = 0$). If the fluid is not charge symmetric, the screening length κ_{B}^{-1} decreases when the coupling strength increases.

Our main results are the following. First, we find that

$$Z_\alpha^{\mathrm{eff\,B}} = Z_\alpha \left\{ 1 + \varepsilon \left[Z_\alpha \frac{\Sigma_3}{\Sigma_2} \frac{\ln 3}{2} + \left(\frac{\Sigma_3}{\Sigma_2} \right)^2 \left(\frac{1}{6} - \frac{\ln 3}{8} \right) \right] + o(\varepsilon) \right\} \tag{16}$$

where $(1/6) - (1/8) \ln 3 > 0$. In the case of a one-component plasma, formula (16) is reduced to that found in Ref. [12] by diagrammatic techniques. (The expression given for a multi-component electrolyte in Ref.[13] corresponds to another definition of the effective charge and does not coincide with our expression (16).) As in the case of the screening length, there is no correction at order ε if the composition of the electolyte is charge symmetric. According to the diagrammatic origin of this correction, the contribution to $Z_\alpha^{\mathrm{eff\,B}}$ from a screened interaction via one intermediate charge has the sign of $Z_\alpha \Sigma_3$ whereas the contribution to $Z_\alpha^{\mathrm{eff\,B}}$ from a screened interaction via two intermediate charges always increases the effective charge. We notice that the existence of the non-linear term Z_α^2 in $Z_\alpha^{\mathrm{eff\,B}}$ implies that $w_{\alpha\alpha'}^{\mathrm{as}}$ cannot be written as $Z_\alpha \psi_{\alpha'}$ where $\psi_{\alpha'}$ would be the total electrostatic potential created at $\mathbf{r}$ by the charge $Z_{\alpha'} e$ at $\mathbf{r}'$ and its screening cloud in the electrolyte. $\psi_{\alpha'}$ does not exist beyond the framework of linear-response theory.

Second, as expected, the screening length in the direction perpendicular to the wall proves to be the same as in the bulk, at least up to first order in ε. Besides, the renormalized charge $Z_\alpha^{\mathrm{eff\,W}}$ defined in (10) and the renormalized charge $Z_\alpha^{\text{eff B}}$ in the bulk do not coincide. However, up to order ε, their ratio is independent of the species α,

$$Z_\alpha^{\text{eff W}} = \left[1 + \gamma^{(1)} + o(\varepsilon)\right] Z_\alpha^{\text{eff B}} \tag{17}$$

with

$$\gamma^{(1)} = C_\phi^{(1)}\left(\frac{\beta e^2}{\epsilon_{\text{solv}} b}, \ln(\kappa_{\text{D}} b), \Delta_{\text{el}}\right) - \varepsilon \left(\frac{\Sigma_3}{\Sigma_2}\right)^2 \left[\frac{a_c(\Delta_{\text{el}})}{4} - \frac{\ln 3}{8}\right]. \tag{18}$$

(We notice that the notation $o(\varepsilon)$ in (17) contains both contributions such as those in (64) and terms of order $\varepsilon \times \kappa_{\text{D}} b$.) As exhibited by their diagrammatic origins, the various terms in $\gamma^{(1)}$ arise both from the nonuniformity of the density profiles and from screened interactions via two intermediate charges. These profiles, which have been calculated explicitly in the limit of vanishing $\kappa_{\text{D}} b$ in Ref.[2], result from the competition between, on one hand, the screened self-energy arising both from the electrostatic response of the wall and its steric deformation of screening clouds, and, on the other hand, the profile of the electrostatic potential drop which these two effects induce in the electrolyte. More precisely, $C_\phi^{(1)}$ written in (146) is the first-order renormalization of the amplitude of $\overline{D}_\phi(x)$ (see (4)), which originates from the nonuniformity of the density profiles. (The screened potential ϕ appears as an auxiliary object in the resummed Mayer diagrammatics, and the expressions of $C_\phi^{(1)}$ and $\overline{G}_\phi^{\exp (1)}(x, x')$ are calculated in Section V.) $C_\phi^{(1)}$ and its sign depend on the composition of the electrolyte, on the closest approach distance b to the wall (through the parameters $\kappa_{\text{D}} b$ and $\beta e^2/(\epsilon_{\text{solv}} b)$), and on the parameter Δ_{el}, which charaterizes the difference between the dielectric permittivity of the wall and that of the solvent,

$$\Delta_{\text{el}} \equiv \frac{\epsilon_{\text{W}} - \epsilon_{\text{solv}}}{\epsilon_{\text{W}} + \epsilon_{\text{solv}}}. \tag{19}$$

The second term in the r.h.s. of (18) originates from the renormalization of the screening length and from the difference in the contributions from four-body effective interactions in the bulk and along the wall. The three-body effective interactions do not contribute to $\gamma^{(1)}$ – so that $\gamma^{(1)}$ is independent of the species α –, because they give the same corrections to the amplitudes of $w_{\alpha\alpha'}^{\text{B}}$ and $w_{\alpha\alpha'}$. The constant $a_c(\Delta_{\text{el}})$ is written in (169). If $\epsilon_{\text{solv}} > \epsilon_W$, as it is the case when the solvent is water and the wall is made of glass, $a_c(\Delta_{\text{el}}) > (1/2) \ln 3$ and the second term decreases the ratio $Z_\alpha^{\text{eff W}}/Z_\alpha^{\text{eff B}}$. We notice that $G_\alpha^{\exp (1)}(x)$ at first order in ε is given in Section VI D. Contrarily to $D_\alpha^{(0)}(x)$, the sign of $D_\alpha^{(1)}(x)$ may vary with the distance x, and it depends on the composition of the electrolyte, on the closest approach distance to the wall b, and on the ratio between the dielectric constant of the wall and that of the solvent.

C. Contents

The paper is organized as follows. The large-distance behaviors of the effective pairwise interactions $w_{\alpha\alpha'}$, in the bulk or along the wall, are investigated through the large-distance decay of the Ursell function $h_{\alpha\alpha'}$ according to relation (1). The latter decay is conveniently studied from Mayer diagrammatics generalized to inhomogeous situations. In Section II we recall the resummed Mayer diagrammatics introduced in Paper I in order to systematically handle with the large-distance nonintegrability of the bare Coulomb potential (far away or near the wall). There appears a screened potential ϕ, which coincides with the interaction defined from the immersion free energy between two infinitesimal external point charges (see Section II B). In the bulk, ϕ is a solution of the usual Debye equation. Near the wall ϕ obeys an inhomogeneous Debye equation, where the inverse screening length depends on x. In Section II C a decomposition of $h_{\alpha\alpha'}$ into four contributions enables one to show how the basic internal- and external-screening sum rules arise in resummed Mayer diagrammatics, and how they are preserved if only some subclass of diagrams is retained. It also allows one to show that, for a symmetric electrolyte, $\sum_\alpha \rho_\alpha(\mathbf{r})h_{\alpha\alpha'}(\mathbf{r},\mathbf{r}')$ decays faster than $h_{\alpha\alpha'}(\mathbf{r},\mathbf{r}')$ (see Sections IV E and VI B). We also recall the graphic reorganization of diagrams devised in Paper I for the study of the general structure of large-distance tails in dilute regimes.

Systematic double-expansions in the dimensionless parameters σ/a and ε can be performed from resummed diagrams. In Section III we exhibit the nature of the first various contributions. This leads us to introduce the scaling regimes (12) and (13) where the correction proportional to the coupling parameter ε is the leading contribution. (We also recall the expression of the pair correlation at any distance at leading order in ε.)

Section IV is devoted to bulk correlations. We take advantage of the full translational invariance in the bulk in order to resum the four geometric series which appear in the Fourier transform of the graphic decomposition of $h^{B}_{\alpha\alpha'}$ recalled in Section II C. Thus, we obtain a compact formula for the large-distance behavior of $h^{B}_{\alpha\alpha'}$, where the contributions of both charges are factorized. This formula is appropriate to obtain systematic ε-expansions of the screening length and of the renormalized charge from the ε-expansions of resummed diagrams.

In Section IV D, we also show how to retrieve the corresponding corrections of order ε by a more cumbersome method which will be useful for the calculations in the vicinity of a wall, where the translational invariance is lost in the direction perpendicular to the wall. In position space every convolution in the graphic representation of $h^{B}_{\alpha\alpha'}$ decays exponentially over the Debye screening length κ_{D}^{-1} at large relative distances r, with an amplitude which is proportional to $1/r$ times a polynomial in r. The resummation of the series of the leading tails in r at every order in ε must be performed in order to get the exponential decay over the screening length κ_{B}^{-1} calculated up to order ε

(see Appendix B). On the contrary, the correction of order ε in the renormalized charge can be retrieved from only a finite number of resummed Mayer diagrams.

In Section V we recall how the screened potential $\phi(x,x',y)$ and the effective dipole $\overline{D}_{\phi}(x)$ in its large-y tail are formally expressed in terms of the density profiles in the vicinity of the wall [1]. Then, the ε-expansion of $\overline{D}_{\phi}(x)$ can be performed from the ε-expansion of the density profiles, by applying the method devised in Ref.[3]. The density profiles, which vary rapidly over the Bjerrum length $\beta e^2/\epsilon_{\text{solv}}$ in the vicinity of a dielectric wall, have been explicitly determined up to order ε in the limit where $\kappa_{\text{D}} b$ vanishes in Ref.[2], and we explicitly calculate $\overline{D}_{\phi}(x)$ up to order ε in the same limit.

In Section VI we recall how the structure of the effective dipole $D_{\alpha}(x)$ in the $1/y^3$ tail of $h_{\alpha\alpha'}(x,x',y)$ is given in terms of the graphic representation written in Section II C. We also derive a sum rule for $\sum_{\alpha} e_{\alpha}\rho_{\alpha}(x)D_{\alpha}(x)$. By using the resummation method checked for the bulk situation in Section IV D, we determine the renormalized value of the screening length in the direction perpendicular to the wall at first order in ε. For that purpose, in Appendix D we show that the leading term in x at every order ε^q is proportional to $(x-b)^q \exp\left[-\kappa_{\text{D}}(x-b)\right]$, and we resum the series of these leading terms. Thus, we check that the correction of order ε in the screening length is indeed the same in the bulk and in the direction perpendicular to the wall. Then, $D_{\alpha}(x)$ is determined up to order ε by only two resummed Mayer diagrams. Explicit calculations are performed in the limit where $\kappa_{\text{D}} b$ vanishes and the expressions of $Z_{\alpha}^{\text{eff B}}$ and $Z_{\alpha}^{\text{eff W}}$ are compared. Their physical interpretation is given thanks to the diagrammatic origins of the various contributions.

II. GENERAL FORMALISM

A. Model

In the primitive model defined above, the hard-core effect between two species α and α' can be taken into account in the pair energy by an interaction v_{SR} which is infinitely repulsive at distances shorter than the sum $(\sigma_{\alpha}+\sigma_{\alpha'})/2$ of the sphere radii of both species. Its Boltzmann factor reads

$$\exp\left[-\beta v_{SR}(|\mathbf{r}-\mathbf{r}'|;\alpha,\alpha')\right] = \begin{cases} 0 \ \text{ if } |\mathbf{r}-\mathbf{r}'| < (\sigma_{\alpha}+\sigma_{\alpha'})/2, \\ 1 \ \text{ if } |\mathbf{r}-\mathbf{r}'| > (\sigma_{\alpha}+\sigma_{\alpha'})/2. \end{cases} \tag{20}$$

Since charges are reduced to points at the centers of excluded-volume spheres with the same dielectric constant as the solvent, the Coulomb interaction between two charges can be written in the whole space (even for $x<0$ or $x'<0$)

as $(Z_\alpha Z_{\alpha'} e^2/\epsilon_{\rm solv}) v(\mathbf{r},\mathbf{r}')$, where $v(\mathbf{r},\mathbf{r}')$ is the solution of Poisson equation for unit point charges with the adequate electrostatic boundary conditions. Since the half-space $x<0$ is occupied by a material with a dielectric constant $\epsilon_{\rm W}$, $v(\mathbf{r},\mathbf{r}')$ in Gauss units reads, for $x>0$ and $x'>0$ and for any $|\mathbf{r}-\mathbf{r}'|>0$ [14],

$$v(\mathbf{r},\mathbf{r}') = \frac{1}{|\mathbf{r}-\mathbf{r}'|} - \Delta_{\rm el}\frac{1}{|\mathbf{r}-\mathbf{r}'^{\star}|}. \tag{21}$$

$\Delta_{\rm el}$, defined in (19), lies between -1 and 1, and $\mathbf{r}'^{\star}$ is the *image* of the position $\mathbf{r}'$ with respect to the plane interface between the solution and the dielectric material. In the bulk the Coulomb potential reads

$$v_B(|\mathbf{r}-\mathbf{r}'|) = \frac{1}{|\mathbf{r}-\mathbf{r}'|}. \tag{22}$$

The total pair energy $U_{\rm pair}$ is

$$U_{\rm pair} = \frac{1}{2}\sum_{i\neq j} v_{SR}(|\mathbf{r}_i-\mathbf{r}_j|;\alpha_i,\alpha_j) + \frac{1}{2}\sum_{i\neq j}\frac{e^2}{\epsilon_{\rm solv}} Z_{\alpha_i} Z_{\alpha_j} v(\mathbf{r}_i,\mathbf{r}_j), \tag{23}$$

where i is the index of a particle.

In the vicinity of the wall, one-body potentials appear in the total energy of the system. For every charge a self-energy $Z_\alpha^2(e^2/\epsilon_{\rm solv})V_{\rm self}$ arises from the work necessary to bring a charge $Z_\alpha e$ from $x=+\infty$ (in the solvent) to a point $\mathbf{r}$ in the vicinity of the wall. According to (21), the wall electrostatic response is equivalent to the presence of an image charge $-\Delta_{\rm el} Z_\alpha e$ at point $\mathbf{r}^{\star}$ inside a wall that would have the same dielectric constant $\epsilon_{\rm solv}$ as the solvent, and

$$V_{\rm self}(x) = -\Delta_{\rm el}\frac{1}{4x}. \tag{24}$$

In the case of a glass wall in contact with water, the relative dielectric constant $\epsilon_W/\epsilon_{\rm solv}$ of the wall with respect to the solvent is of order $(1/80)<1$, $\Delta_{\rm el}$ defined in (19) is negative, and $V_{\rm self}$ is a repulsive potential. The impenetrability of the wall corresponds to a short-ranged potential $V_{SR}(x)$, the Boltzmann factor of which is

$$\exp\left[-\beta V_{SR}(x)\right] = \begin{cases} 0 & \text{if } x<b \\ 1 & \text{if } x>b, \end{cases} \tag{25}$$

where b is the closest approach distance to the wall for the centers of spherical particles, which is the same for all species. The confinement of all particles to the positive-x region and the electrostatic self-energy may be gathered in a one-body potential $V_{\rm wall}$,

$$V_{\rm wall} = \sum_i V_{SR}(x_i;\alpha_i) + \sum_i \frac{e^2}{\epsilon_{\rm solv}} Z_{\alpha_i}^2 V_{\rm self}(x_i). \tag{26}$$

B. Generalized resummed Mayer diagrams

By virtue of definition (1), the leading large-distance behavior $w^{\mathrm{as}}_{\alpha\alpha'}$ of $w_{\alpha\alpha'}$ is proportional to the large-distance behavior $h^{\mathrm{as}}_{\alpha\alpha'}$ of $h_{\alpha\alpha'}$,

$$h^{\mathrm{as}}_{\alpha\alpha'} = -\beta w^{\mathrm{as}}_{\alpha\alpha'}, \tag{27}$$

because any power $[w^{\mathrm{as}}_{\alpha\alpha'}]^n$, with $n \geq 2$, has a faster decay than $w^{\mathrm{as}}_{\alpha\alpha'}$. In an inhomogeneous situation $h^{\mathrm{as}}_{\alpha\alpha'}$ is conveniently studied by means of the Mayer diagrammatic representation of $h_{\alpha\alpha'}$. However, the large-distance behavior of the Coulomb pair interaction $v(\mathbf{r},\mathbf{r}')$ is not integrable, and every integral corresponding to a standard Mayer diagram that is not sufficiently connected diverges when the volume of the region occupied by the fluid becomes infinite.

As shown in Paper I, thanks to a generalization of the procedure introduced by Meeron [15] in order to calculate $h_{\alpha\alpha'}$ in the bulk, the density-expansion of $h_{\alpha\alpha'}$ in the vicinity of the wall can be expressed in terms of resummed Mayer diagrams with integrable bonds F. Since the procedure for the systematic resummation of Coulomb divergences relies on topological considerations, the definitions of Mayer diagrams with resummed bonds are formally the same ones in the bulk or near the wall. The two differences between resummed diagrams in the bulk and near the wall are the following. First, near the wall the point weights are not constant densities but x-dependent density profiles. Second, the screened potential ϕ arising from collective effects described by the systematic resummation of Coulomb divergences is no longer the Debye potential, but it obeys an "inhomogeneous" Debye equation,

$$\Delta_{\mathbf{r}}\phi(\mathbf{r},\mathbf{r}') - \overline{\kappa}^2(x)\phi(\mathbf{r},\mathbf{r}') = -4\pi\delta(\mathbf{r}-\mathbf{r}'). \tag{28}$$

In (28) $\overline{\kappa}^2(x)$ is defined as

$$\overline{\kappa}^2(x) \equiv 4\pi\beta\frac{e^2}{\epsilon_{\mathrm{solv}}}\sum_{\alpha} Z_\alpha^2\rho_\alpha(x), \tag{29}$$

where all densities $\rho_\alpha(x)$'s vanish for $x < b$. ϕ obeys the same boundary conditions as the Coulomb potential v: $\phi(\mathbf{r},\mathbf{r}')$ is continuous everywhere and tends to 0 when $|\mathbf{r}-\mathbf{r}'|$ goes to $+\infty$, while its gradient times the dielectric constant is continuous at the interface with dielectric walls. We recall that particles are supposed to be made of a material with the same dielectric constant as the solvent.

The two resummed bonds F, called F^{cc} and F_{R} respectively, are written in terms of the screened potential ϕ as

$$F^{\mathrm{cc}}(n,m) = -\frac{\beta e^2}{\epsilon_{\mathrm{solv}}} Z_{\alpha_n} Z_{\alpha_m}\phi(\mathbf{r}_n,\mathbf{r}_m) \tag{30}$$

and

$$F_{\mathrm{R}}(n,m) = \exp\left[-\beta v_{SR}(|\mathbf{r}_n - \mathbf{r}_m|) - \frac{\beta e^2}{\epsilon_{\mathrm{solv}}} Z_{\alpha_n} Z_{\alpha_m} \phi(\mathbf{r}_n, \mathbf{r}_m)\right] - 1 + \frac{\beta e^2}{\epsilon_{\mathrm{solv}}} Z_{\alpha_n} Z_{\alpha_m} \phi(\mathbf{r}_n, \mathbf{r}_m), \tag{31}$$

where n and m are point indices in the Mayer diagrams. (In the bond notations, the superscript "cc" stands for "charge-charge" and "R" means "resummed". Indeed, F^{cc} is proportional to the resummed interaction $\phi(\mathbf{r}, \mathbf{r}')$ between point charges; $F_{\mathrm{R}} + F^{\mathrm{cc}}$ is equal to the original Mayer bond where the Coulomb pair interaction $v(\mathbf{r}, \mathbf{r}')$ is replaced by its resummed expression $\phi(\mathbf{r}, \mathbf{r}')$, while the short-range repulsion is left unchanged.) The resummed Mayer diagrammatics of $h_{\alpha\alpha'}$ is

$$h_{\alpha\alpha'}(x, x', \mathbf{y}) = \sum_{\Pi} \frac{1}{S_\Pi} \int_\Lambda \left[\prod_{n=1}^{N} d\mathbf{r}_n \sum_{\alpha_n=1}^{n_s} \rho_{\alpha_n}(x_n)\right] \left[\prod F\right]_\Pi . \tag{32}$$

In (32) the sum runs over all the unlabeled topologically different connected diagrams Π with two root points $(\mathbf{r}, \alpha)$ and $(\mathbf{r}', \alpha')$ (which are not integrated over) and N internal points (which are integrated over) with $N = 0, \ldots, \infty$, and which are built according to the following rules. Each pair of points in Π is linked by at most one bond F, and there is no articulation point. (An articulation point is defined by the fact that, if it is taken out of the diagram, then the latter is split into two pieces, one of which at least is no longer linked to any root point.) Moreover, in order to avoid double counting in the resummation process, diagrams Π must be built with an "excluded-composition" rule : there is no point attached by only two bonds F^{cc} to the rest of the diagram. $[\prod F]_\Pi$ is the product of the bonds F in the Π diagram and S_Π is its symmetry factor, i.e., the number of permutations of the internal points $\mathbf{r}_n$ that do not change this product. Every point has a weight equal to $\rho_\alpha(x)$ that is summed over all species. We have used the convention that, if N is equal to 0, no $\int_\Lambda d\mathbf{r}_n \rho_{\alpha_n}(x_n)$ appears, and $(1/S_\Pi)\,[\prod F]_\Pi$ is reduced to $F(\mathbf{r}, \mathbf{r}')$. Near the wall, Λ denotes a finite-size region bounded by the wall on the left, whereas, in the bulk, Λ stands for a finite-size region far away from the wall. The screened potential ϕ is integrable at large distances. (In the bulk ϕ decays exponentially fast in all directions; near the wall in the large-distance behavior given in (4), $\overline{D}_\phi(x)$ has an exponential decay and the $1/y^3$ tail is integrable.) As a consequence, Π diagrams correspond to convergent integrals in the limit where the volume Λ extends to infinity inside the bulk or on the right of the wall.

C. Graphic reorganization of resummed diagrammatics

In $h_{\alpha\alpha'}(\mathbf{r}_a, \mathbf{r}'_{a'})$ we can distinguish four classes of diagrams by considering whether a single bond F^{cc} is attached to root point a or to root point a'. (a and a' are short notations for the couple of variables $(\mathbf{r}_a, \alpha)$ and $(\mathbf{r}_{a'}, \alpha')$, respectively, which are associated with the root points in a Mayer diagram.) $h_{\alpha\alpha'}$ can be rewritten as the sum

$$h_{\alpha\alpha'} \equiv h^{\rm cc}_{\alpha\alpha'} + h^{\rm c-}_{\alpha\alpha'} + h^{-\rm c}_{\alpha\alpha'} + h^{--}_{\alpha\alpha'} , \tag{33}$$

where in $h^{\rm cc}_{\alpha\alpha'}$ both a and a' carry a single bond $F^{\rm cc}$, in $h^{\rm c-}_{\alpha\alpha'}$ ($h^{-\rm c}_{\alpha\alpha'}$) only a (a') is linked to the rest of the diagram by a single bond $F^{\rm cc}$, and in $h^{--}_{\alpha\alpha'}$ neither a nor a' are linked to the rest of the diagram by only one bond $F^{\rm cc}$.

1. Screening rules

A first interest of decomposition (33) is that it enables one to derive the basic screening rules (recalled hereafter) from the fact that they are already fulfilled by the diagram made of a single bond $F^{\rm cc}$ (because of the corresponding sum rules obeyed by the screened potential $\phi(\mathbf{r},\mathbf{r}')$). Moreover, since the sum rules are linked to the large-distance behavior of the charge-charge correlation function, decomposition (33) also enables one to show that if some diagrams are to be kept for their contributions to $h^{--\,\rm as}_{\alpha\alpha'}$ in some dilute regime, then the corresponding diagrams "dressed" with $F^{\rm cc}$ bonds in $h^{\rm cc}_{\alpha\alpha'}$, $h^{\rm c-}_{\alpha\alpha'}$ and $h^{-\rm c}_{\alpha\alpha'}$ are also to be retained, together with the bond $F^{\rm cc}$, in order to ensure that the screening rules are still satisfied.

The basic screening rules are the following. In a charge fluid with Coulomb interactions, an internal charge of the system, as well as an infinitesimal external charge, are perfectly screened by the fluid: each charge is surrounded by a cloud which carries exactly the opposite charge. These properties can be written in a compact form in terms of the charge-charge correlation defined as

$$C(\mathbf{r},\mathbf{r}') \equiv e^2 \left\{ \sum_{\alpha} Z_\alpha^2 \rho_\alpha(\mathbf{r}) \delta(\mathbf{r}-\mathbf{r}') + \sum_{\alpha,\alpha'} Z_\alpha Z_{\alpha'} \rho_\alpha(\mathbf{r}) \rho_{\alpha'}(\mathbf{r}') h_{\alpha\alpha'}(\mathbf{r},\mathbf{r}') \right\} . \tag{34}$$

The internal-screening rule reads

$$\int d\mathbf{r} \sum_{\alpha} Z_\alpha \rho_\alpha(\mathbf{r}) h_{\alpha\alpha'}(\mathbf{r},\mathbf{r}') = -Z_{\alpha'} , \tag{35}$$

and, by performing the summation $\sum_{\alpha'} Z_{\alpha'}\rho_{\alpha'}(\mathbf{r}') \times$ (35), the internal-screening sum rule implies that

$$\int d\mathbf{r}\, C(\mathbf{r},\mathbf{r}') = 0. \tag{36}$$

By virtue of the linear response theory, the external-screening sum rule reads

$$\frac{\beta}{\epsilon_{\rm solv}} \int d\mathbf{r} \int d\mathbf{r}' v(\mathbf{r}_0,\mathbf{r}') C(\mathbf{r}',\mathbf{r}) = 1. \tag{37}$$

The latter equation, derived for inhomogeneous systems by Carnie and Chan [16], is the generalization of the sum-rule first settled by Stillinger and Lovett [17] for the second moment of $C(\mathbf{r},\mathbf{r}')$ in the homogeneous case (see next paragraph). As a consequence of the internal screening sum rule, (37) holds whatever short-distance regularization may be added to the pure Coulomb interaction $v(\mathbf{r}_0, \mathbf{r}')$ [6].

In the bulk, the translational invariance in all directions implies that sum rules (36) and (37) are relative respectively to the $k = 0$ value and to the coefficient of the k^2-term in the k-expansion of $C^{\mathrm{B}}(k)$. Both sum rules are summarized in the following small-k behavior,

$$C^{\mathrm{B}}(k) \underset{k \to 0}{\sim} \frac{\epsilon_{\mathrm{solv}}}{4\pi\beta} k^2. \tag{38}$$

In the vicinity of a wall, there is translational invariance only in directions parallel to the plane interface, and the Carnie and Chan sum rule (37) takes the form of a dipole sum rule [6, 18],

$$\int_0^{+\infty} dx \int_0^{+\infty} dx' \int d\mathbf{y}\, x' C(x, x', \mathbf{y}) = -\frac{\epsilon_{\mathrm{solv}}}{4\pi\beta}. \tag{39}$$

As shown in Ref. [19], the first moment of $C(x, x', \mathbf{y})$ is linked to the amplitude $f_C(x, x')$ of the $1/y^3$ tail of $C(x, x', \mathbf{y})$,

$$\int_0^{+\infty} dx' \int d\mathbf{y}\, x' C(x, x', \mathbf{y}) = \frac{\epsilon_{\mathrm{solv}}}{\epsilon_W} 2\pi \int_0^{+\infty} dx' f_C(x, x'). \tag{40}$$

$f_C(x, x')$ coincides with $-\beta \sum_{\alpha\alpha'} e^2 Z_\alpha Z_{\alpha'} \rho_\alpha(x) \rho_{\alpha'}(x') f_{\alpha\alpha'}(x, x')$, where $-\beta f_{\alpha\alpha'}(x, x')/y^3$ is the large-distance behavior of $h_{\alpha\alpha'}(x, x', \mathbf{y})$. Therefore, the moment rule (39) can be rewritten as a sum rule for the amplitude $f_{\alpha\alpha'}(x, x')$, first derived in Ref.[20],

$$\int_0^{+\infty} dx \int_0^{+\infty} dx' \sum_{\alpha\alpha'} e^2 Z_\alpha Z_{\alpha'} \rho_\alpha(x) \rho_{\alpha'}(x') f_{\alpha\alpha'}(x, x') = \frac{\epsilon_W}{8\pi^2\beta^2}. \tag{41}$$

(We notice that there is a misprint in Paper I, where the above sum rule is written in Eq.(4) with a an extra spurious coefficient $1/\epsilon_{\mathrm{solv}}$ on the r.h.s.)

Now, we show how the combination of decomposition (33) with sum rules obeyed by ϕ enables one to derive the two basic screening rules. A key ingredient of the derivation is the relations between h^{cc} and $h^{-\mathrm{c}}$ on one hand, and $h^{\mathrm{c}-}$ and h^{--} on the other hand, which arise from their definitions.

In the bulk, because of the full translational invariance, the latter relations take simple forms in Fourier space. They read

$$h^{\mathrm{cc}}_{\alpha\alpha'}(k) = F^{\mathrm{cc}}_{\alpha\alpha'}(k) + \sum_{\gamma_1} \rho^{\mathrm{B}}_{\gamma_1} F^{\mathrm{cc}}_{\alpha\gamma_1}(k) h^{-\mathrm{c}}_{\gamma_1\alpha'}(k), \tag{42}$$

and

$$h^{\mathrm{c}-}_{\alpha\alpha'}(k) = \sum_{\gamma_1} \rho^{\mathrm{B}}_{\gamma_1} F^{\mathrm{cc}}_{\alpha\gamma_1}(k) h^{--}_{\gamma_1\alpha'}(k). \tag{43}$$

(For the sake of clarity, in the present paragraph, we forget superscripts B, except in the densities, in $h_{\alpha\alpha'}$ and in C.) On the other hand, by virtue of the explicit expression (59) of $\phi_{\rm B}$,

$$\sum_{\alpha} Z_\alpha \rho^{\rm B}_\alpha F^{\rm cc}_{\alpha\alpha'}(k=0) = -Z_{\alpha'}. \tag{44}$$

In other words, the part $F^{\rm cc}$ in $h^{\rm B}_{\alpha\alpha'}$ already fulfills the internal-screening sum rule. When relations (42) and (43) are inserted in decomposition (33) of $h^{\rm B}_{\alpha\alpha'}$,

$$h^{\rm B}_{\alpha\alpha'}(k) = F^{\rm cc}_{\alpha\alpha'}(k) + \left[\sum_{\gamma_1} \rho^{\rm B}_{\gamma_1} F^{\rm cc}_{\alpha\gamma_1}(k) h^{-{\rm c}}_{\gamma_1\alpha'}(k) + h^{-{\rm c}}_{\alpha\alpha'}(k)\right] + \left[\sum_{\gamma_1} \rho^{\rm B}_{\gamma_1} F^{\rm cc}_{\alpha\gamma_1}(k) h^{--}_{\gamma_1\alpha'}(k) + h^{--}_{\alpha\alpha'}(k)\right] \tag{45}$$

Then property (44) implies that, in $\sum_\alpha Z_\alpha \rho^{\rm B}_\alpha h^{\rm B}_{\alpha\alpha'}(k=0)$, the contribution from $h^{\rm cc} - F^{\rm cc}$, given in (42), cancels that from $h^{-{\rm c}}$, and the contribution from $h^{{\rm c}-}$, given in (43), compensates that from h^{--}, so that the internal-screening rule is indeed satisfied.

In the case of the bulk external-screening rule (38), the same mechanism operates when the k^2-term in the small-k expansion of $C^{\rm B}(k)$ is considered. The charge-charge correlation $C^{\rm B}_{F^{\rm cc}}$, where $h^{\rm B}_{\alpha\alpha'}$ is replaced by $F^{\rm cc}_{\alpha\alpha'}$, fulfills the second-moment sum-rule,

$$C^{\rm B}_{F^{\rm cc}}(k) \underset{k\to 0}{\sim} \frac{\epsilon_{\rm solv}}{4\pi\beta}\, k^2. \tag{46}$$

Again, by virtue of (44), decomposition (45) implies that the k^2-term in $h^{-{\rm c}}$ is canceled by the part of the k^2-term in $h^{\rm cc} - F^{\rm cc} = \sum_{\gamma_1} \rho^{\rm B}_{\gamma_1} F^{\rm cc}_{\alpha\gamma_1}(k) h^{-{\rm c}}_{\gamma_1\alpha'}(k)$ that arises from the k^2-term in $h^{-{\rm c}}$. Similarly, the k^2-term in h^{--} is canceled by the part of the k^2-term in $h^{{\rm c}-} = \sum_{\gamma_1} \rho^{\rm B}_{\gamma_1} F^{\rm cc}_{\alpha\gamma_1}(k) h^{--}_{\gamma_1\alpha'}(k)$ that arises from the k^2-term in h^{--}. Moreover, (43) and (44) imply that $\sum_{\alpha'} Z_{\alpha'} \rho^{\rm B}_{\alpha'} h^{-{\rm c}}_{\gamma\alpha'}(k=0) = -\sum_{\gamma'} Z_{\gamma'} \rho^{\rm B}_{\gamma'} h^{--}_{\gamma\gamma'}(k=0)$, so that the part of the k^2-term in $h^{\rm cc} - F^{\rm cc}$ that comes from the k^2 term in $F^{\rm cc}$ is opposite to the part of the k^2-term in $h^{{\rm c}-}$ that is generated by the k^2-term in $F^{\rm cc}$. We notice that the present argument is analogous to that found in Ref.[21] for an analogous decomposition in a quantum charge fluid.

In the vicinity of the wall, the derivation of screening rules (35) and (41) also relies on the analog of decomposition (45) and on two sum rules derived for ϕ in Paper I, namely, if $x' > b$,

$$\int_0^{+\infty} dx\, \overline{\kappa}^2(x) \int d\mathbf{y}\, \phi(x, x', \mathbf{y}) = 4\pi, \tag{47}$$

and

$$\int_0^{+\infty} dx \int_0^{+\infty} dx'\, \overline{\kappa}^2(x) \overline{\kappa}^2(x') f_\phi(x, x') = 2\frac{\epsilon_W}{\epsilon_{\rm solv}}. \tag{48}$$

The Fourier transform of a function $f(\mathbf{y})$ at wave vector $\mathbf{l}$ is defined as $f(\mathbf{l}) \equiv \int d\mathbf{y} \exp(i\mathbf{l}\cdot\mathbf{y}) f(\mathbf{y})$. Thanks to the translational invariance in the direction $\mathbf{y}$ parallel to the plane interface, the relations, which arise from their definitions, between $h^{\rm cc}$ and $h^{-\rm c}$ on one hand, and $h^{\rm c-}$ and h^{--} on the other hand, take the simple form,

$$\begin{aligned} h^{\rm cc}_{\alpha\alpha'}(x,x',\mathbf{l}) &= F^{\rm cc}_{\alpha\alpha'}(x,x',\mathbf{l}) \\ &\quad + \int_0^{+\infty} dx_1 \sum_{\gamma_1} \rho_{\gamma_1}(x_1) F^{\rm cc}_{\alpha\gamma_1}(x,x_1,\mathbf{l}) h^{-\rm c}_{\gamma_1\alpha'}(x_1,x',\mathbf{l}), \end{aligned} \tag{49}$$

and

$$h^{\rm c-}_{\alpha\alpha'}(x,x',\mathbf{l}) = \int_0^{+\infty} dx_1 \sum_{\gamma_1} \rho_{\gamma_1}(x_1) F^{\rm cc}_{\alpha\gamma_1}(x,x_1,\mathbf{l}) h^{--}_{\gamma_1\alpha'}(x_1,x',\mathbf{l}). \tag{50}$$

(47) and (48) imply that $F^{\rm cc}$ saturates the internal sum rule (35) and the external sum rule (41), respectively.

The external-screening sum rule (41) in the vicinity of the wall is studied again in Section VI B. We show that, in the case where all species have the same closest approach distance to the wall, decomposition (33) enables one to derive a sum rule fulfilled by the effective dipole amplitude $\overline{D}_\alpha(x)$.

2. Large-distance tails

Another interest of decomposition (33) is that the large-distance behavior of the Ursell function $h_{\alpha\alpha'}$ can be conveniently analyzed from this decomposition, after a suitable reorganization of resummed Mayer diagrams, which has been introduced in Paper I. The resummed Mayer diagrammatics (32) for $h_{\alpha\alpha'}$ is reexpressed in terms of "graphs" made of two kinds of bonds: the bond $F^{\rm cc}$ and the bond I that is defined as the sum of all subdiagrams that either contain no $F^{\rm cc}$ bond or remain connected in a single piece when a bond $F^{\rm cc}$ is cut. $F_{\rm R}$ falls off faster than $F^{\rm cc}$ at large distances (namely, as $[F^{\rm cc}]^2/2$) and the topology of subdiagrams involved in I implies that I decays faster than $F^{\rm cc}$ at large distances in a sufficiently dilute regime. Since the reorganization is purely topological, it is valid for correlations in the bulk as well as in the vicinity of the wall. According to the excluded-composition rule obeyed by resummed Π diagrams, the functions in the r.h.s. of (33) are equal to the series represented in Figs.1-3 respectively,

$$\begin{aligned} h^{\rm cc}_{\alpha\alpha'}(\mathbf{r},\mathbf{r}') = F^{\rm cc}(a,a') &+ \int d\mathbf{r}_1 d\mathbf{r}'_1 \sum_{\gamma_1,\gamma'_1} \rho_{\gamma_1}(\mathbf{r}_1)\rho_{\gamma'_1}(\mathbf{r}'_1) F^{\rm cc}(a,1) I(1,1') F^{\rm cc}(1',a') \\ &+ \int d\mathbf{r}_1 d\mathbf{r}'_1 \sum_{\gamma_1,\gamma'_1} \rho_{\gamma_1}(\mathbf{r}_1)\rho_{\gamma'_1}(\mathbf{r}'_1) \int d\mathbf{r}_2 d\mathbf{r}'_2 \sum_{\gamma_2,\gamma'_2} \rho_{\gamma_2}(\mathbf{r}_2)\rho_{\gamma'_2}(\mathbf{r}'_2) \\ &\qquad F^{\rm cc}(a,1) I(1,1') F^{\rm cc}(1',2) I(2,2') F^{\rm cc}(2',a') + \cdots , \end{aligned} \tag{51}$$

$$\begin{aligned} h^{\mathrm{c}-}_{\alpha\alpha'}(\mathbf{r},\mathbf{r}') \equiv & \int d\mathbf{r}_{c'} \sum_{\gamma'} \rho_{\gamma'}(\mathbf{r}_{c'}) F^{\mathrm{cc}}(a,c') I(c',a') \\ & + \int d\mathbf{r}_{c'} \sum_{\gamma'} \rho_{\gamma'}(\mathbf{r}_{c'}) \int d\mathbf{r}_1 d\mathbf{r}'_1 \sum_{\gamma_1,\gamma'_1} \rho_{\gamma_1}(\mathbf{r}_1)\rho_{\gamma'_1}(\mathbf{r}'_1) \\ & \qquad F^{\mathrm{cc}}(a,1) I(1,1') F^{\mathrm{cc}}(1',c') I(c',a') + \cdots \,, \end{aligned} \tag{52}$$

while $h^{-\mathrm{c}}$ is defined in a symmetric way, and

$$\begin{aligned} h^{--}_{\alpha\alpha'}(\mathbf{r},\mathbf{r}') \equiv I(a,a') & + \int d\mathbf{r}_c \int d\mathbf{r}_{c'} \sum_{\gamma,\gamma'} \rho_\gamma(\mathbf{r}_c)\rho_{\gamma'}(\mathbf{r}_{c'}) I(a,c) F^{\mathrm{cc}}(c,c') I(c',a') \\ & + \int d\mathbf{r}_c \int d\mathbf{r}_{c'} \sum_{\gamma,\gamma'} \rho_\gamma(\mathbf{r}_c)\rho_{\gamma'}(\mathbf{r}_{c'}) \int d\mathbf{r}_1 d\mathbf{r}'_1 \sum_{\gamma_1,\gamma'_1} \rho_{\gamma_1}(\mathbf{r}_1)\rho_{\gamma'_1}(\mathbf{r}'_1) \\ & \qquad I(a,c) F^{\mathrm{cc}}(c,1) I(1,1') F^{\mathrm{cc}}(1',c') I(c',a') + \cdots \,. \end{aligned} \tag{53}$$

In the previous definitions c is a short notation for $(\mathbf{r}_c, \gamma)$, and i stands for $(\mathbf{r}_i, \alpha_i)$.

We notice that, according to previous section, any contribution to I automatically generates a change in $h_{\alpha\alpha'}$ that preserves the two basic screening sum rules. In the bulk, the external-screening rule (38) is also retrieved from the compact formulae obtained by resummations in the graphic expansion (51)–(53), as shown in Section IV E.

III. WEAK-COUPLING REGIME

A. Small parameters

Now we take into account the fact that in an electrolyte all species have charges and diameters of the same magnitude orders e and σ, respectively. Moreover, all bulk densities are comparable, and the typical interparticle distance does not depend on species: it is denoted by a. First, we assume that the densities are so low that the volume fraction $(\sigma/a)^3$ of particles is small,

$$\left(\frac{\sigma}{a}\right)^3 \ll 1. \tag{54}$$

Our second assumption is that the temperature is high enough for the mean closest approach distance between charges of the same sign at temperature T, of order $\beta e^2/\epsilon_{\mathrm{solv}}$, to be small compared with the mean interparticle distance a. In other words, the coulombic coupling parameter Γ between charges of the fluid is negligible,

$$\Gamma \equiv \frac{\beta e^2}{\epsilon_{\mathrm{solv}} a} \propto \left(\frac{a}{\xi_D}\right)^2 \ll 1. \tag{55}$$

(The proportionality relation in (55) arises from definition (5).) The high-dilution condition (54) implies the weak-coupling condition $\Gamma^3 \ll 1$, if $\beta e^2/(\epsilon_{\mathrm{solv}}\sigma)$ is of order unity or smaller than 1.

In fact, conditions (54) and (55) can be realized in two different kinds of expansions in the density and temperature parameters. In the first situation, the density vanishes at fixed temperature; then the ratio between the pair energy at contact and the mean kinetic energy, $\beta e^2/(\epsilon_{\rm solv}\sigma)$, is also fixed, namely

$$\left(\frac{\sigma}{a}\right)^3 \propto \Gamma^3 \quad \text{case (1).} \tag{56}$$

In the second situation the density vanishes while the temperature goes to infinity, so that $\beta e^2/(\epsilon_{\rm solv}\sigma)$ also vanishes, namely

$$\Gamma^3 \ll \left(\frac{\sigma}{a}\right)^3 \quad \text{case (2).} \tag{57}$$

B. Expansions of resummed diagrams

The discussion of the Γ- and (σ/a)-expansions of the integrals associated with resummed Π diagrams is easier if we split the bond $F_{\rm R}$ into two pieces

$$F_{\rm R} = \frac{1}{2}[F^{\rm cc}]^2 + F_{\rm RT}. \tag{58}$$

(The notation $F_{\rm RT}$ refers to the truncation with respect to $F_{\rm R}$.) Diagrams built with bonds $F^{\rm cc}$, $[F^{\rm cc}]^2/2$ and $F_{\rm RT}$ – and with the same exclusion rule for bonds $F^{\rm cc}$ as in Π diagrams – will be called $\widetilde{\Pi}$. The Ursell function $h_{\alpha\alpha'}$ is represented in terms of $\widetilde{\Pi}$ diagrams by the same formula (32) as in the case of Π diagrams. The splitting (58) has already been used for a classical plasma in the vicinity of a dielectric wall in Ref.[3], and its use was detailed for quantum plasmas in the bulk in Refs.[22, 26].

For the sake of simplicity, the scaling analysis of diagrams is now discussed in the case of the bulk. The bulk screened potential ϕ_B obeys (28) far away from any boundary, where $\overline{\kappa}(x)$ no longer depends on x and coincides with the inverse Debye screening length $\kappa_{\rm D}$. Then, (28) is reduced to the usual Debye equation, and, since ϕ_B is a function of $|\mathbf{r}-\mathbf{r}'|$ that vanishes when $|\mathbf{r}-\mathbf{r}'|$ goes to infinity, it is equal to the well-known Debye potential $\phi_{\rm D}$,

$$\phi_{\rm B}(|\mathbf{r}-\mathbf{r}'|) = \phi_{\rm D}(|\mathbf{r}-\mathbf{r}'|) \equiv \frac{e^{-\kappa_{\rm D}|\mathbf{r}-\mathbf{r}'|}}{|\mathbf{r}-\mathbf{r}'|}. \tag{59}$$

The integrals of the diagrams with a single bond can be calculated explicitly, and their orders in Γ and σ/a are the following:

$$\int d\mathbf{r}'\, \rho_\alpha^{\rm B} F^{\rm cc}(\mathbf{r},\mathbf{r}') = \mathcal{O}(\Gamma^0) \tag{60}$$

and

$$\int d\mathbf{r}'\, \rho^{\mathrm{B}}_{\alpha} \frac{1}{2}[F^{\mathrm{cc}}]^2(\mathbf{r},\mathbf{r}') = \mathcal{O}(\Gamma^{3/2}), \tag{61}$$

where $\mathcal{O}(\Gamma^0)$ and $\mathcal{O}(\Gamma^{3/2})$ denote terms of orders unity and $\Gamma^{3/2}$, respectively. According to (31)

$$F_{\mathrm{RT}}(\mathbf{r},\mathbf{r}';\alpha,\alpha') = \begin{cases} -1 - F^{\mathrm{cc}}(\mathbf{r},\mathbf{r}') - \frac{1}{2}\left[F^{\mathrm{cc}}\right]^2(\mathbf{r},\mathbf{r}') & \text{if } |\mathbf{r}-\mathbf{r}'| < (\sigma_{\alpha}+\sigma_{\alpha'})/2 \\ \sum_{n=3}^{+\infty} \frac{1}{n!}\left[F^{\mathrm{cc}}\right]^n(\mathbf{r},\mathbf{r}') & \text{if } |\mathbf{r}-\mathbf{r}'| > (\sigma_{\alpha}+\sigma_{\alpha'})/2. \end{cases} \tag{62}$$

If we assume, for the sake of simplicity, that all particles have the same diameter σ, the expression F^{B}_{RT} of F_{RT} in the bulk leads to [23]

$$\begin{aligned} \int d\mathbf{r}'\, F^{B}_{\mathrm{RT}}(\mathbf{r},\mathbf{r}';\alpha,\alpha') = \;& -\frac{4\pi}{3}\sigma^3 + 2\pi\frac{\beta e^2 Z_{\alpha}Z_{\alpha'}}{\epsilon_{\mathrm{solv}}}\sigma^2 - 2\pi\left(\frac{\beta e^2 Z_{\alpha}Z_{\alpha'}}{\epsilon_{\mathrm{solv}}}\right)^2\sigma \\ & +\frac{2\pi}{3}\left(\frac{\beta e^2 Z_{\alpha}Z_{\alpha'}}{\epsilon_{\mathrm{solv}}}\right)^3\left[C+\ln(3\kappa_{\mathrm{D}}\sigma)\right] \\ & -4\pi\left(\frac{\beta e^2 Z_{\alpha}Z_{\alpha'}}{\epsilon_{\mathrm{solv}}}\right)^3\sum_{n=1}^{+\infty}\frac{(-1)^n}{(n+3)!n}\left(\frac{\beta e^2 Z_{\alpha}Z_{\alpha'}}{\epsilon_{\mathrm{solv}}\sigma}\right)^n + R_{\Gamma^{3/2}}, \end{aligned} \tag{63}$$

where $R_{\Gamma^{3/2}}$ denotes terms which are of relative order $\Gamma^{3/2}$ with respect to those written on the r.h.s. of (63). Therefore, since $\rho^{\mathrm{B}}_{\alpha}$ is of order $1/a^3$, at leading order $\int d\mathbf{r}'\, \rho^{\mathrm{B}}_{\alpha} F_{\mathrm{RT}}(\mathbf{r},\mathbf{r}')$ is a sum of terms with respective orders

$$\left(\frac{\sigma}{a}\right)^3, \quad \left(\frac{\sigma}{a}\right)^2\Gamma, \quad \frac{\sigma}{a}\Gamma^2, \quad \Gamma^3, \quad \Gamma^3\ln\left[\left(\frac{\sigma}{a}\right)^2\Gamma\right], \quad \text{and} \quad \Gamma^3 f\left(\frac{\beta e^2}{\epsilon_{\mathrm{solv}}\sigma}\right), \tag{64}$$

where $\beta e^2/(\epsilon_{\mathrm{solv}}\sigma) = \Gamma/(\sigma/a)$ and the function $f(u) \equiv \sum_{n=1}^{+\infty}(-1)^n u^n/[(n+3)!n]$ vanishes for $u=0$. The last term in (64) arises from the short-distance behavior of the Boltzmann factor, the explosion of which for oppositely charged species is prevented by the cut-off distance σ provided by the hard-core repulsion.

As already noticed in Paper I, the contributions from excluded-volume effects in the primitive model are not involved in F^{cc} but they are contained in F_{R}. Indeed, the potential ϕ solution of (28) describes resummed interactions between point charges at the centers of penetrable spheres, because it corresponds to the integral equation

$$\phi(\mathbf{r},\mathbf{r}') = v(\mathbf{r},\mathbf{r}') - \frac{\beta e^2}{\epsilon_{\mathrm{solv}}}\int d\mathbf{r}''\sum_{\alpha} Z^2_{\alpha}\rho_{\alpha}(x'')v(\mathbf{r},\mathbf{r}'')\phi(\mathbf{r}'',\mathbf{r}'). \tag{65}$$

We notice that, in the bulk, for the primitive model again, in a linearized mean-field Poisson-Boltzmann theory where excluded-volume spheres are taken into account [4], an extra Heaviside function $\theta[|\mathbf{r}''-\mathbf{r}'|-(\sigma_{\alpha''}+\sigma_{\alpha'})/2)]$ appears in an equation analogous to (65), and the effective interaction between two charges e_{α} and $e_{\alpha'}$ behaves as $e_{\alpha}e_{\alpha'}\exp\{-\kappa_{\mathrm{D}}[r-(\sigma_{\alpha}+\sigma_{\alpha'})/2)]\}/\left\{[1+\kappa_{\mathrm{D}}(\sigma_{\alpha}+\sigma_{\alpha'})/2]r\right\}$ at large relative distances r. The latter interaction is equal to $e_{\alpha}e_{\alpha'}\phi_{B}(r)$ up to a steric correction of order $(\kappa_{\mathrm{D}}\sigma)^2 \propto \Gamma(\sigma/a)^2$. This is also the case in the so-called DLVO theory

[24, 25] for another model where every charge is spread over the surface of the excluded-volume sphere instead of being concentrated at its center. In the corresponding effective interaction at large distances, the denominator of the steric factor which multiplies $\exp(-\kappa_{\mathrm{D}} r)/r$ takes the slightly different form $[1+\kappa_{\mathrm{D}}(\sigma_\alpha+\sigma_{\alpha'})/4]^2$. The order $\Gamma(\sigma/a)^2$ of this steric correction is one among the contributions listed in (64).

By using the variable change $\mathbf{r} \equiv \widetilde{\mathbf{r}}/\kappa_{\mathrm{D}}$, it can be shown that, when the number of internal points in a $\widetilde{\Pi}$ diagram increases, then the lowest order in Γ at which it contributes to various integrals also increases. (See e.g. Refs. [22] or [26].)

C. Scaling regimes

As shown in previous section, in the bulk the leading coupling correction is of order $\Gamma^{3/2}$, and the next correction without any steric contribution is of order Γ^3. The orders of the first corrections induced by steric effects involve σ/a and Γ through the combinations written in (64).

In the first scaling regime (56), all terms in (64) are of order Γ^3, and the leading correction is indeed provided by the correction of order $\Gamma^{3/2}$ arising only from Coulomb interactions for point charges in the Debye approximation. Moreover, we notice that in this regime, where the temperature T is fixed, $\Gamma^{3/2}$ is proportional to $\sqrt{\sum_\alpha \rho_\alpha^{\mathrm{B}} Z_\alpha^2}$: the density-expansions prove to involve powers of the square root of a linear combination of densities. (The appearance of such square roots instead of integer powers in density expansions is an effect of the long range of Coulomb interactions, which makes the infinite-dilution and vanishing-coupling limit singular.)

In the second case (57), $\beta e^2/(\epsilon_{\mathrm{solv}}\sigma)$ vanishes, and terms in (64) are of orders $(\sigma/a)^3$ and $(\sigma/a)^3$ times a function of $\beta e^2/(\epsilon_{\mathrm{solv}}\sigma)$ which tends to zero when $\beta e^2/(\epsilon_{\mathrm{solv}}\sigma)$ goes to zero. The explicit calculations will be performed in a subcase where the leading coupling correction of order $\Gamma^{3/2}$ is large compared with all corrections involving steric effects. This property is fulfilled if $(\sigma/a)^3/\Gamma^{3/2}$ goes to zero, and the corresponding subregime reads

$$\Gamma^3 \ll \left(\frac{\sigma}{a}\right)^3 \ll \Gamma^{3/2} \quad \text{subcase}\,(2). \tag{66}$$

In place of Γ, we shall use the parameter ε defined in (11), because the first coupling correction is of order

$$\Gamma^{3/2} \propto \varepsilon. \tag{67}$$

(See (55) and the definition (5) of κ_{D}.) In the first scaling regime, relation (56) can be written as $(\sigma/a)^3 \propto \varepsilon^2$. Then all terms in (64) are of order ε^2, $\varepsilon^2\ln\varepsilon$ and $\varepsilon^2 f(\beta e^2/(\epsilon_{\mathrm{solv}}\sigma))$, and the whole double expansion in powers of ε and σ/a

proves to be a series in integer powers of ε times some possible powers of $\ln\varepsilon$, at fixed $\beta e^2/(\epsilon_{\mathrm{solv}}\sigma)$. In the second regime, condition (57) reads $\varepsilon^2 \ll (\sigma/a)^3$ and the extra condition in (66) is $(\sigma/a)^3 \ll \varepsilon$.

In the following, the so-called "weak-coupling" regime refers to the scaling limits (12) or (13). Moreover the term "ε-expansions" refers to ε- and σ/a- expansions, as if they were always performed in the scaling regime (12).

D. Pair correlation at any distance in the weak-coupling limit

The scaling analysis of ε-expansions for resummed $\widetilde{\Pi}$ diagrams (see Section III B) shows that the ε-expansions of integrals involving I start at least at relative order ε. As a consequence, at any relative distance, the pair correlation $h^{(0)}_{\alpha\alpha'}$ in the infinite-dilution and vanishing-coupling limit arises only from the sum of Π diagrams with a single bond and where the screened potential ϕ is replaced by its leading value $\phi^{(0)}$: $h^{(0)}_{\alpha\alpha'} = F^{\mathrm{cc}\,(0)} + F^{(0)}_{\mathrm{R}}$. (In other words, only the graph with one bond F^{cc} in h^{cc} and the graph I in $h^{--}_{\alpha\alpha'}$ where I is replaced by F_{R} do contribute at finite distances: $h^{\mathrm{cc}\,(0)}_{\alpha\alpha'} = F^{\mathrm{cc}\,(0)}$, $h^{\mathrm{c}-\,(0)}_{\alpha\alpha'} = h^{-\mathrm{c}\,(0)}_{\alpha\alpha'} = 0$, and $h^{--\,(0)}_{\alpha\alpha'} = (1/2)\left[F^{\mathrm{cc}\,(0)}\right]^2 + F^{(0)}_{\mathrm{RT}} = F^{(0)}_{\mathrm{R}}$.) At any finite distance $|\mathbf{r}-\mathbf{r}'|$, $h^{(0)}_{\alpha\alpha'}$ reads

$$h^{(0)}_{\alpha\alpha'}(\mathbf{r},\mathbf{r}') = \theta\left(|\mathbf{r}-\mathbf{r}'| - \frac{\sigma_\alpha + \sigma_{\alpha'}}{2}\right)\exp\left[-\frac{\beta e^2}{\epsilon_{\mathrm{solv}}} Z_\alpha Z_{\alpha'} \phi^{(0)}(\mathbf{r},\mathbf{r}')\right] - 1. \tag{68}$$

In the bulk the inverse screening length $\overline{\kappa}$ in (28) does not depend on x, $\overline{\kappa} = \kappa_{\mathrm{D}}$ and $\phi^{(0)}_{\mathrm{B}} = \phi_{\mathrm{B}}$ given in (59), where ϕ_{B} obeys the Debye equation with the same boundary conditions as the bare Coulomb potential v_B far away from any vessel surface. Near the wall, since the density profiles created by interactions depend on the coupling strength, $\overline{\kappa}^2(x)$ has an ε-expansion, and so has $\phi(x,x',y)$. In the infinite-dilution and vanishing-coupling limit, $\overline{\kappa}^2(x)$ tends to κ^2_{D} and $\phi^{(0)}$ obeys Debye equation with the same boundary conditions as the bare Coulomb potential v, which take into account the dielectric response of the wall.

The large-distance behavior of $h_{\alpha\alpha'}$ at leading order, $h^{\mathrm{as}(0)}_{\alpha\alpha'}$, is equal to the large-distance behavior of $h^{(0)}_{\alpha\alpha'}$, namely

$$h^{\mathrm{as}\,(0)}_{\alpha\alpha'}(\mathbf{r},\mathbf{r}') = -\frac{\beta e^2}{\epsilon_{\mathrm{solv}}} Z_\alpha Z_{\alpha'} \phi^{(0)\,\mathrm{as}}(\mathbf{r},\mathbf{r}'). \tag{69}$$

In other words, since F_{R} decays only as the square of F^{cc}, in the diagrammatic representation $h^{\mathrm{as}\,(0)}_{\alpha\alpha'}$ arises only from the diagram with one bond F^{cc}, where ϕ is replaced by $\phi^{(0)}$. (The diagram with one bond F^{cc} is called $\widetilde{\Pi}_a$ in the following and is shown in Fig.7.) Subsequently, the first term in the ε-expansion of κ is

$$\kappa^{(0)} = \kappa_{\mathrm{D}}. \tag{70}$$

IV. BULK CORRELATIONS

In the bulk, the Ursell function $h_{\alpha\alpha'}$ decays exponentially fast in all directions [27]. In the high-dilution and weak-coupling regime, the leading tail at large distances is a monotonic exponential decay over the screening length $1/\kappa^{\mathrm{B}}$ (see Ref.[28] for a review), while damping might become oscillatory in regimes with higher densities, as expected from various approximate theories (see e.g. Refs.[13] and [29]).

The resummed Meeron diagrammatic expansions used in the present paper enable one to retrieve the existence of an exponential decay in the dilute regime. Indeed, all resummed Mayer diagrams Π are built with bonds F^{cc} (30) and F_{R} (31), the large-distance decays of which are ruled by the screened potential ϕ_{B} that is the solution of (28) in the bulk. By virtue of (59), ϕ_{B} falls off exponentially over the length scale $1/\kappa_{\mathrm{D}}$ defined in (5). The monotonic exponential decay of $h_{\alpha\alpha'}$ over the length scale $1/\kappa_{\mathrm{B}}$ in the dilute regime is expected to be given by partially resumming the tails of Π diagrams, which decrease exponentially over the scale $1/\kappa_{\mathrm{D}}$, though the convergence of the corresponding series is not controlled.

Before going into details, we introduce the following definitions. Let $f(r)$ be a rotationally invariant function that decays exponentially fast at large distances r. Let κ_{D} be the smallest inverse screening length in the exponential tails of f. f may contain several tails $\exp[-\kappa_{\mathrm{D}} r]/r^{\gamma}$ with various exponents γ's, which may be negative. We define the slowest of the exponential tails of f, denoted by $f^{\mathrm{slow}}(r)$ hereafter, as the sum of all tails $\exp(-\kappa_{\mathrm{D}} r)/r^{\gamma}$, with any exponent γ. In other words, $f^{\mathrm{slow}}(r)$ is the large-distance behavior with the largest screening length in the exponential and all possible powers of r. The notation $f^{\mathrm{as}}(r)$ will be restricted to the leading tail in the large-distance behavior of $f(r)$: $f^{\mathrm{as}}(r)$ is the leading term in $f^{\mathrm{slow}}(r)$, namely the contribution in $f^{\mathrm{slow}}(r)$ with the smallest exponent γ. For instance, as argued in Appendix A, if $f=\phi_{\mathrm{D}} * [\phi_{\mathrm{D}}]^2$, $f^{\mathrm{slow}}(r)=a\exp(-\kappa_{\mathrm{D}} r)/r$ and $f^{\mathrm{as}}=f^{\mathrm{slow}}$, whereas, if $f=\phi_{\mathrm{D}} * [\phi_{\mathrm{D}}]^2 * \phi_{\mathrm{D}}$, $f^{\mathrm{slow}}(r)=[b+cr]\exp(-\kappa_{\mathrm{D}} r)/r$ and $f^{\mathrm{as}}=c\exp(-\kappa_{\mathrm{D}} r)$.

A. Resummations of geometric series in Fourier space

The translational invariance in the bulk implies that the graph series in the decomposition (33)–(53) of $h_{\alpha\alpha'}$ are sums of convolutions. In Fourier space, they become geometric series which are resummed into compact formulae. $h^{\mathrm{cc\,B}}_{\alpha\alpha'}(k)$ merely reads

$$h^{\mathrm{cc\,B}}_{\alpha\alpha'}(k)=-\frac{\beta e^2}{\epsilon_{\mathrm{solv}}}Z_{\alpha}Z_{\alpha'}\frac{\phi_{\mathrm{D}}(k)}{1+\phi_{\mathrm{D}}(k)\overline{I}(k)}, \tag{71}$$

where

$$\phi_{\mathrm{D}}(k) = \frac{4\pi}{k^2 + \kappa_{\mathrm{D}}^2} \tag{72}$$

and

$$\overline{I}(k) \equiv \frac{\beta e^2}{\epsilon_{\mathrm{solv}}} \sum_{\gamma,\gamma'} \rho_\gamma^{\mathrm{B}} \rho_{\gamma'}^{\mathrm{B}} Z_\gamma Z_{\gamma'} I(k;\gamma,\gamma'). \tag{73}$$

$h_{\alpha\alpha'}^{\mathrm{cc\,B}}(k)$ is reduced to a fraction

$$h_{\alpha\alpha'}^{\mathrm{cc\,B}}(k) = -\frac{\beta e^2}{\epsilon_{\mathrm{solv}}} \frac{4\pi}{k^2 + \kappa_{\mathrm{D}}^2 + 4\pi\overline{I}(k)} Z_\alpha Z_{\alpha'}. \tag{74}$$

The same geometric series appears in the case of $h_{\alpha\alpha'}^{\mathrm{c-\,B}}$ and $h_{\alpha\alpha'}^{\mathrm{--\,B}}$ with the results

$$h_{\alpha\alpha'}^{\mathrm{c-\,B}}(k) = -\frac{\beta e^2}{\epsilon_{\mathrm{solv}}} \frac{4\pi}{k^2 + \kappa_{\mathrm{D}}^2 + 4\pi\overline{I}(\mathbf{k})} Z_\alpha \sum_{\gamma'} \rho_{\gamma'}^{\mathrm{B}} Z_{\gamma'} I(k;\gamma',\alpha') \tag{75}$$

and

$$h_{\alpha\alpha'}^{\mathrm{--\,B}}(k) = I(k;\alpha,\alpha') - \frac{\beta e^2}{\epsilon_{\mathrm{solv}}} \frac{4\pi}{k^2 + \kappa_{\mathrm{D}}^2 + 4\pi\overline{I}(k)} \sum_{\gamma} \rho_\gamma^{\mathrm{B}} Z_\gamma I(k;\gamma,\alpha) \sum_{\gamma'} \rho_{\gamma'}^{\mathrm{B}} Z_{\gamma'} I(k;\gamma',\alpha'). \tag{76}$$

Finally, $h_{\alpha\alpha'}^{\mathrm{B}}(k)$ takes the half factorized form

$$h_{\alpha\alpha'}^{\mathrm{B}}(k) = I(k;\alpha,\alpha') - \frac{\beta e^2}{\epsilon_{\mathrm{solv}}} \frac{4\pi}{k^2 + \kappa_{\mathrm{D}}^2 + 4\pi\overline{I}(k)} \left[Z_\alpha + \sum_{\gamma} \rho_\gamma^{\mathrm{B}} Z_\gamma I(k;\gamma,\alpha) \right] \left[Z_{\alpha'} + \sum_{\gamma'} \rho_{\gamma'}^{\mathrm{B}} Z_{\gamma'} I(k;\gamma',\alpha') \right]. \tag{77}$$

From this expression we readily get that $\sum_\alpha Z_\alpha \rho_\alpha^{\mathrm{B}} h_{\alpha\alpha'}^{\mathrm{B}}(k=0) = -Z_{\alpha'}$, which is another writing of the internal-screening sum rule (35) in the bulk case. (We also notice that the writing of $h_{\alpha\alpha'}^{\mathrm{B}}(k)$ in (77) is analogous to Eq.(2.110) of Ref.[30], where the authors consider the Feynman diagrammatics for a field theory, with some short-distance regularization, which modelizes a charge fluid.)

B. Large-distance behavior of bulk correlations

When the bulk Ursell function $h_{\alpha\alpha'}(\mathbf{r},\mathbf{r}')$ is only a function of $|\mathbf{r}-\mathbf{r}'|$ and decays faster than any inverse power of $|\mathbf{r}-\mathbf{r}'|$ when $|\mathbf{r}-\mathbf{r}'|$ becomes infinite, its large-distance behavior $h_{\alpha\alpha'}^{\mathrm{as}}(\mathbf{r},\mathbf{r}')$ is determined by the general formulas recalled in Appendix A. As checked at first order in ε in next Section, the singular points of $I(k;\gamma,\gamma')$ in the weak-coupling regime are more distant from the real axis in the upper complex half-plane $k = k' + ik"$ than the pole k_0 of the fraction $1/[k^2 + \kappa_{\mathrm{D}}^2 + \overline{I}(k)]$ that has the smallest positive imaginary part. Moreover, k_0 is purely imaginary, $k_0 = i\kappa_{\mathrm{B}}$, and k_0 is a pole of rank 1.

Therefore, in the weak-coupling regime, the slowest exponential tail of $h^{\rm B}_{\alpha\alpha'}$ is a purely $\exp(-\kappa_{\rm B} r)/r$ function, as well as the slowest exponential tails of $h^{\rm cc\,B}_{\alpha\alpha'}$, $h^{-{\rm c}\,{\rm B}}_{\alpha\alpha'}$, $h^{{\rm c}-\,{\rm B}}_{\alpha\alpha'}$ and $h^{--\,{\rm B}}_{\alpha\alpha'}$. By inserting the property

$$\mathrm{Res}\left[\frac{1}{k^2+\kappa_{\rm D}^2+4\pi\overline{I}(k)}\right]\Bigg|_{k=k_0} = \left[2k_0 + 4\pi \left.\frac{\partial\overline{I}(k)}{\partial k}\right|_{k_0}\right]^{-1} \tag{78}$$

into the general formula (A2) applied to $f = h_{\alpha\alpha'}$ given in (77) with $k_0 = i\kappa_{\rm B}$, we find that the large-distance behavior $h^{\rm B\,as}_{\alpha\alpha'}(r)$ of $h^{\rm B}_{\alpha\alpha'}(r)$ takes the form

$$h^{\rm B\,as}_{\alpha\alpha'}(r) = -\frac{\beta e^2}{\epsilon_{\rm solv}} Z^{\rm eff\,B}_{\alpha} Z^{\rm eff\,B}_{\alpha'} \frac{e^{-\kappa_{\rm B} r}}{r}, \tag{79}$$

where $i\kappa_{\rm B}$ is the pole of $1/[k^2+\kappa_{\rm D}^2+\overline{I}(k)]$ with the positive imaginary part, and

$$Z^{\rm eff\,B}_{\alpha} = \frac{Z_\alpha + \sum_\gamma \rho^{\rm B}_\gamma Z_\gamma I(i\kappa_{\rm B};\gamma,\alpha)}{\sqrt{1 - i(2\pi/\kappa_{\rm B})\partial\overline{I}(k)/\partial k|_{i\kappa_{\rm B}}}}. \tag{80}$$

C. Large-distance tail at order ε

According to the scaling analysis of Section III B, the first term in the ε-expansion of $I(k)$ is $I^{(1)}(k)$ with $I^{(1)} = [F^{\rm cc}]^2/2$. $\overline{I}^{(1)}$ is calculated from the definition (73) of $\overline{I}(k)$ with $I^{(1)}$ in place of I. By using

$$\left[\phi_{\rm D}^2\right](\mathbf{k}) = \frac{4\pi}{k}\arctan\left(\frac{k}{2\kappa_{\rm D}}\right) \tag{81}$$

and

$$\frac{1}{2}\left(\frac{\beta e^2}{\epsilon_{\rm solv}}\right)^3 \left(4\pi\sum_\gamma \rho^{\rm B}_\gamma Z^3_\gamma\right)^2 = \kappa_{\rm D}^3\varepsilon\left(\frac{\Sigma_3}{\Sigma_2}\right)^2, \tag{82}$$

where Σ_m is defined in (15), we get

$$4\pi\overline{I}^{(1)}(\mathbf{k}) = \varepsilon\,\kappa_{\rm D}^2\left(\frac{\Sigma_3}{\Sigma_2}\right)^2 \frac{\kappa_{\rm D}}{k}\arctan\left(\frac{k}{2\kappa_{\rm D}}\right). \tag{83}$$

$I^{(1)}$ and $\overline{I}^{(1)}(k)$ have a branch point at $k = 2i\kappa_{\rm D}$, while $\left[k^2+\kappa_{\rm D}^2+4\pi\overline{I}^{(1)}(k)\right]^{-1}$ has a pole at the value of k equal to

$$i\kappa_{\rm D}\left[1 + \frac{2\pi}{\kappa_{\rm D}^2}\overline{I}^{(1)}(i\kappa_{\rm D}) + o(\varepsilon)\right]. \tag{84}$$

The leading corrections involved in the notation $o(\varepsilon)$ are given in (64). The latter pole is closer to the real axis than the branch point at $k = i2\kappa_{\rm D}$. Therefore, at first order in ε, the singular point in $h^{B}_{\alpha\alpha'}(k)$ that is the closest one to the real axis in the upper complex half-plane of k is the pole of $1/[k^2+\kappa_{\rm D}^2+4\pi\overline{I}^{(1)}(k)]$.

The scenario of Section IV B does happen at leading order in ε and the large-distance behavior $h^{\rm B\,as}_{\alpha\alpha'}(r)$ up to order ε takes the form (79) where $k_0 = i[\kappa_{\rm D} + \delta\kappa^{(1)}_{\rm B}]$ with

$$\delta\kappa^{(1)}_{\rm B} = \frac{2\pi}{\kappa_{\rm D}}\overline{I}^{(1)}(i\kappa_{\rm D}). \tag{85}$$

According to (83) we find

$$\frac{\delta\kappa_{\mathrm{B}}^{(1)}}{\kappa_{\mathrm{D}}}=\varepsilon\left(\frac{\Sigma_3}{\Sigma_2}\right)^2\frac{\ln 3}{4}. \tag{86}$$

We retrieve the formula of Ref.[13] obtained from integral equations. It is reduced to the results obtained by Mitchell and Ninham through diagrammatic techniques for the one-component plasma [12] or for a two-component electrolyte [31]. (The formulae for the one-component plasma can be derived from those calculated for a two-component plasma with charges e_+ and e_- and densities ρ_+ and ρ_- by taking the limit where e_- vanishes while ρ_- diverges under the constraint $e_-\rho_- = -e_+\rho_+$.) The correction $\delta\kappa_{\mathrm{B}}^{(1)}$ vanishes in the case of a 1:1 electrolyte. If the electrolyte is not charge symmetric, the expression (86) shows that the screening length $1/\kappa^{\mathrm{B}}$ is a decreasing function of the coupling parameter ε at first order in ε.

The bulk effective charge $Z_\alpha^{\mathrm{eff\,B}}$ up to order ε is calculated by formula (80). The explicit result is written in (16). In view of the discussion of next Section, we rewrite $Z_\alpha^{\mathrm{eff\,B}}$ as

$$Z_\alpha^{\mathrm{eff\,B}}=Z_\alpha[1+A_\alpha^{(1)}+o(\varepsilon)]. \tag{87}$$

The amplitude (79) of $h_{\alpha\alpha'}^{\mathrm{B\,as}}(r)$ up to order ε can be rewritten as

$$h_{\alpha\alpha'}^{\mathrm{B\,as}}(r)=-\frac{\beta e^2}{\epsilon_{\mathrm{solv}}}\frac{Z_\alpha Z_{\alpha'}}{r}\left\{\left[1+A_\alpha^{(1)}+A_{\alpha'}^{(1)}\right]e^{-(\kappa_{\mathrm{D}}+\delta\kappa_{\mathrm{B}}^{(1)})r}+o(\varepsilon)\right\}. \tag{88}$$

To our knowledge, the amplitude of $h_{\alpha\alpha'}^{\mathrm{B\,as}}(r)$ for a multicomponent plasma has not been calculated in the litterature previously. In the limit of the one-component plasma, it is the same as that found by Mitchell and Ninham in Ref.[12] by a diagrammatic method.

We notice that the use of (80) with $\overline{I}^{(1)}$ in place of $\overline{I}$ is equivalent to replacing the diagrammatic series of $h_{\alpha\alpha'}^{\mathrm{cc\,B}}$, $h_{\alpha\alpha'}^{\mathrm{c-\,B}}$ and $h_{\alpha\alpha'}^{--\,\mathrm{B}}$ shown in Figs.1-3 by the corresponding series represented in Figs.4-6. As shown in Appendix B, the correction $\delta\kappa_{\mathrm{B}}^{(1)}$ to the screening length in $h^{\mathrm{cc\,B}}$, $h^{\mathrm{c-\,B}}$, and $h^{--\,\mathrm{B}}$ arises from the whole series in Figs.4, 5, and 6, respectively.

On the contrary, the first corrections to the effective bulk charges can be seen as arising from only a finite number of diagrams in Figs.4 and 5. This will be shown in next section. The property relies on the following rewriting of $h_{\alpha\alpha'}^{\mathrm{B\,as}}(r)$,

$$h_{\alpha\alpha'}^{\mathrm{B\,as}}(r)=-\frac{\beta e^2}{\epsilon_{\mathrm{solv}}}\frac{Z_\alpha Z_{\alpha'}}{r}\left\{\left[1+A_\alpha^{(1)}+A_{\alpha'}^{(1)}-\delta\kappa_{\mathrm{B}}^{(1)}r\right]e^{-\kappa_{\mathrm{D}}r}+o(\varepsilon)\right\}. \tag{89}$$

We point out that (89) is valid for any distance r. Indeed $\exp[-(\kappa_{\mathrm{D}}+\delta\kappa_{\mathrm{B}}^{(1)})r]=\left(1-\delta\kappa_{\mathrm{B}}^{(1)}r\right)\exp(-\kappa_{\mathrm{D}}r)+o(\varepsilon)$ for any distance, whereas $\exp[-(\kappa_{\mathrm{D}}+\delta\kappa_{\mathrm{B}}^{(1)})r]=\left[1-\delta\kappa_{\mathrm{B}}^{(1)}r+o(\varepsilon)\right]\exp(-\kappa_{\mathrm{D}}r)$ only for distances $r<L_{\max}\equiv\xi_D/\varepsilon^\nu$ with

$\nu < 1/2$. The condition $\nu < 1/2$ ensures that for $r < L_{\max}$ every n^{th} term with $n \geq 2$ in the expansion of the exponential $\exp[-\delta\kappa_{\text{B}}^{(1)} r]$ is indeed a correction, of order $\varepsilon^{n(1-\nu)} = o(\varepsilon)$, with respect to the $\mathcal{O}(\varepsilon^{1-\nu})$-term $\delta\kappa_{\text{B}}^{(1)} r$.

D. Alternative derivation of the bulk large-distance tail at order ε

In view of calculations in the vicinity of a wall, where the infinite series in $f = h^{\text{cc B}}$, $h^{\text{c}-\text{ B}}$ or $h^{--\text{ B}}$ can no longer be resummed in Fourier space, because of the lost of translational invariance in the direction perpendicular to the wall, we show how to retrieve the expression (88) for $h^{\text{B as}}_{\alpha\alpha'}$ in a less systematic way than the method involving the resummed formulae (79) and (80). (For the sake of simplicity we omit the indices α and α' for charge species in the notation f.)

In the general method of Sections IV A and IV B, we performed Fourier transforms, then we resummed the four infinite series $f = h^{\text{cc B}}$, $h^{\text{c}-\text{ B}}$, $h^{-\text{c B}}$, or $h^{--\text{ B}}$ that define $h^{\text{B}}_{\alpha\alpha'}$ through the graphs shown in Figs.1-3, and we got a compact formula for $h^{\text{B}}_{\alpha\alpha'}(k)$ from which we calculated the large-distance behavior $h^{\text{B as}}_{\alpha\alpha'}(r)$ of $h^{\text{B}}_{\alpha\alpha'}(r)$. Here, on the contrary, in each series f we formally calculate the slowest exponential tail $f^{\text{slow}}_m(r)$ of every graph f_m, with m bonds F^{cc}, directly in position space by using the residue theorem, and the large-distance behavior f^{as} of $f = h^{\text{cc}}$, $h^{\text{c}-}$, $h^{-\text{c}}$, or h^{--} is given by the sum (over m) of the slowest tails $f^{\text{slow}}_m(r)$'s in each case. (The slowest exponential tail is defined in the introduction of Section IV.)

The second procedure is more cumbersome, because the series sums $f(k)$'s have a pole of rank 1 at $k = i\kappa_{\text{B}}$ and their inverse Fourier transform decay as $\exp(-\kappa_{\text{B}} r)/r$, whereas each term $f_m(k)$ in the series has a multiple pole of rank m at $k = i\kappa_{\text{D}}$ and its inverse Fourier transform behaves as $\exp(-\kappa_{\text{D}} r)/r$ times a polynomial in r of degree $m-1$. We point out that, in the present ε-expansion of $f^{\text{as}}(r)$ around its $\exp[-\kappa_{\text{D}} r]/r$ limit behavior in the infinite-dilution and vanishing-coupling limit (where only the bond F^{cc} contributes), for every graph f_m we must retain the entire slowest tail f^{slow}_m – namely the entire polynomial in r –, and we only disregard tails $\exp[-l\kappa_{\text{D}} r]/r$ with $l \geq 2$. (See example in (A5).) The procedure is legitimate as long as dilution is sufficiently high. Details are given in Appendix B and we give only a summary in the present section.

1. *General structure of the ε-expansion of $h^{\text{as}}_{\alpha\alpha'}$*

As long as densities are low enough, the graph I decays faster than the bond F^{cc}, and, as shown in Appendix B, the slowest tail $f^{\text{slow}}_m(r)$ of $f_m(r)$ is equal to $\exp[-\kappa_{\text{D}} r]/r$ times a polynomial in r of rank $m-1$, $\sum_{p=0}^{m-1} F_{m,p} r^p$. As a consequence, the ε-expansion of the large-distance behavior of $h^{B}_{\alpha\alpha'}$ reads

$$h^{\mathrm{B\,as}}_{\alpha\alpha'}(r) = \frac{e^{-\kappa_{\mathrm{D}} r}}{r} \sum_{p=0}^{+\infty} r^p \, H_p(\alpha,\alpha';\varepsilon), \tag{90}$$

where the coefficient $H_p(\alpha,\alpha';\varepsilon)$ – which is the the sum of the contributions from $h^{\mathrm{cc\,B}}$, $h^{\mathrm{c-\,B}}$, $h^{\mathrm{-c\,B}}$, and $h^{\mathrm{--\,B}}$ – arises only from the graphs f_m with $m \geq p+1$ in the series representations shown in Figs.1-3. (We recall that ε is a short notation for parameters ε and σ/a in the scaling regimes (56) and (66), as explained at the end of Section III C.)

Moreover, according to the scaling analysis for ε-expansions in Section III B, all coefficients $F_{m,p}$ in the polynomial in the slowest tail of every graph f_m with $m \geq 1$ start at order ε^{n_0+m-1}, where $n_0 = 0$ if $f = h^{\mathrm{cc\,B}}$, $n_0 = 1$ if $f = h^{\mathrm{c-\,B}}$ or $h^{\mathrm{-c\,B}}$, and $n_0 = 2$ if $f = h^{\mathrm{--\,B}}$. Therefore, the ε-expansion of $H_p(\alpha,\alpha';\varepsilon)$ starts at order ε^p, and, after reversing the summation orders,

$$h^{\mathrm{B\,as}}_{\alpha\alpha'}(r) = \frac{e^{-\kappa_{\mathrm{D}} r}}{r} \sum_{q=0}^{+\infty} \varepsilon^q \sum_{p=0}^{q} r^p \, H_p^{(q)}(\alpha,\alpha') \tag{91}$$

with

$$H_q^{(q)}(\alpha,\alpha') = F^{(q)}_{q+1,q}\left(f = h^{\mathrm{cc\,B}}_{\alpha\alpha'}\right). \tag{92}$$

(91) displays that, in the ε-expansion of $h^{B\,\mathrm{as}}_{\alpha\alpha'}(r)$ around its $\exp[-\kappa_{\mathrm{D}} r]/r$ behavior in the limit where ε vanishes, the leading tail of $h^{\mathrm{B\,as}}_{\alpha\alpha'}(r)$ at order ε^q behaves as r^q times $\exp[-\kappa_{\mathrm{D}} r]/r$. Moreover, by virtue of (92), it coincides with the first term in the ε-expansion of the leading tail in the slowest exponential decay $f^{\mathrm{slow}}_{q+1}(r)$ of the graph f_{q+1} with $(q+1)$ bonds F^{cc} in $f = h^{\mathrm{cc\,B}}_{\alpha\alpha'}$.

2. Renormalization of the screening length

As shown in Appendix B, for each $f = h^{\mathrm{cc\,B}}$, $h^{\mathrm{c-\,B}}$, $h^{\mathrm{-c\,B}}$, or $h^{\mathrm{--\,B}}$, the sum $f^{\mathrm{as}\,\star}(r)$ of the leading tails at every order ε^{n_0+q} in the ε-expansion of $f^{\mathrm{as}}(r)$ around its lowest-order $\varepsilon^{n_0} \exp[-\kappa_{\mathrm{D}} r]/r$ limit can be performed explicitly. (Indeed, the coefficient $a_q^{(n_0+q)}\varepsilon^{n_0+q}$ of the leading $r^q \exp[-\kappa_{\mathrm{D}} r]/r$ tail at order ε^{n_0+q} in the ε-expansion of f^{as} coincides with the first term in the ε-expansion of the coefficient $F_{q+1,q}$ of the leading $r^q \exp[-\kappa_{\mathrm{D}} r]/r$ term in the slowest exponential decay $f^{\mathrm{slow}}_{q+1}(r)$ of the graph f_{q+1} with $(q+1)$ bonds F^{cc}, and the formal expression of $F_{q+1,q}$ in terms of I is given in (B7).) $f^{\mathrm{as}\,\star}(r)$ proves to be equal to $\exp[-\delta\kappa^{\star}_{\mathrm{B}}\, r]$ times $f_1^{\mathrm{as}(n_0)}$, the value at the first order ε^{n_0} of the large-distance behavior of the graph f_1 with only one bond F^{cc}. As a consequence, the sum $h^{\mathrm{B\,as}\,\star}_{\alpha\alpha'}(r)$ of the leading $r^q \exp[-\kappa_{\mathrm{D}} r]/r$

tails at every order ε^q in the ε-expansion of $h^{\mathrm{B\,as}}_{\alpha\alpha'}(r)$ around its lowest-order $\exp[-\kappa_{\mathrm{D}}r]/r$ limit, namely

$$h^{\mathrm{B\,as}\,\star}_{\alpha\alpha'}(r) \equiv \sum_{q=0}^{+\infty} H_q^{(q)}(\alpha,\alpha')\varepsilon^q r^q \frac{e^{-\kappa_{\mathrm{D}}r}}{r}, \tag{93}$$

reads

$$h^{\mathrm{B\,as}\,\star}_{\alpha\alpha'}(r) = F^{\mathrm{cc}\,(0)}(r)\, e^{-\delta\kappa_{\mathrm{B}}^{\star}\, r}. \tag{94}$$

It arises from the leading $\varepsilon^q r^q \exp[-\kappa_{\mathrm{D}}r]/r$ tails of $h^{\mathrm{cc\,B}}_{\alpha\alpha'}$ only.

Moreover, $\delta\kappa_{\mathrm{B}}^{\star}$ coincides with the first-order correction $\delta\kappa_{\mathrm{B}}^{(1)}$ to the bulk screening length (see (85)) calculated from the exact procedure of Section IV B,

$$\delta\kappa_{\mathrm{B}}^{\star} = \delta\kappa_{\mathrm{B}}^{(1)}. \tag{95}$$

Eventually, the resummation of the series of leading tails at every order in ε for $h^{\mathrm{cc\,B}}$ proves to be a way to retrieve the value of $\delta\kappa_{\mathrm{B}}^{(1)}$.

3. Diagrams with slowest exponential tails of order ε

As already seen in Section III D, diagram $\widetilde{\Pi}_a$ in Fig.7 is the only diagram whose slowest exponential tail (proportional to $\exp(-\kappa_{\mathrm{D}}r)/r$) has an amplitude of order $\varepsilon^0 \times \beta e^2/\epsilon_{\mathrm{solv}}$. Diagrams whose slowest exponential tails have amplitudes of order ε are diagrams $\widetilde{\Pi}_b$, $\widetilde{\Pi}_{b^\star}$ and $\widetilde{\Pi}_c$ shown in Figs.8 and 9 (which come from the series $h^{\mathrm{c}-}$, $h^{-\mathrm{c}}$ and h^{cc}, respectively, where I is replaced by $I^{(1)}$, as shown in Figs.4 and 5). The contribution of $\widetilde{\Pi}_b$ to $h^{\mathrm{B\,as}}_{\alpha\alpha'}(r)$ reads

$$-\frac{\beta e^2}{\epsilon_{\mathrm{solv}}} Z_\alpha Z_{\alpha'}^2 \varepsilon \frac{\Sigma_3}{\Sigma_2}\frac{\ln 3}{2}\frac{e^{-\kappa_{\mathrm{D}}r}}{r}, \tag{96}$$

while the contribution of $\widetilde{\Pi}_c$ is

$$-\frac{\beta e^2}{\epsilon_{\mathrm{solv}}} Z_\alpha Z_{\alpha'} \left[-\varepsilon\left(\frac{\Sigma_3}{\Sigma_2}\right)^2 \frac{\ln 3}{4}\kappa_{\mathrm{D}}r + 2\varepsilon\left(\frac{\Sigma_3}{\Sigma_2}\right)^2\left(\frac{1}{6}-\frac{\ln 3}{8}\right)\right]\frac{e^{-\kappa_{\mathrm{D}}r}}{r}. \tag{97}$$

Indeed, the contribution of diagram $\widetilde{\Pi}_b$ is proportional to the convolution $\phi_{\mathrm{D}} * [\phi_{\mathrm{D}}]^2$ calculated in (A3), while the diagram $\widetilde{\Pi}_c$ involves the convolution $\phi_{\mathrm{D}} * [\phi_{\mathrm{D}}]^2 * \phi_{\mathrm{D}}$, whose expression at any distance is given by (A5). We notice that the diagrams $\widetilde{\Pi}_b$, $\widetilde{\Pi}_{b^\star}$ and $\widetilde{\Pi}_c$ have already been calculated in the case of the electron gas [12].

By virtue of (96) and (97), the sum of the slowest exponential tails of diagrams $\widetilde{\Pi}_b$, $\widetilde{\Pi}_{b^\star}$ and $\widetilde{\Pi}_c$ coincides with the expression (89) of $h^{\mathrm{B\,as}}_{\alpha\alpha'}$ up to order ε, where $\delta\kappa_{\mathrm{B}}^{(1)}$ is given in (86) and

$$A_\alpha^{(1)} = Z_\alpha \overline{A}_{[b]}^{(1)} + A_{[c]}^{(1)} \tag{98}$$

with

$$\overline{A}^{(1)}_{[b]} = \varepsilon \frac{\Sigma_3}{\Sigma_2} \frac{\ln 3}{2} \tag{99}$$

and

$$A^{(1)}_{[c]} = \varepsilon \left(\frac{\Sigma_3}{\Sigma_2} \right)^2 \left(\frac{1}{6} - \frac{\ln 3}{8} \right) . \tag{100}$$

The $-\delta\kappa_{\mathrm{B}}^{(1)} r$ term in (89) comes from diagram $\widetilde{\Pi}_c$. The term $Z_\alpha \overline{A}^{(1)}_{[b]}$ $(Z_{\alpha'} \overline{A}^{(1)}_{[b]})$ proportional to Z_α $(Z_{\alpha'})$ in $A^{(1)}_\alpha$ comes from $\widetilde{\Pi}_b$ $(\widetilde{\Pi}_{b^\star})$, whereas the other term, $A^{(1)}_{[c]}$, arises from $\widetilde{\Pi}_c$.

Therefore, the constants $A^{(1)}_\alpha$ and $A^{(1)}_{\alpha'}$ are determined by the exponential tails of only three diagrams $\widetilde{\Pi}_b$, $\widetilde{\Pi}_{b^\star}$, and $\widetilde{\Pi}_c$. (See the comment after (89) for a comparison with the exact method of Section IV C.) Moreover, as a consequence of the analysis summarized in Section IV D 2, the coefficient of the r-term in the amplitude of the slowest tail of diagram $\widetilde{\Pi}_c$ with two F^{cc} bonds (See Fig.9) must coincide with the opposite of the first-order correction $\delta\kappa_{\mathrm{B}}^{(1)}$ in the inverse screening length.

E. Density-density and charge-charge correlation

By virtue of the bulk local charge neutrality,

$$\sum_\alpha e_\alpha \rho_\alpha^{\mathrm{B}} = 0, \tag{101}$$

the Fourier transform of the density-density correlation function takes the form

$$\sum_{\alpha,\alpha'} \rho_\alpha^{\mathrm{B}} \rho_{\alpha'}^{\mathrm{B}} h^{\mathrm{B}}_{\alpha\alpha'}(k) = \sum_{\alpha,\alpha'} \rho_\alpha^{\mathrm{B}} \rho_{\alpha'}^{\mathrm{B}} I(k;\alpha,\alpha') - \frac{\beta e^2}{\epsilon_{\mathrm{solv}}} \frac{4\pi}{k^2 + \kappa_{\mathrm{D}}^2 + 4\pi \overline{I}(k)} \left[\sum_\alpha \rho_\alpha^{\mathrm{B}} \sum_\gamma \rho_\gamma^{\mathrm{B}} Z_\gamma I(k;\gamma,\alpha) \right]^2 , \tag{102}$$

while the charge-charge structure factor, defined from (34),

$$C^{\mathrm{B}}(k) \equiv e^2 \left\{ \sum_\alpha \rho_\alpha^{\mathrm{B}} Z_\alpha^2 + \sum_{\alpha,\alpha'} \rho_\alpha^{\mathrm{B}} \rho_{\alpha'}^{\mathrm{B}} Z_\alpha Z_{\alpha'} h_{\alpha\alpha'}(k) \right\} , \tag{103}$$

reads

$$C^{\mathrm{B}}(k) = \frac{\epsilon_{\mathrm{solv}}}{4\pi\beta} \left\{ \kappa_{\mathrm{D}}^2 + 4\pi \overline{I}(k) - \frac{\left[\kappa_{\mathrm{D}}^2 + 4\pi \overline{I}(k) \right]^2}{k^2 + \kappa_{\mathrm{D}}^2 + 4\pi \overline{I}(k)} \right\} . \tag{104}$$

As announced in Subsection II C 1, the expression (104) of the charge-charge structure factor $C^{\mathrm{B}}(k)$ indeed obeys the sum rule (38), which summarizes both the internal-screening sum rule (36) and the external-screening sum rule (37). (If a phase transition gave rise to nonintegrable algebraic tails in $\overline{I}(r)$ and subsequent non-analytic terms of order k^η with $\eta \leq 0$ in the Fourier transform $\overline{I}(k)$, then $C^{\rm B}(k)$ would still vanish at $k = 0$, but the coefficient of the k^2-term would be different from the universal value in (38), as exhibited in the exactly-soluble spherical model of Ref.[32].)

We stress that the k^2-term in the Fourier expansion of $C^{\rm B}(k)$ is independent of the short-range potential $v_{SR}(|\mathbf{r} - \mathbf{r}|; \alpha, \alpha')$, which must be introduced in three dimensions in order to avoid the collapse under the attraction between charges with opposite signs. This property is a consequence of the internal screening rule [6], and it is retrieved from the structure of expression (104). On the contrary, the k^2-term in $\sum_{\alpha,\alpha'} \rho^{\rm B}_\alpha \rho^{\rm B}_{\alpha'} h^{\rm B}_{\alpha\alpha'}(k)$ given in (102) has not any universal value: it depends on the short-distance repulsion in the generic case. However, this is not the case for a symmetric 1:1 electrolyte in two-dimensions [34, 35], where the pure logarithmic Coulomb interaction needs not be regularized at short distances and is scale-invariant. Then, for point charges, scale-invariance arguments lead to a value of the dimensionless second-moment of $\sum_{\alpha,\alpha'} \rho^{\rm B}_\alpha \rho^{\rm B}_{\alpha'} h^{\rm B}_{\alpha\alpha'}(r)$ that depends only on the coupling parameter βe^2. We also notice that formulae (102) and (104) enable one to retrieve the leading low-density values of the coefficients of the k^2 and k^4 terms in the Fourier transforms of the density-density correlation and of the charge-charge structure factor derived for a symmetric 1:1 electrolyte in Ref.[33].

When there is no charge symmetry in the composition of the electrolyte, the same argument as that used in Section IV B implies that, according to (102) and (104), the large-distance behaviors of the density-density and charge-charge correlations in the high-dilution and weak-coupling regime are determined by the zero $k_0 = i\kappa_{\rm B}$ of $k^2 + \kappa_{\rm D}^2 + \overline{I}(k)$: they decay over the same screening length as the correlation $h^{\rm B}_{\alpha\alpha'}$.

In the case of a symmetric electrolyte made of two species with opposite charges $+Ze$ and $-Ze$ and with the same radii, $\sum_\alpha \rho^{\rm B}_\alpha \sum_\gamma \rho^{\rm B}_\gamma Z_\gamma I(\mathbf{k}; \gamma, \alpha)$ vanishes by virtue of the local neutrality (101) and of the symmetries ($I(\mathbf{k}; ++) = I(\mathbf{k}; --)$ and $I(\mathbf{k}; +-) = I(\mathbf{k}; -+)$). As a consequence, $\sum_\alpha \rho^{\rm B}_\alpha h_{\alpha\alpha'}(r)$ and $\sum_{\alpha,\alpha'} \rho^{\rm B}_\alpha \rho^{\rm B}_{\alpha'} h_{\alpha\alpha'}(r)$ decay as $I(r; \alpha, \alpha')$ by virtue of (102). $I(r; \alpha, \alpha')$ is expected to decay over the length $1/(2\kappa_{\rm B})$, by analogy with the infinite-dilution and vanishing-coupling limit where it behaves as the diagram $[F^{\rm cc}]^2/2$, which falls off over the scale $1/(2\kappa_{\rm D})$. Therefore, in this peculiar case, the "screening" length of the density-density correlation is expected to be $1/(2\kappa_{\rm B})$ at low density, in agreement with the result of Ref.[33].

V. SCREENED POTENTIAL ALONG THE WALL

A. Formal expression of the screened potential

Near the plane dielectric wall located at $x = 0$, interactions create density profiles and (28) is an inhomogeneous Debye equation, where the inverse squared screening length $\overline{\kappa}^2$ depends on the distance x to the wall. Moreover, $\phi(\mathbf{r}, \mathbf{r}')$ obeys the same boundary conditions as $v(\mathbf{r}, \mathbf{r}')$ (defined after (20)),

$$\lim_{x \to 0^-} \frac{\epsilon_{\mathrm{W}}}{\epsilon_{\mathrm{solv}}} \frac{\partial \phi}{\partial x}(\mathbf{r}, \mathbf{r}') = \lim_{x \to 0^+} \frac{\partial \phi}{\partial x}(\mathbf{r}, \mathbf{r}') \tag{105}$$

and

$$\lim_{x \to b^-} \frac{\partial \phi}{\partial x}(\mathbf{r}, \mathbf{r}') = \lim_{x \to b^+} \frac{\partial \phi}{\partial x}(\mathbf{r}, \mathbf{r}'), \tag{106}$$

since particles are made of a material with the same dielectric constant as the solvent. In order to take advantage of the invariance along directions parallel to the wall, we introduce the Fourier transform with respect to the $\mathbf{y}$ variable, and we write

$$\phi(x, x', \mathbf{y}) = \kappa_{\mathrm{D}} \int \frac{d^2\mathbf{q}}{(2\pi)^2}\, e^{-i\mathbf{q}\cdot(\kappa_{\mathrm{D}}\mathbf{y})} \widetilde{\phi}(\kappa_{\mathrm{D}} x, \kappa_{\mathrm{D}} x'; \mathbf{q}). \tag{107}$$

In the following, the tilde index denotes dimensionless quantities, such as the Fourier transform $\widetilde{\phi}(\kappa_{\mathrm{D}} x, \kappa_{\mathrm{D}} x'; \mathbf{q})$ and the dimensionless coordinate $\widetilde{x} \equiv \kappa_{\mathrm{D}} x$.

The solution of the inhomogeneous Debye equation (28) requires one to distinguish only three regions: region I for $x < 0$, region II for $0 < x < b$ and region III for $b < x$. In regions I and II, $\overline{\kappa}(x)$ vanishes by virtue of (29). According to (28), the dimensionless Fourier transform $\widetilde{\phi}(\widetilde{x}, \widetilde{x}'; \mathbf{q})$ obeys a one-dimensional differential equation. When $x' > b$ it reads

$$\left\{ \frac{\partial^2}{\partial \widetilde{x}^2} - \mathbf{q}^2 \right\} \widetilde{\phi}(\widetilde{x}, \widetilde{x}'; \mathbf{q}) = 0 \quad \text{if } \widetilde{x} < \widetilde{b}. \tag{108}$$

The solution with boundary conditions (105) and (106) is

$$\widetilde{\phi}(\widetilde{x}, \widetilde{x}', |\mathbf{q}|) = \begin{cases} B(\widetilde{x}', |\mathbf{q}|)\,(1 - \Delta_{\mathrm{el}})\, e^{|\mathbf{q}|\widetilde{x}} & \text{if } \quad \widetilde{x} < 0, \\ B(\widetilde{x}', |\mathbf{q}|)\, \left[e^{|\mathbf{q}|\widetilde{x}} - \Delta_{\mathrm{el}} e^{-|\mathbf{q}|\widetilde{x}} \right] & \text{if } 0 < \widetilde{x} < \widetilde{b}. \end{cases} \tag{109}$$

(A similar equation is solved in Ref.[2] with a misprint in Eq.(4.20).)

In region III, when x goes to $+\infty$, $\overline{\kappa}(x)$ tends to the inverse Debye length κ_{D}^{-1} (5), and we rewrite the Fourier transform of (28) as

$$\left\{ \frac{\partial^2}{\partial \widetilde{x}^2} - \left(1 + \mathbf{q}^2\right) - U(\widetilde{x}) \right\} \widetilde{\phi}(\widetilde{x}, \widetilde{x}'; \mathbf{q}) = -4\pi\delta(\widetilde{x} - \widetilde{x}') \quad \text{if } \widetilde{x} > \widetilde{b} \tag{110}$$

with

$$U(\widetilde{x}) \equiv \frac{4\pi\beta e^2}{\epsilon_{\text{solv}}\kappa_{\text{D}}^2}\sum_\alpha Z_\alpha^2[\rho_\alpha(x) - \rho_\alpha^{\text{B}}]. \tag{111}$$

The solution of the one-dimensional equation (110) can be written in terms of the solutions h of the associated "homogeneous" equation (with a zero in place of the Dirac distribution) which is valid for $-\infty < x < +\infty$. Indeed, the general solution of (110) for $x > b$ and $x' > b$ is the following sum: a linear combination of two independent solutions h^+ and h^- plus a particular solution ϕ_{sing} of (110), which is singular when $x = x'$ and which is calculated in terms of h^+ and h^- by the so-called Wronskian method [36]. In the following, h^+ (h^-) is chosen to be a solution which vanishes (diverges) when x tends to $+\infty$. In the bulk, $\overline{\kappa}(x)$ is a constant equal to the inverse Debye length κ_{D}: h^+ and h^- can be chosen to be equal to $\exp[\mp x\sqrt{1+\mathbf{q}^2}]$. When $\overline{\kappa}$ depends on x, we look for the solutions h^+ and h^- in terms of the bulk solutions as

$$e^{\mp\widetilde{x}\sqrt{1+\mathbf{q}^2}}[1 + H^\pm(\widetilde{x}, \mathbf{q}^2)]. \tag{112}$$

Moreover, the particular solutions H^+ and H^- can be chosen to vanish at $\widetilde{x} = \widetilde{b}$. As shown in Ref.[3], when $\widetilde{x} > b$ and $\widetilde{x}' > b$

$$\widetilde{\phi}(\widetilde{x}, \widetilde{x}', \mathbf{q}) = \widetilde{\phi}_{\text{sing}}(\widetilde{x}, \widetilde{x}', \mathbf{q}^2) + Z(|\mathbf{q}|)e^{-(\widetilde{x}+\widetilde{x}')\sqrt{1+\mathbf{q}^2}}[1 + H^+(\widetilde{x}, \mathbf{q}^2)][1 + H^+(\widetilde{x}', \mathbf{q}^2)] \tag{113}$$

and

$$\widetilde{\phi}_{\text{sing}}(\widetilde{x}, \widetilde{x}', q) = -\frac{4\pi}{W(\mathbf{q}^2)}e^{-|\widetilde{x}-\widetilde{x}'|\sqrt{1+\mathbf{q}^2}}[1 + H^-(\inf(\widetilde{x}, \widetilde{x}'), \mathbf{q}^2)][1 + H^+(\sup(\widetilde{x}, \widetilde{x}'), \mathbf{q}^2)], \tag{114}$$

where $\inf(\widetilde{x}, \widetilde{x}')$ ($\sup(\widetilde{x}, \widetilde{x}')$) is the infimum (supremum) of $\widetilde{x}$ and $\widetilde{x}'$. Since H^+ and H^- vanish at $\widetilde{x} = \widetilde{b}$, $\partial H^-/\partial\widetilde{x}|_{\widetilde{x}=\widetilde{b}}$ is also equal to zero, as can be checked from the formal solutions given in next paragraph. Therefore the Wronskian $W(\mathbf{q}^2)$ takes the simple form

$$W(\mathbf{q}^2) = -2\sqrt{1+\mathbf{q}^2} + \left.\frac{\partial H^+(\widetilde{x}, \mathbf{q}^2)}{\partial\widetilde{x}}\right|_{\widetilde{x}=\widetilde{b}}. \tag{115}$$

For the same reasons, the value of $Z(|\mathbf{q}|)$ depends only on $\partial H^+/\partial\widetilde{x}|_{\widetilde{x}=\widetilde{b}}$. Indeed, $Z(|\mathbf{q}|)$ is entirely determined by the ratio of the continuity equations (105) and (106) obeyed by $\widetilde{\phi}$ and $\partial\widetilde{\phi}/\partial\widetilde{x}$ at $\widetilde{x} = \widetilde{b}$, and the amplitude $B(\widetilde{x}', |\mathbf{q}|)$ in region $0 < \widetilde{x} < \widetilde{b}$ (see (109)) disappears in the latter ratio.

As shown in Ref.[3], H^+ can be represented by a formal alternating series, which will be used in the following,

$$H^+(\widetilde{x}, \mathbf{q}^2) = -\mathcal{T}^+[1](\widetilde{x}; \mathbf{q}^2) + \mathcal{T}^+\left[\mathcal{T}^+[1]\right](\widetilde{x}; \mathbf{q}^2) - \cdots, \tag{116}$$

where the operator $\mathcal{T}^+$ acting on a function $f(\widetilde{x})$ reads

$$\mathcal{T}^+[f](\widetilde{x};\mathbf{q}^2) \equiv \int_{\widetilde{b}}^{\widetilde{x}} dv\, e^{2\sqrt{1+\mathbf{q}^2}\,v} \int_v^{+\infty} dt\, e^{-2\sqrt{1+\mathbf{q}^2}\,t}\, U(t) f(t). \tag{117}$$

Similarly $H^-(\widetilde{x},\mathbf{q}^2)$ is equal to the series

$$H^-(\widetilde{x},\mathbf{q}^2) = \mathcal{T}^-[1](\widetilde{x};\mathbf{q}^2) + \mathcal{T}^-\left[\mathcal{T}^-[1]\right](\widetilde{x};\mathbf{q}^2) + \cdots \tag{118}$$

with

$$\mathcal{T}^-[f](\widetilde{x};\mathbf{q}^2) \equiv \int_{\widetilde{b}}^{\widetilde{x}} dv\, e^{-2\sqrt{1+\mathbf{q}^2}\,v} \int_{\widetilde{b}}^{v} dt\, e^{2\sqrt{1+\mathbf{q}^2}\,t}\, U(t) f(t). \tag{119}$$

In the infinite-dilution and vanishing-coupling limit, density profiles become uniform and $\overline{\kappa}^2(x)$ tends to κ_{D}^2. The corresponding screened potential $\phi^{(0)}$ obeys the Debye equation and satisfies the same boundary conditions as the bare Coulomb potential v. In other words, H^+ and H^- in expressions (113) vanish for $\widetilde{\phi}^{(0)}(\widetilde{x},\widetilde{x}',\mathbf{q})$ according to their definitions (112), while the expression (115) is reduced to $-2\sqrt{1+\mathbf{q}^2}$ for $W^{(0)}(\mathbf{q}^2)$. $Z^{(0)}(|\mathbf{q}|)$ is then determined by the continuity equations (105) and (106). The result reads

$$\phi^{(0)}(x,x',\mathbf{y}) = \phi^{(0)}_{\mathrm{sing}}(\mathbf{r}-\mathbf{r}') + \kappa_{\mathrm{D}} \int \frac{d^2\mathbf{q}}{(2\pi)^2}\, e^{-i\mathbf{q}\cdot(\kappa_{\mathrm{D}}\mathbf{y})} Z^{(0)}(|\mathbf{q}|) e^{-(\widetilde{x}+\widetilde{x}')\sqrt{1+\mathbf{q}^2}}, \tag{120}$$

where

$$Z^{(0)}(|\mathbf{q}|) = \frac{2\pi}{\sqrt{1+\mathbf{q}^2}} e^{2\widetilde{b}\sqrt{1+\mathbf{q}^2}} \frac{1-\Delta_{\mathrm{el}} e^{-2\widetilde{b}|\mathbf{q}|}(\sqrt{1+\mathbf{q}^2}+|\mathbf{q}|)^2}{(\sqrt{1+\mathbf{q}^2}+|\mathbf{q}|)^2 - \Delta_{\mathrm{el}} e^{-2\widetilde{b}|\mathbf{q}|}}. \tag{121}$$

The particular solution $\phi^{(0)}_{\mathrm{sing}}(\mathbf{r}-\mathbf{r}')$ that is singular when $\mathbf{r}=\mathbf{r}'$ coincides with the bulk screened potential in Debye theory,

$$\begin{aligned}\phi^{(0)}_{\mathrm{sing}}(\mathbf{r}-\mathbf{r}') = {} & \kappa_{\mathrm{D}} \int \frac{d^2\mathbf{q}}{(2\pi)^2}\, e^{-i\mathbf{q}\cdot(\kappa_{\mathrm{D}}\mathbf{y})} \frac{2\pi}{\sqrt{1+\mathbf{q}^2}} e^{-|\widetilde{x}-\widetilde{x}'|\sqrt{1+\mathbf{q}^2}} \\ = {} & \phi_{\mathrm{D}}(\mathbf{r}-\mathbf{r}')\end{aligned} \tag{122}$$

where ϕ_{D} is written in (59).

B. Large-distance tail of the screened potential

When $x > b$ and $x' > b$, $\phi(x,x',\mathbf{y})$ falls off as $1/y^3$, because of the boundary conditions at the interface $x = b$. The reason is the following. The appearance of an $1/y^3$ tail in the large-y behavior of a function $f(\mathbf{y})$ corresponds to the existence of a term proportional to $|\mathbf{q}|$, which is not analytical in the Cartesian components of $\mathbf{q}$, in the small-$\mathbf{q}$

expansion of $f(\mathbf{q})$ [37]. Functions different from $Z(\mathbf{q})$ in $\widetilde{\phi}(\widetilde{x},\widetilde{x}',\mathbf{q})$ [see (113)] prove to be functions of $\mathbf{q}^2$, but the boundary conditions at $\widetilde{x}=\widetilde{b}$ imply that, as well as the small-$\mathbf{q}$ expansion of $\widetilde{\phi}(\widetilde{x},\widetilde{x}',\mathbf{q})$ when $\widetilde{x}<\widetilde{b}$ (and $\widetilde{x}'>\widetilde{b}$) [see (109)], the small-$\mathbf{q}$ expansion of $Z(\mathbf{q})$ contains a term proportional to $|\mathbf{q}|$.

As shown in Paper I, the $1/y^3$ tail of ϕ takes the product structure (3) where

$$\overline{D}_\phi(x)=-\sqrt{\frac{(-B_Z)}{2\pi}}\,\frac{e^{-\widetilde{x}}}{\kappa_{\rm D}}[1+H^+(\widetilde{x},\mathbf{q}^2=\mathbf{0})]. \tag{123}$$

In (123) B_Z is the coefficient of the $|\mathbf{q}|$-term in the small-$\mathbf{q}$ expansion of $Z(|\mathbf{q}|)$,

$$Z(|\mathbf{q}|)=Z(\mathbf{q}=\mathbf{0})+B_Z|\mathbf{q}|+O(|\mathbf{q}|^2). \tag{124}$$

We notice that, as shown in Paper I, sum rules obeyed by $\phi(x,x',y)$ imply that $\overline{D}_\phi(x)$ has the same sign for all x's, and the $1/y^3$ tail of $\phi(x,x',y)$ is repulsive at all distances x and x' from the wall. In (123) the minus sign in front of the square root is *a priori* arbitrary. It has been introduced, because in the infinite-dilution and vanishing-coupling limit and in the case of a plain wall ($\epsilon_W=\epsilon_{\rm solv}$), $\overline{D}_\phi(x)$ is expected to have the same sign as the dipole $d(x)$ carried by the set made of a positive unit charge and its screening cloud repelled from the wall, and $H^+(\widetilde{x},\mathbf{q}^2=\mathbf{0})$ vanishes in this limit.

The large-distance behavior of $\phi(x,x',y)$ at leading order, $\phi^{{\rm as}\,(0)}$, is equal to the leading tail $\phi^{(0)\,{\rm as}}$ of $\phi^{(0)}$: $\phi^{{\rm as}\,(0)}=\overline{D}_\phi^{(0)}(x)\overline{D}_\phi^{(0)}(x')/y^3$ with $\overline{D}_\phi^{(0)}=\overline{D}_{\phi^{(0)}}$. $\overline{D}_{\phi^{(0)}}(x)$ is given by (123), where H^+ vanishes and B_Z is calculated for $\phi^{(0)}$, namely, $B_Z^{(0)}$ is equal to the coefficient of the $|\mathbf{q}|$-term in the small-$\mathbf{q}$ expansion of $Z_{\phi^{(0)}}(\mathbf{q})\equiv Z^{(0)}(\mathbf{q})$. According to (121)

$$Z^{(0)}(|\mathbf{q}|)=2\pi e^{2\widetilde{b}}\left[1-2\frac{\epsilon_W}{\epsilon_{\rm solv}}|\mathbf{q}|\right]+O(|\mathbf{q}|^2) \tag{125}$$

and the resulting expression for $\overline{D}_{\phi^{(0)}}$ is written in (7). The expression of the distance $y_\star^{(0)}(x)$ at which the $1/y^3$ tail in $\phi^{(0)}$ overcomes the exponential tails in $\phi^{(0)}$ has been estimated in Paper I. In the case where the solvent is water and where the dielectric wall is made of glass, $\epsilon_W/\epsilon_{\rm solv}\sim 1/80$ and $y_\star^{(0)}(x=b)=7\xi_D$, $y_\star^{(0)}(x=b+\xi_D)=10\xi_D$, $y_\star^{(0)}(x=b+3\xi_D)=15\xi_D$ and $y_\star^{(0)}(x=b+5\xi_D)=20\xi_D$.

C. Large-distance tail of the screened potential up to order ε

1. *Formal ε-expansion of the tail*

Because of the nonuniformity of the density profiles in the vicinity of the wall, ϕ has an ε-expansion. More precisely, the ε-expansion of the screened potential ϕ originating from the ε-expansion of density profiles can be determined by

(113) from the ε-expansion of the functions H^+ and H^-, which themselves are derived from the formal series (116) and (118) respectively.

According to (123) and with the notations of (4), the first correction $\overline{D}_\phi^{(1)}(x)$ in the ε-expansion of $\overline{D}_\phi(x)$ is obtained from $H^{+(1)}(\widetilde{x}, \mathbf{q}^2 = 0)$ and from the ε-expansion of the coefficient of $|\mathbf{q}|$ in the small-$\mathbf{q}$ expansion (124) of $Z(|\mathbf{q}|)$, $B_Z = B_Z^{(0)} + B_Z^{(1)} + o(\varepsilon)$. It reads

$$\overline{D}_\phi^{(1)}(x) = \overline{D}_\phi^{(0)}(x)\left[C_\phi^{(1)} + \overline{G}_\phi^{\exp\,(1)}(\widetilde{x})\right], \tag{126}$$

where the constant $C_\phi^{(1)}$ is equal to

$$C_\phi^{(1)} = \frac{B_Z^{(1)}}{2B_Z^{(0)}} + \lim_{\widetilde{x}\to+\infty} H^{+\,(1)}(\widetilde{x}, \mathbf{q}^2 = 0), \tag{127}$$

and the function $\overline{G}_\phi^{\exp\,(1)}(\widetilde{x})$, which vanishes exponentially fast when $\widetilde{x}$ goes to infinity, is

$$\overline{G}_\phi^{\exp\,(1)}(\widetilde{x}) = H^{+\,(1)}(\widetilde{x}, \mathbf{q}^2 = 0) - \lim_{\widetilde{x}\to+\infty} H^{+\,(1)}(\widetilde{x}, \mathbf{q}^2 = 0). \tag{128}$$

If we write the ε-expansion of $Z(|\mathbf{q}|)$ up to order ε as $Z(|\mathbf{q}|) = Z^{(0)}(|\mathbf{q}|) + Z^{(1)}(|\mathbf{q}|) + o(\varepsilon)$, then $B_Z^{(0)} = B_{Z^{(0)}}$ and $B_Z^{(1)} = B_{Z^{(1)}}$. By virtue of (125), $B_{Z^{(0)}} = -4\pi(\epsilon_W/\epsilon_{\text{solv}})\exp(2\widetilde{b})$. As already mentioned in Section V A, $Z(|\mathbf{q}|)$, and subsequently B_Z, is entirely determined from the expression of $\partial H^+/\partial\widetilde{x}$ at $\widetilde{x} = \widetilde{b}$ by the ratio of the continuity equations (105) and (106). When the ε-expansions of $Z(|\mathbf{q}|)$ and $\partial H^+/\partial\widetilde{x}|_{\widetilde{b}}$ up to order ε are introduced in the expression (113) of $\widetilde{\phi}(\widetilde{x}, \widetilde{x}', \mathbf{y})$, the continuity equations at $\widetilde{x} = \widetilde{b}$ lead to

$$\begin{aligned} Z^{(1)}(|\mathbf{q}|) = \quad & Z^{(0)}(|\mathbf{q}|)\left.\frac{\partial H^+(\widetilde{x}, \mathbf{q}^2)}{\partial\widetilde{x}}\right|_{\widetilde{x}=\widetilde{b}}^{(1)} \times \frac{1}{2\sqrt{1+\mathbf{q}^2}} \\ \times \quad & \frac{3\sqrt{1+\mathbf{q}^2} + |\mathbf{q}| - \Delta_{\text{el}}e^{-2\widetilde{b}|\mathbf{q}|}(3\sqrt{1+\mathbf{q}^2} - |\mathbf{q}|)}{\sqrt{1+\mathbf{q}^2} + |\mathbf{q}| - \Delta_{\text{el}}e^{-2\widetilde{b}|\mathbf{q}|}(\sqrt{1+\mathbf{q}^2} - |\mathbf{q}|)}. \end{aligned} \tag{129}$$

Then the coefficient $B_{Z^{(1)}}$ of the $|\mathbf{q}|$-term in the $\mathbf{q}$-expansion of $Z^{(1)}(|\mathbf{q}|)$ is determined by using (125), and the expression of $C_\phi^{(1)}$ is given by (127) where

$$\frac{B_Z^{(1)}}{2B_Z^{(0)}} = \left.\frac{\partial H^+(\widetilde{x}, \mathbf{q}^2 = 0)}{\partial\widetilde{x}}\right|_{\widetilde{x}=\widetilde{b}}^{(1)}. \tag{130}$$

The expression of $H^{+(1)}(\kappa_{\text{D}}x, \mathbf{q}^2 = 0)$ is calculated from $\sum_\alpha Z_\alpha^2\rho_\alpha(x)$ as the term of order ε in the ε-expansion of the formal series (116). The first term in the latter series reads

$$\mathcal{T}^+[1](\widetilde{x}; \mathbf{q}^2) = \int_{\widetilde{b}}^{\widetilde{x}} dv\, e^{2\,v\sqrt{1+\mathbf{q}^2}} \int_v^{+\infty} dt\, e^{-2\,t\sqrt{1+\mathbf{q}^2}} \left[\frac{\overline{\kappa}^2(t/\kappa_{\text{D}})}{\kappa_{\text{D}}^2} - 1\right]. \tag{131}$$

As shown in next section, the contribution to $\overline{\kappa}^2(x)$ from each species varies over two length scales, $\beta e^2/\epsilon_{\text{solv}}$ (times Z_α^2) and $1/\kappa_{\text{D}}$. Therefore, $\mathcal{T}^+[1](\widetilde{x}; \mathbf{q})$, as well as all other terms in the series (116), can be expanded in powers of the ratio $2\varepsilon = \kappa_{\mathrm{D}}\beta e^2/\epsilon_{\mathrm{solv}}$ of these two lengths. As shown in Ref.[3], for an operator $\mathcal{T}^+$ associated with a function similar to $\overline{\kappa}^2(x)$, the ε-expansion of $\mathcal{T}^+[1](\widetilde{x};\mathbf{q})$ starts at order ε (for any value of $\widetilde{b}$), and the ε-expansions of next terms in the formal series (116) are of larger order in ε. Therefore $H^{+(1)}$ is reduced to the contribution from $\mathcal{T}^+[1]$

$$H^{+(1)}(\widetilde{x},\mathbf{q}^2) = -\,\mathcal{T}^+[1](\widetilde{x};\mathbf{q})\big|^{(1)}. \tag{132}$$

Similarly, $\partial H^+/\partial\widetilde{x}|^{(1)}_{\widetilde{x}=\widetilde{b}} = -\,\partial\mathcal{T}^+[1](\widetilde{x};\mathbf{q})/\partial x|^{(1)}$. We notice that the latter derivative originates both from the derivative of $\mathcal{T}^+[1](\widetilde{x};\mathbf{q})|^{(1)}$ and of $\mathcal{T}^+[1](\widetilde{x};\mathbf{q})|^{(2)}$, because the latter term can be written as ε times a function of the two arguments $\widetilde{x}$ and $\widetilde{x}/\varepsilon$ (see Appendix C). Similar results hold for $H^{-(1)}$, with $H^{-(1)}(\widetilde{x},\mathbf{q}^2) = \mathcal{T}^-[1](\widetilde{x};\mathbf{q})|^{(1)}$.

2. ε-expansion of density profiles

The density profiles in the vicinity of a dielectric wall have been calculated in the high-dilution and weak-coupling regime in Refs.[3] and [2]. (The systematic approach in [3] is based on the Mayer diagrammatics for the fugacity expansions of density profiles. Resummations of Coulomb divergences are performed along a scheme which is similar to – but more complicated than – the procedure used in Section II B, because of differences in the topological definition of Mayer diagrams in the two cases.) Up to corrections of first order in the coupling parameter ε, for $\kappa_{\mathrm{D}}b$ and $\beta e^2/(\epsilon_{\mathrm{solv}}b)$ fixed, the density profile reads

$$\rho_\alpha(x) = \rho_\alpha^{\mathrm{B}}\exp\left[-Z_\alpha^2\frac{\beta e^2}{\epsilon_{\mathrm{solv}}}V_{\mathrm{im}}^{B\,\mathrm{sc}}(x;\kappa_{\mathrm{D}})\right]\times\left[1 - Z_\alpha^2\varepsilon\overline{L}(\kappa_{\mathrm{D}}x;\kappa_{\mathrm{D}}b) - Z_\alpha\beta e\Phi^{(1)}\left(x;\kappa_{\mathrm{D}},\kappa_{\mathrm{D}}b,\frac{\beta e^2}{\epsilon_{\mathrm{solv}}b}\right) + \mathcal{O}(\varepsilon^2)\right]. \tag{133}$$

In (133) $\mathcal{O}(\varepsilon^2)$ is a short notation for terms of orders written in (64) with $\Gamma\propto\varepsilon^{2/3}$.

More precisely, in (133) $(Z_\alpha^2e^2/\epsilon_{\mathrm{solv}})V_{\mathrm{im}}^{B\,\mathrm{sc}}(x;\kappa_{\mathrm{D}})$, called the bulk-screened self-image interaction in the following, is the part of the screened self-energy that is reduced to a mere *bulk* Debye exponential screening of the bare self-image interaction (24) due to the dielectric response of the wall. For two charges separated by a distance $2x$, the bulk screening factor at leading order is $\exp(-2\kappa_{\mathrm{D}}x)$. After multiplication by β,

$$\beta\frac{(Z_\alpha e)^2}{\epsilon_{\mathrm{solv}}}V_{\mathrm{im}}^{B\,\mathrm{sc}}(x;\kappa_{\mathrm{D}}) = -Z_\alpha^2\,\Delta_{\mathrm{el}}\frac{\beta e^2}{\epsilon_{\mathrm{solv}}}\frac{e^{-2\kappa_{\mathrm{D}}x}}{4x} = Z_\alpha^2\,f_{\mathrm{im}}\left(\kappa_{\mathrm{D}}x,\frac{\beta e^2}{\epsilon_{\mathrm{solv}}x}\right). \tag{134}$$

The other part of the screened self-energy comes from the deformation of the set made by a charge, its screening cloud inside the electrolyte, and their images inside the wall, with respect to the spherical symmetry of a charge and its screening cloud in the bulk. The deformation stems both from the impenetrability of the wall (steric effect) and from the contribution of its electrostatic response if $\Delta_{\mathrm{el}}\neq 0$ (polarization effect). When it is multiplied by β, one gets

$$\beta\frac{(Z_\alpha e)^2}{\epsilon_{\mathrm{solv}}}\,\frac{1}{2}\,\kappa_{\mathrm{D}}\,\overline{L}(\kappa_{\mathrm{D}}x;\kappa_{\mathrm{D}}b) = Z_\alpha^2\,\varepsilon\,\overline{L}(\kappa_{\mathrm{D}}x;\kappa_{\mathrm{D}}b) \tag{135}$$

$\Phi^{(1)}$ is the electrostatic potential created by the charge-density profile at first order in ε. It is given by

$$\Phi^{(1)}\left(x;\kappa_{\mathrm{D}},\kappa_{\mathrm{D}}b,\frac{\beta e^2}{\epsilon_{\mathrm{solv}}b}\right) = \frac{e}{\epsilon_{\mathrm{solv}}}\int_b^{+\infty} dx'\int d\mathbf{y}\,\phi^{(0)}(x,x',\mathbf{y})\sum_{\gamma} Z_\gamma \rho_\gamma^{\mathrm{B}}\exp\left[-Z_\gamma^2\frac{\beta e^2}{\epsilon_{\mathrm{solv}}}V_{\mathrm{im}}^{B\,\mathrm{sc}}(x';\kappa_{\mathrm{D}})\right]\times\left\{1-Z_\gamma^2\varepsilon\overline{L}(\kappa_{\mathrm{D}}x';\kappa_{\mathrm{D}}b)\right\}\Bigg|^{(1)} \tag{136}$$

where $\phi^{(0)}(x,x',\mathbf{y})$ is written in (120) and $|^{(1)}$ means that the integral must be calculated at first order in ε with $\kappa_{\mathrm{D}}b$ and $\beta e^2/(\epsilon_{\mathrm{solv}}b)$ kept fixed. As a consequence,

$$Z_\alpha\,\beta e\Phi^{(1)}\left(x;\kappa_{\mathrm{D}},\kappa_{\mathrm{D}}b,\frac{\beta e^2}{\epsilon_{\mathrm{solv}}b}\right) = Z_\alpha\,\varepsilon\,f_\Phi\left(\kappa_{\mathrm{D}}x;\kappa_{\mathrm{D}}b,\frac{\beta e^2}{\epsilon_{\mathrm{solv}}b}\right) \tag{137}$$

$\overline{L}$ and $\Phi^{(1)}$ are functions of x which are bounded in the interval $0<x<+\infty$, and which decay exponentially fast over a few κ_{D}^{-1}'s when x goes to $+\infty$. In the case of an electrolyte confined between two walls, the density profile exhibits an analogous structure [39].

3. *Explicit results in the limit $\kappa_{\mathrm{D}}b\ll 1$ at fixed $\beta e^2/(\epsilon_{\mathrm{solv}}b)$*

Density profiles have been explicitly calculated at leading order in a double expansion in ε and $\kappa_{\mathrm{D}}b$ with $\beta e^2/(\epsilon_{\mathrm{solv}}b)$ fixed in Ref.[2]. Indeed, in regimes where $\kappa_{\mathrm{D}}b\ll 1$ the density profile written in (133) can be explicitly calculated at leading order by considering the limit of $\varepsilon\overline{L}(\kappa_{\mathrm{D}}x;\kappa_{\mathrm{D}}b)$ and of $\varepsilon\,f_\Phi\left(\kappa_{\mathrm{D}}x;\kappa_{\mathrm{D}}b,\beta e^2/(\epsilon_{\mathrm{solv}}b)\right)$ when $\kappa_{\mathrm{D}}b$ vanishes at fixed $\beta e^2/(\epsilon_{\mathrm{solv}}b)$, and by keeping only the terms of order $\varepsilon\ln(\kappa_{\mathrm{D}}b)$ and ε. The corresponding expressions are valid in regime (1) where the temperature is fixed (see (12)). In regime (2) (see (13)), the temperature goes go infinity, and the density profiles are obtained from those of regime (1) by taking the limit where $\beta e^2/(\epsilon_{\mathrm{solv}}b)$ vanishes while $\kappa_{\mathrm{D}}b$ is kept fixed.

We notice that the corresponding results enables one to calculate the surface tension of the electrolyte-wall interface at leading order in ε and $\kappa_{\mathrm{D}}b$ at fixed $\beta e^2/(\epsilon_{\mathrm{solv}}b)\propto\varepsilon/\widetilde{b}$ [40]. From the generic expression, one retrieves results already known in some special cases.

In regime (1) $\kappa_{\mathrm{D}}b$ vanishes at fixed $\beta e^2/(\epsilon_{\mathrm{solv}}b)$, and the explicit expressions of functions in (133) are the following.

$$\overline{L}(\widetilde{x};\widetilde{b}) = (1-\Delta_{\mathrm{el}}^2)\int_1^\infty dt\,\frac{e^{-2t\widetilde{x}}}{\left(t+\sqrt{t^2-1}\right)^2-\Delta_{\mathrm{el}}}+O(\widetilde{b}) \tag{138}$$

and

$$
\begin{aligned}
&-\beta e\Phi^{(1)}\left(x;\kappa_{\rm D},\widetilde{b},\frac{\beta e^2}{\epsilon_{\rm solv} b}\right)\\
&\qquad=\varepsilon\left\{\frac{\Sigma_3}{\Sigma_2}\overline{M}(\widetilde{x})+\frac{\Delta_{\rm el}}{2}\left[\frac{\Sigma_3}{\Sigma_2}\left(C+\frac{\ln 3}{2}+\ln\widetilde{b}\right)+\frac{\sum_\gamma Z_\gamma^3\rho_\gamma^{\rm B}g_\gamma}{\Sigma_2}\right]e^{-\widetilde{x}}+\frac{\Delta_{\rm el}}{4}\frac{\Sigma_3}{\Sigma_2}e^{-2\widetilde{x}}S_-(\widetilde{x})\right\}+\mathcal{O}(\varepsilon\widetilde{b}), \quad (139)
\end{aligned}
$$

where $\mathcal{O}(\varepsilon\widetilde{b})$ stands for a term of order $\varepsilon\widetilde{b}$. By virtue of (136), the electrostatic potential profile $\Phi^{(1)}(x)$ at first order in ε arises from the screened self-energy: the term with $\overline{M}$ comes from the deformation of screening clouds with respect to the bulk spherical symmetry, which is described by $\overline{L}$ (135), and the other terms originate from the bulk-screened self-image interaction $V_{\rm im}^{B\,{\rm sc}}(x)$ (134). If $\Delta_{\rm el}=0$, $\Phi^{(1)}(x)$ is reduced to $\varepsilon\,(\Sigma_3/\Sigma_2)\overline{M}(\widetilde{x})$. In (139)

$$
\overline{M}(\widetilde{x})=\int_1^\infty dt\,\frac{e^{-2t\widetilde{x}}-2te^{-\widetilde{x}}}{1-(2t)^2}\,\frac{1-\Delta_{\rm el}^2}{\left(t+\sqrt{t^2-1}\right)^2-\Delta_{\rm el}}\ , \tag{140}
$$

C is the Euler constant,

$$
g_\gamma\equiv g\left(\frac{\Delta_{\rm el}}{4}Z_\gamma^2\frac{\beta e^2}{\epsilon_{\rm solv}b}\right), \tag{141}
$$

where

$$
g(u)\equiv -1+\frac{e^u-1}{u}-\int_0^u dt\frac{e^t-1}{t}. \tag{142}
$$

S_- is defined by

$$
S_\pm(u)\equiv e^{3u}{\rm Ei}(-3u)\pm e^u{\rm Ei}(-u), \tag{143}
$$

where ${\rm Ei}(-x)$ is the Exponential-Integral function: for $x>0$

$$
{\rm Ei}(-x)\equiv-\int_x^{+\infty}dt\,\frac{e^{-t}}{t}\ =\ C+\ln x+\int_0^x dt\frac{e^{-t}-1}{t}. \tag{144}
$$

$S_-(u)$ decays proportionally to $1/u$ when u goes to ∞, since ${\rm Ei}(-u)$ behaves as $\exp(-u)/u$ for large u.

We notice that, in the calculation of the part in $\Phi^{(1)}(x)$ that comes from the bulk- screened image contribution $V_{\rm im}^{B\,{\rm sc}}$, a key ingredient is the decomposition (C13) combined with the expression of the Exponential-Integral function (144). $g(u)$ arises because

$$
\int_{\widetilde{b}}^{+\infty}dv\left[e^{(\eta/v)}-1-\frac{\eta}{v}\right]=-\eta\,g\left(\frac{\eta}{\widetilde{b}}\right). \tag{145}
$$

We point out that $g(u{=}0)=0$.

In regime (2) (see (13)), $\beta e^2/(\epsilon_{\rm solv}b)$ vanishes, whatever the sign of $\Delta_{\rm el}$ is, because $(\beta e^2/\epsilon_{\rm solv})\ll b\ll\xi_D$. In this regime, ε vanishes faster than $\widetilde{b}$, and $\varepsilon/\widetilde{b}$ must be set to zero while $\widetilde{b}$ is kept fixed in $\ln\widetilde{b}+g_\gamma(\varepsilon/\widetilde{b})$; then the latter sum is reduced to $\ln \widetilde{b}$. The result is the same as if the exponential involving the bulk-screened self-image interaction $V_{\mathrm{im}}^{B\,\mathrm{sc}}(x')$ in the expression (139) of $\Phi^{(1)}(x)$ had been linearized at all distances x', as it is the case in the second integral in decomposition (C13). In the following, we write expressions only for the more general regime where ε and $\widetilde{b}$ vanish with their ratio kept fixed.

In regime (1) (see (12)), $\beta e^2/(\epsilon_{\mathrm{solv}} b)$ is finite. For an electrostatically attractive wall ($\Delta_{\mathrm{el}} > 0$), we cannot consider the limit $b \ll (\beta e^2/\epsilon_{\mathrm{solv}}) \ll \xi_D$, where $\Delta_{\mathrm{el}}\beta e^2/(\epsilon_{\mathrm{solv}} b)$ tends to $+\infty$: there is an irreducible dependence on b. On the contrary, for an electrostatically repulsive wall ($\Delta_{\mathrm{el}} < 0$), we can take the previous limit, where $\Delta_{\mathrm{el}}\beta e^2/(\epsilon_{\mathrm{solv}} b)$ goes to $-\infty$. In this limit, $\widetilde{b}$ vanishes faster than ε, and we must set $\kappa_{\mathrm{D}} b = 0$ at fixed ε in the term $\ln \widetilde{b} + g_\gamma(\varepsilon/\widetilde{b})$ in (139); then this term becomes equal to $\ln\left(|\Delta_{\mathrm{el}}| Z_\gamma^2 \varepsilon/2\right) + C - 1$.

From the expression of the density profiles up to order ε in the vanishing-$\widetilde{b}$ limit, we explicitly calculate the vanishing-$\widetilde{b}$ limit of the term $\overline{D}_\phi^{(1)}(x)$ of order ε in the coefficient $\overline{D}_\phi(x)$. The formal expression of $\overline{D}_\phi^{(1)}(x)$ has been derived in Section V C 1. The calculations of the zero-$\widetilde{b}$ limits of $H^{+(1)}(\widetilde{x}, \mathbf{q}^2 = 0)$ and $\partial H^+/\partial \widetilde{x}|^{(1)}(\widetilde{b}, \mathbf{q}^2 = 0)$ are performed in Appendix C. $C_\phi^{(1)}$ and $\overline{G}_\phi^{\exp\,(1)}(\widetilde{x})$ in (126) are given by

$$\frac{C_\phi^{(1)}}{\varepsilon} = \frac{\Delta_{\mathrm{el}}}{2}\left[\frac{\Sigma_4}{\Sigma_2}\left(C + \frac{3}{2}\ln 2 + \ln \widetilde{b}\right) + \frac{\sum_\gamma \rho_\gamma^{\mathrm{B}} Z_\gamma^4 g_\gamma}{\Sigma_2}\right] \tag{146a}$$

$$+\frac{\Sigma_4}{\Sigma_2}\int_1^\infty dt\, \frac{1-\Delta_{\mathrm{el}}^2}{\left(t+\sqrt{t^2-1}\right)^2 - \Delta_{\mathrm{el}}}\left[\frac{t+1/2}{2t(t+1)}\right] \tag{146b}$$

$$+\frac{1}{4}\left(\frac{\Sigma_3}{\Sigma_2}\right)^2\left\{\int_1^\infty dt\, \frac{1-\Delta_{\mathrm{el}}^2}{\left(t+\sqrt{t^2-1}\right)^2 - \Delta_{\mathrm{el}}}\,\frac{1}{t^2-1/4}\left[\frac{t+1/2}{2t(t+1)} - \frac{4}{3}t\right]\right\} \tag{146c}$$

$$-\frac{\Delta_{\mathrm{el}}}{3}\frac{\Sigma_3}{\Sigma_2}\left[\frac{\sum_\gamma \rho_\gamma^{\mathrm{B}} Z_\gamma^3 g_\gamma}{\Sigma_2} + \frac{\Sigma_3}{\Sigma_2}\left(C + \frac{\ln 3}{2} + \ln \widetilde{b}\right)\right] \tag{146d}$$

$$+\frac{\Delta_{\mathrm{el}}}{4}\left(\frac{\Sigma_3}{\Sigma_2}\right)^2\left[\frac{2}{3}\ln 2 - \ln 3\right] \tag{146e}$$

and

$$\frac{\overline{G}_\phi^{\exp\,(1)}(\widetilde{x})}{\varepsilon} = \frac{\Delta_{\mathrm{el}}}{4}\frac{\Sigma_4}{\Sigma_2}\left\{e^{2\widetilde{x}}\mathrm{Ei}(-4\widetilde{x}) - \mathrm{Ei}(-2\widetilde{x})\right\} \tag{147a}$$

$$-\frac{\Sigma_4}{\Sigma_2}\int_1^\infty dt\, \frac{1-\Delta_{\mathrm{el}}^2}{\left(t+\sqrt{t^2-1}\right)^2 - \Delta_{\mathrm{el}}}\,\frac{e^{-2t\widetilde{x}}}{4t(t+1)} \tag{147b}$$

$$+\frac{1}{4}\left(\frac{\Sigma_3}{\Sigma_2}\right)^2\left\{\int_1^\infty dt\, \frac{1-\Delta_{\mathrm{el}}^2}{\left(t+\sqrt{t^2-1}\right)^2 - \Delta_{\mathrm{el}}}\,\frac{1}{t^2-1/4}\left[\frac{2}{3}te^{-\widetilde{x}} - \frac{e^{-2t\widetilde{x}}}{4t(t+1)}\right]\right\} \tag{147c}$$

$$+\frac{\Delta_{\mathrm{el}}}{6}\frac{\Sigma_3}{\Sigma_2}\left[\frac{\sum_\gamma \rho_\gamma^{\mathrm{B}} Z_\gamma^3 g_\gamma}{\Sigma_2} + \frac{\Sigma_3}{\Sigma_2}\left(C + \frac{\ln 3}{2} + \ln \widetilde{b}\right)\right] e^{-\widetilde{x}} \tag{147d}$$

$$+\frac{\Delta_{\mathrm{el}}}{4}\left(\frac{\Sigma_3}{\Sigma_2}\right)^2\left[\frac{1}{3}e^{2\widetilde{x}}\mathrm{Ei}(-4\widetilde{x}) + \mathrm{Ei}(-2\widetilde{x}) - \frac{1}{3}e^{-\widetilde{x}}\mathrm{Ei}(-\widetilde{x}) - e^{\widetilde{x}}\mathrm{Ei}(-3\widetilde{x})\right]. \tag{147e}$$

The expressions (146a) and (147a) arise from the contribution of the screened self-image interaction $V_{\mathrm{im}}^{B\,\mathrm{sc}}$ (134) to the density profile (133). The terms (146b) and (147b) originate from the deformation of screening clouds described by the function $\overline{L}$ given in (138), which does not vanish even when $\epsilon_W = \epsilon_{\text{solv}}$. The three last ligns in $C_{\phi}^{(1)}/\varepsilon$ and $\overline{G}_{\phi}^{\exp\,(1)}(\widetilde{x})/\varepsilon$ come from the contribution of the electrostatic potential $\Phi(x)$ to the density profile. More precisely, (146c)-(147c), (146d)-(147d) and (146e)-(147e) originate from the functions $\overline{M}(\widetilde{x})$, $\exp(-\widetilde{x})$ and $\exp(-2\widetilde{x})S_{-}(\widetilde{x})$, in (139), respectively.

VI. CORRELATIONS ALONG THE WALL

A. Tails at large distances along the wall

The Ursell function $h_{\alpha\alpha'}$ cannot decay faster than $1/y^3$. Indeed, by an argument based on linear response theory and screening in macroscopic electrostatics, the correlation between global surface-charge densities at points separated by a distance y is shown to decay as $1/y^3$ with a universal negative amplitude [20]: $f_{\alpha\alpha'}$ in the amplitude $-\beta f_{\alpha\alpha'}$ of the $1/y^3$ tail of $h_{\alpha\alpha'}$ obeys sum rule (41). The latter sum rule holds whether all species have the same closest approach distance b_α to the wall or not. We recall that it is a consequence of external screening, as sum rule (38).

On the other hand, as a consequence of the $1/y^3$ decay of the screened potential ϕ, according to (30) and (31), the bonds F^{cc} and F_{R} in resummed Mayer diagrams behave as $1/y^3$ and $1/y^6$, respectively, at large distances y. Since $h_{\alpha\alpha'}$ does not fall off faster than $1/y^3$, no compensation mechanism kills the $1/y^3$ tail arising from the slowest one among the algebraic bonds in the Mayer diagrammatics. Thereore, in a regime where only a finite number of Mayer diagrams – or only some infinite class of diagrams – contribute to the large-distance behavior of $h_{\alpha\alpha'}$, $h_{\alpha\alpha'}$ indeed decays as $1/y^3$. This is the case in the dilute regime studied hereafter. (We notice that if, in some regime, the summation of some infinite series of subdiagrams led to an infinite contribution to $f_{\alpha\alpha'}(x,x')$, then $h_{\alpha\alpha'}$ would fall off more slowly than $1/y^3$. However, since $h_{\alpha\alpha'}$ is integrable by definition, it cannot decay more slowly than $1/y^2$.)

As shown in Paper I, the large-y behavior of $h_{\alpha\alpha'}$ along the wall is conveniently studied from the decomposition described by (33)–(53), as in the case of bulk correlations. In the latter graphic representation of $h_{\alpha\alpha'}$, the topology of diagrams involved in I implies that the bond I decays algebraically faster than F^{cc} at large distances y (see Section II C). Moreover, as exhibited in Figs.1-3, all graphs in h^{cc}, $h^{-\text{c}}$, $h^{\text{c}-}$, and h^{--} are chain graphs, and, because of the translation invariance in the direction parallel to the wall, the chain graphs can be seen as multiple convolutions with respect to the variable $\mathbf{y}$. Therefore, every term, except I, in the graphic representation of h^{cc}, $h^{-\text{c}}$, $h^{\text{c}-}$ and h^{--} has $1/y^3$ tails arising from all its F^{cc} bonds. The $1/y^3$ tail of every graph in h^{cc}, $h^{\text{c}-}$, $h^{-\text{c}}$ and h^{--} (see Figs.1-3) is a sum of contributions, each of which is determined by replacing one of the bonds $F^{\rm cc}$ by its $1/y^3$ behavior at large y, while the other part of the graph is replaced by its Fourier transform at the value $\mathbf{q}=\mathbf{0}$.

Eventually, as shown in Paper I, when all species have the same closest approach distance to the wall,

$$h_{\alpha\alpha'}(x,x',y) \underset{y\to+\infty}{\sim} -\beta\frac{D_\alpha(x)D_{\alpha'}(x')}{y^3} \tag{148}$$

and

$$D_\alpha(x)=\frac{e}{\sqrt{\epsilon_{\rm solv}}}\Big\{Z_\alpha\left[\overline{D}_\phi(x)+\overline{C}^{\rm c-}(x)\right]+C^{--}_\alpha(x)\Big\}, \tag{149}$$

where $C^{--}_\alpha(x)$ and $\overline{C}^{\rm c-}(x)$ are related to $h^{--}_{\alpha\alpha'}$ and $h^{\rm c-}_{\alpha\alpha'}$, respectively, by

$$C^{--}_\alpha(x)\equiv\int dx''\sum_{\gamma''}\rho_{\gamma''}(x'')Z_{\gamma''}\overline{D}_\phi(x'')h^{--}_{\alpha\gamma''}(x,x'',\kappa_{\rm D}\mathbf{q}=\mathbf{0}) \tag{150}$$

and

$$Z_\alpha\overline{C}^{\rm c-}(x)\equiv\int dx''\sum_{\gamma''}\rho_{\gamma''}(x'')Z_{\gamma''}\overline{D}_\phi(x'')h^{\rm c-}_{\alpha\gamma''}(x,x'',\kappa_{\rm D}\mathbf{q}=\mathbf{0}). \tag{151}$$

An advantage of the resummed Mayer diagrammatic representation is that the contribution from every diagram $\widetilde{\Pi}$ can be associated with some physical effect. For instance, diagram $\widetilde{\Pi}_a$ made of the single bond $F^{\rm cc}$ describes Coulomb screening at leading order, the sum of the two diagrams made of bonds $[F^{\rm cc}]^2/2$ and $F_{\rm RT}$ respectively contains the short-distance repulsion, while diagrams $\widetilde{\Pi}_b$ $\widetilde{\Pi}_{b^\star}$ and $\widetilde{\Pi}_c$ shown in Figs.8-9 involve many-body corrections to the mean-field contribution from $\widetilde{\Pi}_a$.

In order to trace back the physical effects, we have to identify the contributions to $D_\alpha(x)D_{\alpha'}(x')$ from the various diagrams $\widetilde{\Pi}$ defined in Section III B. In other words, we have to recognize in (148)-(149) the tails of $h^{\rm cc}_{\alpha\alpha'}$, $h^{\rm c-}_{\alpha\alpha'}$, $h^{-\rm c}_{\alpha\alpha'}$ and $h^{--}_{\alpha\alpha'}$, the sum of which is equal to $h_{\alpha\alpha'}$. As shown in the Appendix of Paper I, the latter tails read

$$h^{\rm cc}_{\alpha\alpha'}(x,x',\mathbf{y}) \underset{y\to+\infty}{\sim} -\frac{\beta e^2}{\epsilon_{\rm solv}}Z_\alpha Z_{\alpha'}\left[\overline{D}_\phi(x)+\overline{C}^{\rm c-}(x)\right]\left[\overline{D}_\phi(x')+\overline{C}^{\rm c-}(x')\right]\frac{1}{y^3}, \tag{152}$$

$$h^{\rm c-}_{\alpha\alpha'}(x,x',\mathbf{y}) \underset{y\to+\infty}{\sim} -\frac{\beta e^2}{\epsilon_{\rm solv}}Z_\alpha\left[\overline{D}_\phi(x)+\overline{C}^{\rm c-}(x)\right]C^{--}_{\alpha'}(x')\frac{1}{y^3}, \tag{153}$$

$$h^{--}_{\alpha\alpha'}(x,x',\mathbf{y}) \underset{y\to+\infty}{\sim} -\frac{\beta e^2}{\epsilon_{\rm solv}}C^{--}_\alpha(x)C^{--}_{\alpha'}(x')\frac{1}{y^3}. \tag{154}$$

B. Sum rule for the effective dipole $D_\alpha(x)$

According to (148), $f_{\alpha\alpha'}(x,x') = D_\alpha(x)D_{\alpha'}(x')$ so that the sum rule (41) for $f_{\alpha\alpha'}(x,x')$ can be rewritten as

$$\int_0^{+\infty} dx \sum_\alpha e_\alpha \rho_\alpha(x) D_\alpha(x) = \sqrt{\frac{\epsilon_W}{8\pi^2\beta^2}}. \tag{155}$$

Similarly to what happens for the internal-screening rule (35), the latter external-screening sum rule can be derived from the decomposition (149), the integral relation (50) between $h^{\mathrm{c}-}$ and h^{--}, and two sum rules obeyed by ϕ, namely (47) and a sum rule for $\overline{D}_\phi(x)$ in the $f_\phi(x,x')/y^3$ tail of $\phi(x,x',y)$,

$$\int_0^{+\infty} dx\, \overline{\kappa}^2(x)\overline{D}_\phi(x) = \sqrt{\frac{2\epsilon_W}{\epsilon_{\mathrm{solv}}}}. \tag{156}$$

The latter equation arises from the sum rule (48) obeyed by the amplitude $f_\phi(x,x')$ (derived in Paper I), and from the fact that $f_\phi(x,x')$ takes the factorized form $\overline{D}_\phi(x)\overline{D}_\phi(x')$ in the case where all species have the same closest approach distance b to the wall.

More precisely, the derivation of (155) is as follows. The integral relation (50) between $h^{\mathrm{c}-}$ and h^{--} and sum rule (47) imply that the contributions from $C_\alpha^{--}(x)$ and $Z_\alpha \overline{C}^{\mathrm{c}-}(x)$ to the integral in (155) cancel each other. On the other hand, sum rule (156) ensures that the contribution from $Z_\alpha \overline{D}_\phi(x)$ to the integral in (155) is already equal to the constant in the r.h.s. of the equation. In other words, the bond F^{cc}, namely diagram $\widetilde{\Pi}_a$, already fulfulls sum rule (155).

As a consequence, if some diagrams are to be kept for their contributions to $C_\alpha^{--}(x)$ in some dilute regime, then the corresponding diagrams "dressed" with a bond F^{cc} must also be retained in $Z_\alpha \overline{C}^{\mathrm{c}-}(x)$ in order to ensure that screening rule (155) is still obeyed.

In the case of a symmetric electrolyte made of two species with opposite charges $+Ze$ and $-Ze$ and with the same radii, $\sum_\alpha \rho_\alpha(x) h_{\alpha\alpha'}(\mathbf{r},\mathbf{r}')$ decays faster than $h_{\alpha\alpha'}(\mathbf{r},\mathbf{r}')$ in the y-direction, similarly to what happens in the bulk (see Section IV E). Indeed, symmetries enforce that the local neutrality is satisfied not only in the bulk, where $\rho_+^{\mathrm{B}} = \rho_-^{\mathrm{B}}$, but also in the vicinity of the wall, where $\rho_+(x) = \rho_-(x)$. As a consequence, by virtue of (149), $\rho_+(x)D_+(x) + \rho_-(x)D_-(x) = (e/\sqrt{\epsilon_{\mathrm{solv}}})\sum_\alpha \rho_\alpha(x) C_\alpha^{--}(x)$. Symmetries also imply that $h_{++}^{--} = h_{--}^{--}$ and $h_{+-}^{--} = h_{-+}^{--}$, and the definition (150) of $C_\alpha^{--}(x)$ yields $\rho_+(x)D_+(x) + \rho_-(x)D_-(x) = 0$. Subsequently, $\rho_+ h_{+\alpha'} + \rho_- h_{-\alpha'}$ decays faster than $1/y^3$. The latter property has been exhibited in Eq.(3.4) of Ref.[38], where the density-density correlation $\sum_{\alpha,\alpha'} \rho_\alpha(x)\rho_{\alpha'}(x')h_{\alpha\alpha'}(\mathbf{r},\mathbf{r}')$ in the infinite-dilution and vanishing-coupling limit (where $\rho_\alpha(x) = \rho_\alpha^{\mathrm{B}}$) is shown to decay as $\exp[-2\kappa_{\mathrm{D}}(x+x')]/y^6$.

C. ε-expansions

1. *Method*

In the general formula (149) for $D_\alpha(x)$, $Z_\alpha\overline{C}^{\mathrm{c}-}(x)$, as well as $C_\alpha^{--}(x)$, is a series of functions, each of which decays as a polynomial in x times $\exp(-\kappa_{\mathrm{D}}x)$, plus functions which vanish faster (see the general structure (4) of $\overline{D}_\phi(x)$ in the introduction). However, since there is no translational invariance in the direction perpendicular to the wall, the series $C_\alpha^{--}(x)$ and $Z_\alpha\overline{C}^{\mathrm{c}-}(x)$ cannot be expressed as sums of geometric series that could be calculated by such a simple formula as (77). Therefore, the expression of $(Z_\alpha^{\mathrm{eff\,W}}/\kappa)\exp[-\kappa(x-b)]$ in the large-distance behavior (10) of $D_\alpha(x)$ cannot be calculated by the mere determination of the pole of an analytic function and the calculation of a residue.

Though the lost of translational invariance in the direction perpendicular to the wall prevents one from performing systematic resummations, $D_\alpha(x)$ can be determined up to order ε at any distance x (in the sense of the comment after (89)) by the alternative procedure derived for bulk correlations in Section IV D. In a first step, the correction of order ε in the screening length κ^{-1} of the leading exponential decay of $D_\alpha(x)$ has to be calculated by the partial resummation mechanism whose validity has been checked in the case of bulk correlations (see Section IV D 2). In a second step, the amplitude factor in $D_\alpha(x)$ up to order ε is determined as follows. First, we calculate $D_\alpha^{(1)}(x)$ in a form analogous to (89), which arises from the contributions of only a few diagrams whose amplitude is of order ε and which decay at large x as $\exp[-\kappa_{\mathrm{D}}(x-b)]$ times a possible linear term in x; in a second step we check that the coefficient of the $(x-b)\exp[-\kappa_{\mathrm{D}}(x-b)]$ term, which arises from the second diagram $\widetilde{\Pi}_c$ in h^{cc}, indeed coincides with the opposite of the first correction to the screening length in the direction perpendicular to the wall, which has already been calculated independently.

The ε-expansions of $\widetilde{\Pi}$ diagrams are more complicated than in the case of the bulk, because the screened potential ϕ also has an ε-expansion when the vicinity of the wall is studied. The first correction to $\phi^{(0)}$ yields $\overline{D}_\phi^{(1)}(x)$ in the expression (149) of $D_\alpha^{(1)}(x)$. The leading term in the ε-expansion of $C_\alpha^{--}(x)$ or $Z_\alpha\overline{C}^{\mathrm{c}-}(x)$ is obtained as follows: densities ρ_γ's are replaced by their bulk values ρ_γ^{B}'s and both functions $\phi(x,x',\mathbf{q}=\mathbf{0})$ and $I(x,x',\mathbf{q}=\mathbf{0})$ are replaced by their leading values $\phi^{(0)}(x,x',\mathbf{q}=\mathbf{0})$ and $I^{(1)}(x,x',\mathbf{q}=\mathbf{0})=(1/2)[F^{\mathrm{c\,c}\,(0)}]^2(x,x',\mathbf{q}=\mathbf{0})$, respectively. As in the bulk case, only the subseries shown in Figs.4-6 do contribute to $D_\alpha^{(1)}(x)$.

2. Renormalization of the screening length

We recall that, in the bulk case, the leading tail at order ε^q in the ε-expansion of the large-distance behavior $h^{\mathrm{cc\,B\,as}}_{\alpha\alpha'}$ of $h^{\mathrm{cc\,B}}_{\alpha\alpha'}$ around its $\exp[-\kappa_{\mathrm{D}} r]/r$ limit decays as r^q times $\exp[-\kappa_{\mathrm{D}} r]/r$, and the sum $h^{\mathrm{cc\,B\,as}\,\star}_{\alpha\alpha'}$ of the latter tails decays as $\exp\left[-(\kappa_{\mathrm{D}}+\delta\kappa^\star_B)r\right]$, with $\delta\kappa^\star_B=\delta\kappa^{(1)}_{\mathrm{B}}$ (see Section IV D 2). In the vicinity of the wall, the contribution from $h^{\mathrm{cc}}_{\alpha\alpha'}$ to $D_\alpha(x)$ is equal to $Z_\alpha\left[\overline{D}_\phi(x)+\overline{C}^{c-}(x)\right]$ according to (152). As shown in Appendix D, in the ε-expansion of $Z_\alpha\overline{C}^{\mathrm{c}-}(x)$, at order ε^q the leading term at large x is proportional to $(x-b)^q\exp[-\kappa_{\mathrm{D}}(x-b)]$. The sum over q of the latter leading terms is proportional to $\exp\left[-(\kappa_{\mathrm{D}}+\delta\kappa^\star)(x-b)\right]$ with

$$\delta\kappa^\star=\delta\kappa^{(1)}_{\mathrm{B}}. \tag{157}$$

According to the discussion of Section IV D 2, the latter partial resummation determines the correction $\delta\kappa^{(1)}$ of order ε to κ_{D} in the x-direction, $\delta\kappa^\star=\delta\kappa^{(1)}$. According to (157), the correction $\delta\kappa^{(1)}$ to the screening length in the direction perpendicular to the wall coincides at first order in ε with the value found for bulk correlations,

$$\delta\kappa^{(1)}=\delta\kappa^{(1)}_{\mathrm{B}}. \tag{158}$$

3. Renormalization of the amplitude of $D_\alpha(x)$

According to the general method summarized above, the amplitude of $D^{(1)}_\alpha(x)$ can be determined from only a few diagrams in $C^{--}_\alpha(x)$ and $Z_\alpha\overline{C}^{\mathrm{c}-}(x)$. Before turning to the explicit calculations in the regime $\widetilde{b}\ll 1$, we interpret the various contributions in $D_\alpha(x)D_{\alpha'}(x')/y^3$ in terms of diagrams which are representative of physical effects. The diagrams that are involved in the determination of the $1/y^3$ tail of $h_{\alpha\alpha'}(x,x',y)$ up to order in ε are the same as in the case of the bulk. Diagram $\widetilde{\Pi}_a$ in Fig.7 describes the leading screening effect and therefore gives the zeroth-order contribution

$$D^{(0)}_\alpha(x)D^{(0)}_{\alpha'}(x')=\frac{e^2}{\epsilon_{\mathrm{solv}}}Z_\alpha Z_{\alpha'}\overline{D}^{(0)}_\phi(x)\overline{D}^{(0)}_\phi(x'). \tag{159}$$

Contrary to the bulk case, because of the nonuniformity of the density profiles in the vicinity of the wall, ϕ has an ε-expansion, and the first correction $\phi^{(1)}$ to $\phi^{(0)}$ gives a correction of order ε in the $1/y^3$ tail of $\widetilde{\Pi}_a$. The contribution from diagram $\widetilde{\Pi}_a$ to the correction of order ε

$$\left[D_\alpha(x)D_{\alpha'}(x')\right]^{(1)}=D^{(0)}_\alpha(x)D^{(1)}_{\alpha'}(x')+D^{(1)}_\alpha(x)D^{(0)}_{\alpha'}(x') \tag{160}$$

reads

$$\frac{e^2}{\epsilon_{\rm solv}} Z_\alpha Z_{\alpha'} \left[\overline{D}_\phi^{(0)}(x)\overline{D}_\phi^{(1)}(x') + \overline{D}_\phi^{(1)}(x)\overline{D}_\phi^{(0)}(x')\right]. \tag{161}$$

The other contributions to (160) arise from diagrams $\widetilde{\Pi}_b$ $\widetilde{\Pi}_{b^\star}$ and $\widetilde{\Pi}_c$, shown in Figs.8-9, where fixed charges interact through screened interactions via one or two other charges. (The ε-expansions of the contributions from the latter diagrams to the $1/y^3$ tail of $h_{\alpha\alpha'}(x)$ start at the order ε, because they all involve a bond $(1/2)\left[F^{\rm cc}\right]^2$.) The contribution to (160) from diagram $\widetilde{\Pi}_b$ reads

$$\frac{e^2}{\epsilon_{\rm solv}} Z_\alpha \overline{D}_\phi^{(0)}(x)\overline{C}_{\alpha'}^{--\,(1)}(x'), \tag{162}$$

while $\widetilde{\Pi}_{b^\star}$ leads to a symmetric term in the variables x and x', and $\widetilde{\Pi}_c$ yields

$$\frac{e^2}{\epsilon_{\rm solv}} Z_\alpha Z_{\alpha'} \left[\overline{C}_\alpha^{-{\rm c}\,(1)}(x)\overline{D}_\phi^{(0)}(x') + \overline{D}_\phi^{(0)}(x)\overline{C}_{\alpha'}^{-{\rm c}\,(1)}(x')\right]. \tag{163}$$

D. Explicit results in the limit $\kappa_{\rm D} b \ll 1$ at fixed $\beta e^2/(\epsilon_{\rm solv} b)$

1. *Separate contributions*

In the limit $\widetilde{b} \ll 1$, $D_\alpha^{(0)}(x)$ is given by (7) where the $\exp(\kappa_{\rm D} b)$ term disappears in the expression of $\overline{D}_\phi^{(0)}(x)$. $D_\alpha^{(1)}(x)$ is calculated from formula (149). $\overline{D}_\phi^{(1)}(x)$ has been studied in Section V, and in the limit $\widetilde{b} \ll 1$ $\overline{D}_\phi^{(1)}(x)$ is given by (126), (146), and (147). The other contributions $C_\alpha^{--\,(1)}(x)$ and $Z_\alpha \overline{C}^{{\rm c}-\,(1)}(x)$ are obtained by replacing $\rho_{\gamma''}(x'')$ by $\rho^B_{\gamma''}$, ϕ by $\phi^{(0)}$, h^{--} and $h^{{\rm c}-}$ by the graphs with one I in their series representations, and I by $[F^{{\rm c\,c}\,(0)}]^2/2$ in the expressions (150) and (151) for $C_\alpha^{--}(x)$ and $Z_\alpha \overline{C}^{{\rm c}-}(x)$, respectively. The contribution from $C_\alpha^{--}(x)$ is

$$C_\alpha^{--\,(1)}(x) = \overline{D}_\phi^{(0)}(x) Z_\alpha^2 \left[\overline{B}_{[b]}^{(1)} + \overline{G}_{[b]}^{\exp\,(1)}(\widetilde{x})\right], \tag{164}$$

where

$$\overline{B}_{[b]}^{(1)} = \varepsilon \frac{\ln 3}{2}\frac{\Sigma_3}{\Sigma_2} \tag{165}$$

and

$$\overline{G}_{[b]}^{\exp\,(1)}(\widetilde{x}) = \varepsilon \frac{\Sigma_3}{\Sigma_2}\frac{1}{2}\left\{ -e^{-\widetilde{x}} S_-(\widetilde{x}) \right.$$
$$\left. + \int_1^\infty dt\, \frac{e^{(1-2t)\widetilde{x}}}{\left[t+\sqrt{t^2-1}-\Delta_{\rm el}(t-\sqrt{t^2-1})\right]^2}\left[2(1-\Delta_{\rm el})^2 + \frac{(1-\Delta_{\rm el})^2(1-2e^{-\widetilde{x}}) - 8\Delta_{\rm el}(t^2-1)(1-e^{-\widetilde{x}})}{t+1/2}\right]\right\} \tag{166}$$

with $S_-(\widetilde{x})$ defined in (143). The contribution from $Z_\alpha\overline{C}^{\mathrm{c}-}(x)$ reads

$$Z_\alpha\overline{C}^{\mathrm{c}-\,(1)}(x) = Z_\alpha\overline{D}_\phi^{(0)}(x)\left[-\varepsilon\frac{\ln 3}{4}\left(\frac{\Sigma_3}{\Sigma_2}\right)^2\widetilde{x} + B_{[c]}^{(1)} + G_{[c]}^{\exp\,(1)}(\widetilde{x})\right]. \tag{167}$$

In (167) the coefficient of the linear term $\widetilde{x}$ coincides with $-\delta\kappa_{\mathrm{B}}^{(1)}$ given by (86), while

$$B_{[c]}^{(1)} = \varepsilon\frac{1}{2}\left[\frac{1}{3} - \frac{\ln 3}{2} - \frac{a_c(\Delta_{\mathrm{el}})}{2}\right]\left(\frac{\Sigma_3}{\Sigma_2}\right)^2 \tag{168}$$

with

$$a_c(\Delta_{\mathrm{el}}) \equiv \int_1^\infty dt\,\frac{1}{\left[t+\sqrt{t^2-1}-\Delta_{\mathrm{el}}(t-\sqrt{t^2-1})\right]^2}\left[\frac{(1-\Delta_{\mathrm{el}})^2\left[16t^4(t+1/2)-1\right]}{8t(t-1/2)^2(t+1/2)^2(t+1)} - \frac{\Delta_{\mathrm{el}}(t-1)(4t^2+2t+1)}{t(t-1/2)(t+1/2)^2}\right]. \tag{169}$$

If $\epsilon_{\mathrm{solv}}/\epsilon_W = 80$, $a_c = 1.2$, and if $\epsilon_{\mathrm{solv}} = \epsilon_W$, $a_c = 0.84$. $G_{[c]}^{\exp\,(1)}(\widetilde{x})$ is the exponentially decaying function

$$G_{[c]}^{\exp\,(1)}(\widetilde{x}) = -\frac{\varepsilon}{4}\left(\frac{\Sigma_3}{\Sigma_2}\right)^2 \left\{\frac{4}{3}e^{-\widetilde{x}} + \int_1^\infty dt\,\frac{e^{(1-2t)\widetilde{x}}}{\left[t+\sqrt{t^2-1}-\Delta_{\mathrm{el}}(t-\sqrt{t^2-1})\right]^2}\,\frac{4\Delta_{\mathrm{el}}(t^2-1)-(1-\Delta_{\mathrm{el}})^2(t+1)}{(t-1/2)(t+1/2)^2}\right.$$
$$\left. + e^{-\widetilde{x}}\left[-S_-(\widetilde{x}) + \widetilde{x}S_+(\widetilde{x})\right] + \int_1^\infty dt\,\frac{e^{-2t\widetilde{x}}\left[(1-\Delta_{\mathrm{el}})^2 - 4\Delta_{\mathrm{el}}(t^2-1)\right]}{t(t+1)(t+1/2)\left[t+\sqrt{t^2-1}-\Delta_{\mathrm{el}}(t-\sqrt{t^2-1})\right]^2}\right\}. \tag{170}$$

2. Global results

Eventually, the sum of the various contributions at order ε reads

$$D_\alpha^{(1)}(x) = \left[-\varepsilon\frac{\ln 3}{4}\left(\frac{\Sigma_3}{\Sigma_2}\right)^2\widetilde{x} + B_\alpha^{(1)} + G_\alpha^{\exp\,(1)}(\widetilde{x})\right] D_\alpha^{(0)}(x), \tag{171}$$

where $B_\alpha^{(1)}$ is the sum of the various constants,

$$B_\alpha^{(1)} \equiv C_\phi^{(1)} + Z_\alpha\overline{B}_{[b]}^{(1)} + B_{[c]}^{(1)}, \tag{172}$$

and

$$G_\alpha^{\exp\,(1)}(\widetilde{x}) \equiv G_{[a]}^{\exp\,(1)}(\widetilde{x}) + Z_\alpha\overline{G}_{[b]}^{\exp\,(1)}(\widetilde{x}) + G_{[c]}^{\exp\,(1)}(\widetilde{x}). \tag{173}$$

$G_\alpha^{\exp\,(1)}(\widetilde{x})$ is a bounded function of order ε which decays to zero at least as $\exp(-\widetilde{x})$ when $\widetilde{x}$ goes to infinity. The coefficient of the term $(-x)\exp[-\kappa_{\mathrm{D}}x]$ in $D_\alpha^{(1)}(x)$ indeed coincides with the first-order correction $\delta\kappa^{(1)}$ to the screening length in the direction perpendicular to the wall calculated in Appendix D with the result (158). Therefore the ε-expansion of $D_\alpha(x)$ can be rewritten in terms of the explicit expression (7) of $D_\alpha^{(0)}(x)$ as

$$\begin{aligned} D_\alpha(x) = &-\sqrt{\frac{2\epsilon_W}{\epsilon_{\text{solv}}}}\frac{e}{\sqrt{\epsilon_{\text{solv}}}}\frac{Z_\alpha}{\kappa_{\text{D}}} \\ &\times\left\{e^{-(\kappa_{\text{B}}+\delta\kappa_{\text{B}}^{(1)})x}\left[1+B_\alpha^{(1)}+G_\alpha^{\exp\,(1)}(\widetilde{x})\right]+o(\varepsilon)\right\}. \end{aligned} \tag{174}$$

The effective dipole associated with a charge at leading order in ε, $D_\alpha^{(0)}(x)$, is proportional to the mere exponential function $\exp(-\kappa_{\text{D}}x)$. (174) shows that, when first-order corrections are taken into account, the effective dipole varies with the distance from the wall in a more complicated way described by $G_\alpha^{\exp\,(1)}(\widetilde{x})$, the value of which is derived from (173). The sign of $B_\alpha^{(1)}+G_\alpha^{\exp\,(1)}(\widetilde{x})$ may vary with the distance x from the wall and depends drastically upon the composition of the electrolyte, the value of the closest approach distance b, and the relative dielectric constant of the wall with respect to that of the solvent.

Since $G_\alpha^{\exp\,(1)}(\widetilde{x})$ tends to zero at large x, the effective charge near the wall $Z_\alpha^{\text{eff W}}$, defined from the dipolar interaction by (10), reads

$$Z_\alpha^{\text{eff W}} = Z_\alpha\left[1+B_\alpha^{(1)}+\frac{\delta\kappa_{\text{B}}^{(1)}}{\kappa_{\text{B}}}+o(\varepsilon)\right], \tag{175}$$

where the term $\delta\kappa_{\text{B}}^{(1)}/\kappa_{\text{B}}$ arises from the $1/\kappa$ coefficient in the definition (10). By virtue of (172) and (86)

$$Z_\alpha^{\text{eff W}} = Z_\alpha\left\{1+C_\phi^{(1)}+Z_\alpha\varepsilon\frac{\ln 3}{2}\frac{\Sigma_3}{\Sigma_2}-\varepsilon\left[\frac{a_c(\Delta_{\text{el}})}{4}-\frac{1}{6}\right]\left(\frac{\Sigma_3}{\Sigma_2}\right)^2+o(\varepsilon)\right\}. \tag{176}$$

As exhibited by their diagrammatic origins, the various terms in $Z_\alpha^{\text{eff W}}$ arise both from the nonuniformity of the density profiles described by diagram $\widetilde{\Pi}_a$ at order ε and from the leading screened interactions via one or two other charges that appear in diagrams $\widetilde{\Pi}_b$ and $\widetilde{\Pi}_{b^\star}$ (Fig.8) and in diagram $\widetilde{\Pi}_c$ (Fig.9). If $\epsilon_{\text{solv}}>\epsilon_W$, $a_c(\Delta_{\text{el}})>(2/3)$ and the four-body effective interactions tend to decrease $Z_\alpha^{\text{eff W}}$ with respect to its bulk value.

The comparison of the effective charge $Z_\alpha^{\text{eff W}}$ near the wall with its value $Z_\alpha^{\text{eff B}}$ in the bulk given in (87) leads to

$$\frac{Z_\alpha^{\text{eff W}}}{Z_\alpha^{\text{eff B}}} = 1+B_\alpha^{(1)}-A_\alpha^{(1)}+\frac{\delta\kappa_{\text{B}}^{(1)}}{\kappa_{\text{B}}}+o(\varepsilon). \tag{177}$$

where

$$B_\alpha^{(1)}-A_\alpha^{(1)} = C_\phi^{(1)}+B_{[c]}^{(1)}-A_{[c]}^{(1)}. \tag{178}$$

Indeed, according to (99) and (165) $\overline{B}_{[b]}^{(1)}=\overline{A}_{[b]}^{(1)}$: the contributions in the bulk and along the wall from diagram $\widetilde{\Pi}_b$ compensate each other and there is no term proportional to Z_α^2 in the ratio $Z_\alpha^{\text{eff W}}/Z_\alpha^{\text{eff B}}$. The final result is written in (18).

VII. CONCLUSION

In the present Paper we have introduced the renormalized charge $Z_{\alpha}^{\text{eff w}}$ associated with the large-distance dipolar-like effective interaction between two charges along an insulating wall, when all charges have the same closest approach distance to the wall. This charge has been explicitly calculated up to order ε in some limit of infinite dilution and weak coupling when the wall is neutral.

The renormalized charge could also be calculated in the case of an insulating wall with an external surface charge on it, as it is the case for instance when the wall mimicks a cell membrane. Indeed, the general method presently devised for the calculation of $Z_{\alpha}^{\text{eff w}}$ holds for any density profiles when the ε-expansions of the latters are known. On the other hand, such ε-expansions could be obtained by a generalization of the method presented in Refs.[2] and [3], where the external one-body potential created by the surface charge would be incorporated in the fugacity.

APPENDIX A:

The present Appendix is devoted to the determination of the large-distance behaviors of exponentially decaying functions, such as those which appear in the resummed Mayer diagrammatics for bulk correlations. When a function $f(\mathbf{r})$ is rotationally invariant, its Fourier transform $f(\mathbf{k}) \equiv \int d\mathbf{r} \exp[-i\mathbf{k}\cdot\mathbf{r}] f(\mathbf{r})$ depends only on the modulus k of $\mathbf{k}$. On the other hand, when $f(\mathbf{r})$ decays faster than any inverse power law of the modulus r of $\mathbf{r}$, then its Fourier transform is an analytic function of the components of $\mathbf{k}$. When both conditions are fulfilled by $f(\mathbf{r})$, the $\mathbf{k}$-expansion of $f(\mathbf{k})$ contains only powers of $\mathbf{k}^2$. Then the analytic continuation of $f(\mathbf{k}) = f(k)$ to negative values of k is an even function of k and its inverse Fourier transform can be rewritten as the following integral

$$f(r) = -\frac{i}{4\pi^2}\frac{1}{r}\int_{-\infty}^{+\infty} dk\, e^{ikr} k f(k), \tag{A1}$$

where $f(k)$ is a derivable function of k. The one-dimensional integral in (A1) can be performed by the method of contour integrals in the complex plane $k = k' + ik''$. (We notice that, when $f(\mathbf{r})$ decays algebraically, then the small-$\mathbf{k}$ expansion of $f(\mathbf{k})$ contains nonanalytic terms involving either $\ln|\mathbf{k}|$ or odd powers of $|\mathbf{k}|$ [37], and the present method does not hold.)

The slowest exponential tail $f^{\text{slow}}(r)$ of f, defined at the begining of Section IV, is determined by the singular point of $f(k)$ that is the closest one to the real axis $k'' = 0$ in the upper complex half-plane. If the latter singular point is a pole k_0, its contribution to $f(r)$ is given by the residue theorem

$$f^{\text{slow}}(r) = \frac{1}{2\pi r}\, \text{Res}\left[e^{ikr} k f(k)\right]\big|_{k=k_0}\,. \tag{A2}$$

In the present paper we consider functions $f(k)$ that contain no exponential term and such that k_0 is purely imaginary, $k_0 = i\kappa_{\text{D}}$. In that case the inverse decay length of $f^{\text{slow}}(r)$ is equal to the imaginary part of the pole k_0. (If there were two poles with the same imaginary part and opposite real parts, then $f^{\text{slow}}(r)$ would be an oscillatory exponential tail.)

Moreover, when $k_0 = i\kappa_{\text{D}}$ is a pole of rank 1, $f^{\text{slow}}(r)$ is a pure $\exp(-\kappa_{\text{D}} r)/r$ function, whereas if $k_0 = i\kappa_{\text{D}}$ is a pole of rank m, $f^{\text{slow}}(r)$ is equal to $\exp(-\kappa_{\text{D}} r)/r$ times a polynomial in r of rank $m-1$. For instance, if f is equal to the convolution $\phi_{\text{D}} * [\phi_{\text{D}}]^2$, the complete contour integral which determines the r.h.s. of (A1) gives the expression of $\phi_{\text{D}} * [\phi_{\text{D}}]^2$ at any distance r. According to (72) and (81), ϕ_{D} has a pole at $k = i\kappa_{\text{D}}$, while $[\phi_{\text{D}}]^2$ has a cut that starts at $k = 2i\kappa_{\text{D}}$ and goes along the imaginary axis up to $+i\infty$. As a consequence,

$$\left[\frac{e^{-\kappa_{\text{D}} r}}{r} * \left(\frac{e^{-\kappa_{\text{D}} r}}{r}\right)^2\right](r) = 2\pi \ln 3\, \frac{e^{-\kappa_{\text{D}} r}}{\kappa_{\text{D}} r} + \frac{e^{-2\kappa_{\text{D}} r}}{\kappa_{\text{D}} r} F_b(\kappa_{\text{D}} r), \tag{A3}$$

where the first term comes from the residue of $\exp[ikr]kf(k)$ at the pole $k = i\kappa_{\text{D}}$ of $\phi_{\text{D}}(\mathbf{k})$, while the second term arises from the cut in the definition of $[\phi_{\text{D}}^2](\mathbf{k})$. At large distances the first term falls off as ϕ_{D} and the second term as $[\phi_{\text{D}}^2]$, because $F_b(\kappa_{\text{D}} r)$ decays as a constant times $1/(\kappa_{\text{D}} r)$. Indeed,

$$\begin{aligned} F_b(\kappa_{\text{D}} r) &\equiv -8\pi \int_0^{+\infty} dt \frac{e^{-2\kappa_{\text{D}} r\, t}}{4(1+t)^2 - 1} \\ &= -2\pi \left[e^{3\kappa_{\text{D}} r} \text{Ei}(-3\kappa_{\text{D}} r) - e^{\kappa_{\text{D}} r} \text{Ei}(-\kappa_{\text{D}} r)\right], \end{aligned} \tag{A4}$$

where $\text{Ei}(-x)$ is the Exponential-Integral function defined in (144). (The large-distance behavior of the convolution $\phi_{\text{D}} * [\phi_{\text{D}}]^2$ is indeed dominated by the pole of $\phi_{\text{D}}(\mathbf{k})$ at $k = i\kappa_{\text{D}}$ and not by the branch point of the Fourier transform of $[\phi_{\text{D}}(r)]^2$ at $k = 2i\kappa_{\text{D}}$.) In the case of $\phi_{\text{D}} * [\phi_{\text{D}}]^2$, the corresponding slowest exponential tail $f^{\text{slow}}(r)$ is exactly proportional to $\phi_{\text{D}} = \exp[-\kappa_{\text{D}} r]/r$, since the pole at $k_0 = i\kappa_{\text{D}}$ is of rank 1.

For the convolution $\phi_{\text{D}} * [\phi_{\text{D}}]^2 * \phi_{\text{D}}$, $[\phi_{\text{D}}(\mathbf{k})]^2$ has a pole of rank 2, and a calculation similar to the previous one gives

$$\left[\frac{e^{-\kappa_{\text{D}} r}}{r} * \left(\frac{e^{-\kappa_{\text{D}} r}}{r}\right)^2 * \frac{e^{-\kappa_{\text{D}} r}}{r}\right](r) = 16\pi^2 \frac{1}{\kappa_{\text{D}}^2} \left[\frac{\ln 3}{4} \kappa_{\text{D}} r + \left(\frac{\ln 3}{4} - \frac{1}{3}\right)\right] \frac{e^{-\kappa_{\text{D}} r}}{\kappa_{\text{D}} r} + \frac{e^{-2\kappa_{\text{D}} r}}{\kappa_{\text{D}} r} F_c(\kappa_{\text{D}} r), \tag{A5}$$

where $F_c(\kappa_{\text{D}} r)$ decays as a constant times $1/(\kappa_{\text{D}} r)$, since

$$F_c(\kappa_{\text{D}} r) \equiv 32\pi^2 \frac{1}{\kappa_{\text{D}}^2} \int_0^{+\infty} dt \frac{e^{-2\kappa_{\text{D}} r t}}{\left[4(1+t)^2 - 1\right]^2}. \tag{A6}$$

The slowest exponential tail $f^{\rm slow}(r)$ of $f(r) = \phi_{\rm D} * [\phi_{\rm D}]^2 * \phi_{\rm D}$ is given by the pole of $f(k)$ at $k = i\kappa_{\rm D}$, which is of order 2, and $f^{\rm slow}(r)$ is equal to $\exp[-\kappa_{\rm D} r]/r$ times a polynomial in r of rank 1: it is not merely equal to $\phi_{\rm D}$.

APPENDIX B:

In the present Appendix we study the ε-expansion of the large-distance behavior $h^{\rm as}_{\alpha\alpha'}$. The meaning of ε-expansions is detailed in Section III C.

First, we calculate the expression of the slowest exponential tail of the graph f_m with exactly m bonds $F^{\rm cc}$ in the definitions (51)-(53) of $f = h^{\rm cc\,B}$, $h^{\rm c-\,B}$, $h^{\rm -c\,B}$ or $h^{\rm --\,B}$. (For the sake of simplicity we omit the indices for charge species.) The slowest exponential tail has been defined at the beginning of Section IV. For $h^{\rm cc\,B}$ and $h^{\rm c-\,B}$, f_1 corresponds to the first graph in Figs.1 and 2 respectively, whereas, in the case of $h^{\rm --\,B}$, f_1 corresponds to the second graph in Fig.3. Since $F^{\rm cc}$ decays slower than I (at least in the high-dilution and weak-coupling regime) ,

$$f_1(k) = \frac{4\pi}{\mathbf{k}^2 + \kappa_{\rm D}^2} g(k), \tag{B1}$$

where the poles or branch points of $g(k)$ in the upper complex half-plane are more distant from the real axis than the pole $k = i\kappa_{\rm D}$ of $1/(\mathbf{k}^2 + \kappa_{\rm D}^2)$. (For $h^{\rm cc\,B}$, $g(k) = 1$, while, for $h^{\rm c-\,B}$, $g(k)$ is given by (75) with $\overline{I}(\mathbf{k}) = 0$ and, for $h^{\rm --\,B}$, $g(\mathbf{k})$ is given by the second term in the r.h.s. of (76) with $\overline{I}(\mathbf{k}) = 0$.) Subsequently, the slowest exponential tail $f_1^{\rm slow}(r)$ of $f_1(r)$ is obtained from (A2) by calculating the residue of $\exp[ikr] k f_1(k)$ at $k = i\kappa_{\rm D}$, with the result

$$f_1^{\rm slow}(r) = \frac{1}{2\pi r} \left[e^{ikr} k f_1(k)(k - i\kappa_{\rm D}) \right] \Big|_{k=i\kappa_{\rm D}} . \tag{B2}$$

$f_1^{\rm slow}(r)$ takes the form

$$f_1^{\rm slow}(r) = \frac{e^{-\kappa_{\rm D} r}}{r} F_{1,0}. \tag{B3}$$

According to definitions (51)-(53) and (73), the Fourier transform of the graph f_m with m bonds $F^{\rm cc}$ ($m \geq 1$) reads

$$f_m(k) = \left[\frac{-4\pi \overline{I}(k)}{k^2 + \kappa_{\rm D}^2} \right]^{m-1} f_1(k). \tag{B4}$$

According to the argument leading to (B2), $k = i\kappa_{\rm D}$ is the singular point of $f_m(k)$ that is the closest one to the real axis in the complex upper-half plane, and the slowest exponential tail $f_m^{\rm slow}(r)$ of $f_m(r)$ is given by the residue of $\exp[ikr] k f_m(k)/(2\pi)$ at $k = i\kappa_{\rm D}$ according to (A2). Since $k = i\kappa_{\rm D}$ is a simple pole for f_1, it is a multiple pole of rank m for f_m, and the latter residue is equal to

$$\frac{1}{2\pi} \times \frac{1}{(m-1)!} \left[\frac{\partial^{m-1}}{\partial k^{m-1}} \left(e^{ikr} k f_m(k)(k - i\kappa_{\rm D})^m \right) \right] \Bigg|_{k=i\kappa_{\rm D}} . \tag{B5}$$

The expression (B5) is equal to $\exp[-\kappa_{\mathrm{D}} r]$ times a polynomial in r of rank $m-1$, $\sum_{p=0}^{m-1} F_{m,p} r^p$, so that

$$f_m^{\mathrm{slow}}(r) = \frac{e^{-\kappa_{\mathrm{D}} r}}{r} \sum_{p=0}^{m-1} F_{m,p}\, r^p . \tag{B6}$$

The leading term $F_{m,m-1}\, r^{m-1} \exp[-\kappa_{\mathrm{D}} r]$ in the residue (B5) arises from the $(m-1)^{\mathrm{th}}$ derivative of $\exp[ikr]$. Relation (B4) and comparison of (B2) with (B5) imply that

$$F_{m,m-1} = \frac{1}{(m-1)!} \left[-2\pi \frac{\overline{I}(i\kappa_{\mathrm{D}})}{\kappa_{\mathrm{D}}} \right]^{m-1} F_{1,0} . \tag{B7}$$

The large-distance behavior $f^{\mathrm{as}}(r)$ of $f(r)$ is the sum of the slowest exponential tails of all graphs f_m,

$$f^{\mathrm{as}}(r) = \sum_{m=1}^{+\infty} f_m^{\mathrm{slow}}(r) . \tag{B8}$$

It reads

$$f^{\mathrm{as}}(r) = \frac{e^{-\kappa_{\mathrm{D}} r}}{r} \sum_{p=0}^{+\infty} r^p \sum_{m=p+1}^{+\infty} F_{m,p} , \tag{B9}$$

and the large-distance behavior $h_{\alpha\alpha'}^{\mathrm{B\,as}}$ of $h_{\alpha\alpha'}^{\mathrm{B}}$ takes the form (90).

We now turn to ε-expansions of the previous slowest tails. The ε-expansion of $\overline{I}(\mathbf{k})$, written as κ_{D}^2 times a function of k/κ_{D} (see (83)), generates an ε-expansion for f_m through (B1) and (B4). We recall that $f_1(k)$ is the generic notation for the Fourier transform of the graphs with only one bond F^{cc} in Figs.1-3. Since the ε-expansion of $\overline{I}(k)$ starts at order ε (see (83)), the ε-expansion of $f_1(k)$ begins at order ε^{n_0} with $n_0 = 0$ if $f = h^{\mathrm{cc\,B}}$, $n_0 = 1$ if $f = h^{\mathrm{c-\,B}}$ or $f = h^{\mathrm{-c\,B}}$, and $n_0 = 2$ if $f = h^{\mathrm{--\,B}}$. For the same reason, the ε-expansion of f_m starts at the order ε^{n_0+m-1}, and so does the ε-expansion of the coefficient $F_{m,p}$ of r^p in (B6),

$$F_{m,p} = \varepsilon^{n_0} \sum_{q=m-1}^{+\infty} F_{m,p}^{(n_0+q)} \varepsilon^q . \tag{B10}$$

As a consequence, the large-distance tail $f^{\mathrm{as}}(r)$ of $f(r)$ defined in (B8) has an ε-expansion of the form

$$\begin{aligned} f^{\mathrm{as}}(r) &= \frac{e^{-\kappa_{\mathrm{D}} r}}{r} \varepsilon^{n_0} \sum_{p=0}^{+\infty} r^p \sum_{q=p}^{+\infty} a_p^{(n_0+q)} \varepsilon^q \\ &= \frac{e^{-\kappa_{\mathrm{D}} r}}{r} \varepsilon^{n_0} \sum_{q=0}^{+\infty} \varepsilon^q \sum_{p=0}^{q} a_p^{(n_0+q)}\, r^p , \end{aligned} \tag{B11}$$

with $a_p^{(n_0+q)} = \sum_{m=p+1}^{q+1} F_{m,p}^{(n_0+q)}$, and the ε-expansion of $h_{\alpha\alpha'}^{\mathrm{B\,as}}(r)$ has the structure (91). In (B11) the coefficient $a_q^{(n_0+q)}$ of $\varepsilon^{n_0+q} r^q$ has a simple expression,

$$a_q^{(n_0+q)} = F_{q+1,q}^{(n_0+q)} . \tag{B12}$$

The leading tail at order ε^{n_0+q} in the ε-expansion of $f^{\rm as}$ is proportional to $r^q \exp[-\kappa_{\rm D} r]/r$. It comes from the leading r^q-term in the slowest tail $f_{q+1}^{\rm slow}(r)$ of the graph with $q+1$ bonds calculated at its lowest order in ε, namely ε^{n_0+q}.

The sum $f^{{\rm as}\,\star}(r)$ of the leading tails at every order in ε in the ε-expansion of $f^{\rm as}$ reads

$$f^{{\rm as}\,\star}(r) \equiv \frac{e^{-\kappa_{\rm D} r}}{r} \varepsilon^{n_0} \sum_{q=0}^{+\infty} a_q^{(n_0+q)} \, (\varepsilon r)^q \, . \tag{B13}$$

It can be calculated explicitly by virtue of (B12), because $F_{q+1,q}^{(n_0+q)}$ is given by (B7), where $\overline{I}(k)$ is replaced by $\overline{I}^{(1)}(k)$, while $F_{1,0}$ is replaced by the first term in its ε-expansion, namely $F_{1,0}^{(n_0)}$. We get

$$\varepsilon^{n_0+q} F_{q+1,q}^{(n_0+q)} = \frac{1}{q!} \left[-2\pi \frac{\overline{I}^{(1)}(i\kappa_{\rm D})}{\kappa_{\rm D}} \right]^q \varepsilon^{n_0} F_{1,0}^{(n_0)} . \tag{B14}$$

(B14) implies that the coefficient of r^q in the definition (B13) of $f^{{\rm as}\,\star}(r)$ is indeed such that $f^{{\rm as}\,\star}(r)$ coincides with the series of an exponential,

$$f^{{\rm as}\,\star}(r) = \frac{1}{r} e^{-(\kappa_{\rm D}+\delta\kappa_{\rm B}^{\star})r} \, \varepsilon^{n_0} F_{1,0}^{(n_0)} \quad \text{with} \quad \delta\kappa_{\rm B}^{\star} = 2\pi \frac{\overline{I}^{(1)}(i\kappa_{\rm D})}{\kappa_{\rm D}} \tag{B15}$$

According to (85), $\delta\kappa_{\rm B}^{\star}$ coincides with the correction of order ε in $\kappa^{\rm B}$, $\delta\kappa_{\rm B}^{\star} = \delta\kappa_{\rm B}^{(1)}$. By comparison with (B3), the relation (B15) can be rewritten as

$$f^{{\rm as}\,\star}(r) = e^{-\delta\kappa_{\rm B}^{(1)} r} \, f_1^{{\rm as}\,(n_0)}(r), \tag{B16}$$

where $f_1^{{\rm as}\,(n_0)} = f_1^{{\rm slow}\,(n_0)}$ is proportional to $\exp[-\kappa_{\rm D} r]/r$. In other words, the sum $f^{{\rm as}\,\star}(r)$ of the leading tails at every order in ε in the ε-expansion of $f^{\rm as}(r)$ around its $\exp[-\kappa_{\rm D} r]/r$ behavior in the vanishing-ε limit is equal to $\exp[-\delta\kappa_{\rm B}^{(1)} r]$ times the large-distance behavior of the graph f_1 with only one bond $F^{\rm cc}$ calculated at the first order ε^{n_0}. When $f = h^{\rm cc\,B}$, $n_0 = 0$ and $f_1^{{\rm as}\,(n_0)}$ coincides with the diagram $\widetilde{\Pi}_a = F^{\rm cc}$ shown in Fig.7. When $f = h^{\rm c-\,B}$ or $h^{\rm -c\,B}$, $n_0 = 1$ and $f_1^{{\rm as}\,(n_0)}$ is the $\exp[-\kappa_{\rm D} r]/r$ tail of diagram $\widetilde{\Pi}_b$ or $\widetilde{\Pi}_{b^\star}$, respectively (see Fig.8), the amplitude of which is of order ε with respect to that of $F^{\rm cc}$. When $f = h^{\rm --\,B}$, $n_0 = 2$ and $f_1^{{\rm as}\,(n_0)}$ is the $\exp[-\kappa_{\rm D} r]/r$ tail of the diagram built with $(1/2)\,[F^{\rm cc}]^2 * F^{\rm cc} * (1/2)\,[F^{\rm cc}]^2$, the amplitude of which is of order ε^2 with respect to that of $F^{\rm cc}$.

APPENDIX C:

In the present Appendix, we consider the limit $\widetilde{b} \ll 1$ at fixed $\beta e^2/(\epsilon_{\rm solv} b)$ and we calculate the explicit values of $C_\phi^{(1)}$ and $\overline{G}_\phi^{\exp\,(1)}(\widetilde{x})$ [see definition (126)] up to terms of order ε times $\ln \widetilde{b}$ plus a function of $\beta e^2/(\epsilon_{\rm solv} b)$. According to (127), (128) and (130), the values are determined from $H^+(\widetilde{x}, \mathbf{q}^2 = 0)$ and from its derivative with respect to $\widetilde{x}$ at point $\widetilde{x} = \widetilde{b}$.

First, we calculate $H^{+(1)}(\widetilde{x}, \mathbf{q}^2 = 0)$. According to (132), at first order in ε, $H^{+(1)} = -\left.\mathcal{T}^+[1]\right|^{(1)}$. In the following, the definition (131) of $\mathcal{T}^+[1]$ is rewritten for $\mathbf{q}^2 = 0$, thanks to an integration by parts, as

$$\mathcal{T}^+[1](\widetilde{x}; \mathbf{q}^2 = 0) = K(\widetilde{b}) - K(\widetilde{x}) \tag{C1}$$

with

$$K(\widetilde{x}) = \frac{1}{2\Sigma_2} \int_{\widetilde{x}}^{+\infty} du \left[1 - e^{-2(u - \widetilde{x})}\right] \sum_{\alpha} \rho_\alpha^{\mathrm{B}} Z_\alpha^2 \left[\frac{\rho_\alpha(u/\kappa_{\mathrm{D}})}{\rho_\alpha^{\mathrm{B}}} - 1\right]. \tag{C2}$$

With these definitions

$$\lim_{\widetilde{x} \to +\infty} H^{+\,(1)}(\widetilde{x}, \mathbf{q}^2 = 0) = -K^{(1)}(\widetilde{b}), \tag{C3}$$

and (128) is rewritten as

$$\overline{G}_\phi^{\exp\,(1)}(\widetilde{x}) = K^{(1)}(\widetilde{x}). \tag{C4}$$

From now on, we consider the regime $\widetilde{b} \ll 1$ at fixed $\beta e^2/(\epsilon_{\mathrm{solv}} b)$. $K^{(1)}(\widetilde{x})$ is determined from the density profiles up to order ε given in (133). At leading order in the limit where $\widetilde{b}$ vanishes, by virtue of (138) and (139),

$$-Z_\alpha^2 \varepsilon \overline{L}(\widetilde{x}; \widetilde{b}) - Z_\alpha \beta e \Phi^{(1)}\left(x; \kappa_{\mathrm{D}}, \widetilde{b}, \frac{\beta e^2}{\epsilon_{\mathrm{solv}} b}\right) = \varepsilon R_\alpha(\widetilde{x}) + \mathcal{O}(\varepsilon \widetilde{b}), \tag{C5}$$

where $R_\alpha(\widetilde{x})$ is a linear combination of functions of $\widetilde{x}$, where one coefficient involves $\ln \widetilde{b}$ plus a function of $\beta e^2/(\epsilon_{\mathrm{solv}} b)$ in such a way that the limit of this sum is finite if $\Delta_{\mathrm{el}} \leq 0$ and $\widetilde{b} = 0$. $\mathcal{O}(\varepsilon \widetilde{b})$ is a short notation for terms of order $\varepsilon \widetilde{b}$. Then, the expression of the density profiles at order ε can be rewritten at leading order in $\widetilde{b}$ as

$$\frac{\rho_\alpha(x)}{\rho_\alpha^{\mathrm{B}}} - 1 = \left\{\exp\left[-Z_\alpha^2 \frac{\beta e^2}{\epsilon_{\mathrm{solv}}} V_{\mathrm{im}}^{B\,\mathrm{sc}}(x)\right] - 1\right\} + \varepsilon R_\alpha(\widetilde{x}) + \left\{\exp\left[-Z_\alpha^2 \frac{\beta e^2}{\epsilon_{\mathrm{solv}}} V_{\mathrm{im}}^{B\,\mathrm{sc}}(x)\right] - 1\right\} \varepsilon R_\alpha(\widetilde{x}) + \mathcal{O}(\varepsilon \widetilde{b}, \varepsilon^2), \tag{C6}$$

where $\mathcal{O}(\varepsilon^2)$ stands both for terms of orders written in (64) with $\Gamma \propto \varepsilon^{2/3}$ (as in (133)), and for terms of order ε^2 times a possible sum of a $\ln \widetilde{b}$ term and a function of $(\beta e^2/\epsilon_{\mathrm{solv}})$, which is similar to the coefficient in $R_\alpha(\widetilde{x})$ (see the comment after (C5)). $\varepsilon R_\alpha(\widetilde{x})$ is a bounded integrable function of only $\widetilde{x} = \kappa_{\mathrm{D}} x$, while $(\beta e^2/\epsilon_{\mathrm{solv}}) V_{\mathrm{im}}^{B\,\mathrm{sc}}(x)$ is a function of both $x/(\beta e^2/\epsilon_{\mathrm{solv}})$ and $\kappa_{\mathrm{D}} x$. As already noticed in Section 3.3 of Ref.[2], an integral where $\left\{\exp\left[-Z_\alpha^2 (\beta e^2/\epsilon_{\mathrm{solv}}) V_{\mathrm{im}}^{B\,\mathrm{sc}}(x)\right] - 1\right\}$ is multiplied by ε times a bounded integrable function of $\widetilde{x}$ is of order ε^2 times a function of $\widetilde{b}$ and $\beta e^2/(\epsilon_{\mathrm{solv}} b)$, which has a structure similar to $R_\alpha(\widetilde{x})$ in (C6). Thus, according to (C2) and (C6), the expression of $K(\widetilde{x})$ at order ε, $K^{(1)}(\widetilde{x})$, can be written at leading order in $\widetilde{b}$ as the sum of only two contributions

$$K^{(1)}(\widetilde{x}) = K_{\mathrm{im}}^{(1)}(\widetilde{x}) + \varepsilon K_R(\widetilde{x}) + \mathcal{O}(\varepsilon \widetilde{b}), \tag{C7}$$

where $K_{\rm im}(\widetilde{x})$ and $K_R(\widetilde{x})$ are defined as $K(\widetilde{x})$ by replacing $[\rho_\alpha(u/\kappa_{\rm D})/\rho_\alpha^{\rm B}]-1$ in (C2) by $\left\{\exp\left[-Z_\alpha^2(\beta e^2/\epsilon_{\rm solv})V_{\rm im}^{B\,{\rm sc}}(u/\kappa_{\rm D})\right]-1\right\}$ and $R_\alpha(u)$, respectively. $R_\alpha(u)$ defined in (C5) is given by the explicit expressions (138) and (139). $K_R(\widetilde{x})$ is calculated by reversing the order of the integrations $\int du$ from the definition of K_R and $\int dt$ from the expressions of $\overline{L}$ and $\Phi^{(1)}$ in $R_\alpha(u/\kappa_{\rm D})$. Eventually,

$$K_R(\widetilde{x})=K_{\overline{L}}(\widetilde{x})+K_{\overline{M}}(\widetilde{x})+K_{\rm Exp}(\widetilde{x})+K_{S_-}(\widetilde{x}), \tag{C8}$$

where the four contributions arising from the terms in the density profiles involving either $\overline{L}(x)$, $\overline{M}(x)$, $\exp(-\widetilde{x})$ or S_- are written in (147b), (147c), (147d) and (147e), respectively, by virtue of (C4).

Now we show that

$$K_{\rm im}^{(1)}(\widetilde{x})=K_{\rm im}^{\rm lin}(\widetilde{x})+\mathcal{O}(\varepsilon\widetilde{b}), \tag{C9}$$

where $K_{\rm im}^{\rm lin}(\widetilde{x})$ is deduced from $K_{\rm im}(\widetilde{x})$, defined after (C7), by linearizing the exponential that contains the bulk-screened self-image interaction $Z_\alpha^2(e^2/\epsilon_{\rm solv})V_{\rm im}^{B\,{\rm sc}}$. Indeed, $K_{\rm im}(\widetilde{x})-K_{\rm im}^{\rm lin}(\widetilde{x})=Q(\widetilde{x})$ with

$$Q(\widetilde{x})\equiv\frac{1}{2\Sigma_2}\int_{\widetilde{x}}^{+\infty}du\left[1-e^{-2(u-\widetilde{x})}\right]\sum_\alpha\rho_\alpha^{\rm B}Z_\alpha^2\left[\exp\left(\frac{\Delta_{\rm el}}{2}Z_\alpha^2\frac{\varepsilon}{u}e^{-2u}\right)-1-\frac{\Delta_{\rm el}}{2}Z_\alpha^2\frac{\varepsilon}{u}e^{-2u}\right]. \tag{C10}$$

Since the functions in the square brackets are positive and $1-\exp[-2(u-\widetilde{x})]\le1-\exp[-2(u-\widetilde{b})]$ for $\widetilde{x}\ge\widetilde{b}$,

$$0\le Q(\widetilde{x})\le Q(\widetilde{b})=Q\left(\widetilde{b},\varepsilon;\frac{\beta e^2}{\epsilon_{\rm solv}b}\right). \tag{C11}$$

The double expansion of $Q(\widetilde{b},\varepsilon;\beta e^2/(\epsilon_{\rm solv}b))$ in powers of ε and $\widetilde{b}$ at fixed $\beta e^2/(\epsilon_{\rm solv}b)$ can be calculated thanks to the following formula (already used in Ref.[3]). We set $\varepsilon_\alpha\equiv Z_\alpha^2\varepsilon/2$. The function f in the integrand of (C10) is a function of u that depends on ε_α as if f were a function of the two independent variables u and $u_1=u/\varepsilon_\alpha$. We write it as

$$f\left(u,\frac{u}{\varepsilon_\alpha}\right)=g(\varepsilon_\alpha u_1,u_1). \tag{C12}$$

Since $\widetilde{b}\ll1$ the integral $\int_{\widetilde{b}}^{+\infty}$ can be split into the sum of integrals $\int_{\widetilde{b}}^{\widetilde{l}}$ and $\int_{\widetilde{l}}^{+\infty}$ with $\widetilde{b}<\widetilde{l}$ and $\varepsilon_\alpha\ll\widetilde{l}\ll1$. Then

$$\underset{\varepsilon_\alpha\to0}{\rm Exp}\left[\int_{\widetilde{b}}^{+\infty}du\,f\left(u,\frac{u}{\varepsilon_\alpha}\right)\right]= \tag{C13}$$
$$\underset{(\widetilde{l}/\varepsilon_\alpha)\to+\infty}{\rm Exp}\;\varepsilon_\alpha\int_{\widetilde{b}/\varepsilon_\alpha}^{\widetilde{l}/\varepsilon_\alpha}du_1\,\underset{\varepsilon_\alpha\to0}{\rm Exp}\;g(\varepsilon_\alpha u_1,u_1)+\underset{\widetilde{l}\to0}{\rm Exp}\int_{\widetilde{l}}^{+\infty}du\,\underset{\varepsilon_\alpha\to0}{\rm Exp}\;f\left(u,\frac{u}{\varepsilon_\alpha}\right),$$

where $\underset{\delta\to0}{\rm Exp}$ denotes an δ-expansion. The identity holds, because when $u_1<\widetilde{l}/\varepsilon_\alpha$ then $\varepsilon_\alpha u_1\ll1$, and when $u>\widetilde{l}$ then $(\varepsilon_\alpha/u)\ll1$. When (C13) is applied to the calculation of $Q(\widetilde{b},\varepsilon;\beta e^2/(\epsilon_{\rm solv}b))$, the second integral in (C13) gives a term of order $\varepsilon_\alpha^2 \propto \varepsilon^2$, while $\underset{\varepsilon_\alpha \to 0}{\mathrm{Exp}} \left\{1 - \exp\left[-2(\varepsilon_\alpha u_1 - \widetilde{b}\right]\right\}$ behaves as $-2\widetilde{b}$, so that the first integral provides a contribution which starts at order $\varepsilon\widetilde{b}$; more precisely,

$$Q\left(\widetilde{b}, \varepsilon; \frac{\beta e^2}{\epsilon_{\mathrm{solv}} b}\right) = \varepsilon \widetilde{b} \frac{\Delta_{\mathrm{el}}}{2} \frac{\sum_\alpha \rho_\alpha^{\mathrm{B}} Z_\alpha^4 g_\alpha}{\Sigma_2} + \mathcal{O}(\varepsilon^2), \tag{C14}$$

where g_α has been defined in (141)–(145), and $\mathcal{O}(\varepsilon^2)$ is equal to ε^2 times a function with a structure similar to that of $R_\alpha(x)$ in (C5). The result (C14) combined with inequalities (C11) leads to (C9). Eventually (C7) can be written as

$$K^{(1)}(\widetilde{x}) \equiv K_{\mathrm{im}}^{\mathrm{lin}}(\widetilde{x}) + \varepsilon K_R(\widetilde{x}) + \mathcal{O}(\varepsilon\widetilde{b}). \tag{C15}$$

$K_R(\widetilde{x})$ is given in (C8) and, according to its definition,

$$K_{\mathrm{im}}^{\mathrm{lin}}(\widetilde{x}) = \varepsilon \, \frac{\Delta_{\mathrm{el}}}{4} \, \frac{\Sigma_4}{\Sigma_2} \left[e^{2\widetilde{x}} \mathrm{Ei}(-4\widetilde{x}) - \mathrm{Ei}(-2\widetilde{x}) \right], \tag{C16}$$

where $\mathrm{Ei}(u)$ is the Exponential-Integral function defined in (144).

The derivative $\partial H^+(\widetilde{x}, \mathbf{q}^2 = 0)/\partial\widetilde{x}$ at first order in ε must be performed more carefully. The reason that leads to $H^{+(1)} = -\mathcal{T}^{+(1)}[1]$ also implies that

$$\left.\frac{\partial H^+}{\partial \widetilde{x}}\right|^{(1)} = \left.\frac{dK}{d\widetilde{x}}\right|^{(1)}, \tag{C17}$$

and, similarly to (C7),

$$\left.\frac{dK}{d\widetilde{x}}\right|^{(1)} = \left.\frac{dK_{\mathrm{im}}}{d\widetilde{x}}\right|^{(1)} + \varepsilon \frac{dK_R}{d\widetilde{x}} + \mathcal{O}(\varepsilon\widetilde{b}). \tag{C18}$$

The decomposition (C13) leads to

$$\left.\frac{dK_{\mathrm{im}}}{d\widetilde{x}}\right|^{(1)}_{\widetilde{x}=\widetilde{b}} = \frac{\Delta_{\mathrm{el}}}{2} \, \varepsilon \left\{ \frac{\sum_\gamma \rho_\gamma^{\mathrm{B}} Z_\gamma^4 g_\gamma}{\Sigma_2} - \frac{\Sigma_4}{\Sigma_2} \left[C + \ln\left(4\widetilde{b}\right) \right] \right\}. \tag{C19}$$

We notice that

$$\left.\frac{dK_{\mathrm{im}}}{d\widetilde{x}}\right|^{(1)} \neq \frac{dK_{\mathrm{im}}^{(1)}}{d\widetilde{x}}. \tag{C20}$$

The reason is that, though $K_{\mathrm{im}}^{(1)}$ is only a function of $\widetilde{x}$, $K_{\mathrm{im}}^{(2)}$ involves a contribution that is equal to ε^2 times a function of the two variables $\widetilde{x}$ and $\widetilde{x}/\varepsilon$, and the derivative of the latter contribution with respect to the second argument $\widetilde{x}/\varepsilon$ is of order ε. The existence of such a contribution in $K_{\mathrm{im}}^{(2)}$ is due to the fact that the function $Z_\alpha^2(\beta e^2/\epsilon_{\mathrm{solv}}) V_{\mathrm{im}}^{B\,\mathrm{sc}}(x; \kappa_{\mathrm{D}})$ in the expression (134) of the density profile varies both over the Bjerrum length $\beta e^2/\epsilon_{\mathrm{solv}}$ and over the screening length ξ_D. (This structure arises directly when the equation obeyed by H^+ is solved by a multi-scale expansion method.)

APPENDIX D:

In the present Appendix we consider the large-x behavior $D^{\mathrm{c\,as}}_{\alpha}(x)$ of the dipole $D^{\mathrm{c}}_{\alpha}(x)$ that appears in the large-y tail $D^{\mathrm{c}}_{\alpha}(x)D^{\mathrm{c}}_{\alpha'}(x')/y^3$ of $h^{\mathrm{cc}}_{\alpha\alpha'}$. Calculations are not as straightforwrd as for $h^{\mathrm{cc\,B}}_{\alpha\alpha'}$ in the bulk, and we calculate only the sum $D^{\mathrm{c\,as}\,\star}_{\alpha}(x)$ of the leading large-x terms at every order ε^q in the ε-expansion of $D^{\mathrm{c\,as}}_{\alpha}(x)$ around its infinite-dilution and vanishing-coupling limit $D^{\mathrm{c\,as}\,(0)}_{\alpha}(x)$. According to (152),

$$D^{\mathrm{c}}_{\alpha}(x) \equiv \frac{e}{\sqrt{\epsilon_{\mathrm{solv}}}} Z_\alpha \left[\overline{D}_\phi(x) + \overline{C}^{\mathrm{c}-}(x)\right] . \tag{D1}$$

After insertion of the graphic representation (52) of $h^{\mathrm{c}-}$ in the definition (151) of $\overline{C}^{\mathrm{c}-}(x)$, the latter can be written as

$$\overline{C}^{\mathrm{c}-}(x) = \sum_{m=1}^{+\infty} J_m(x), \tag{D2}$$

where $J_m(x)$ is the contribution to $\overline{C}^{\mathrm{c}-}(x)$ from the graph in $h^{\mathrm{c}-}_{\alpha\gamma''}$ with m bonds F^{cc}(see Fig.2).

The graph with m bonds F^{cc} in $h^{\mathrm{c}-}_{\alpha\gamma''}$ also contains m bonds I. Therefore, according to the scaling analysis of Section III B, the ε-expansion of $J_m(x)$ starts at order ε^m, $J_m(x) = \sum_{q=m}^{+\infty} J^{(q)}_m(x)$, where $J^{(q)}_m(x)$ denotes the term of order ε^q. Therefore, the leading tail at order ε^q in the large-x behavior $\overline{C}^{\mathrm{c}-\,\mathrm{as}}(x)$ of $\overline{C}^{\mathrm{c}-}(x)$ can arise only from the leading tails of the $J_m(x)$'s with $m \leq q$. Though we are not able to derive the leading tail of $J_m(x)$ systematically, we expect, by analogy with the F_m's in the bulk case, that the leading tail of $J_m(x)$ has the same x-dependence as the leading tail of the first term $J^{(m)}_m(x)$ in the ε-expansion of $J_m(x)$. As shown herefater, the leading tail $J^{(m)\,\mathrm{as}}_m(x)$ of $J^{(m)}_m(x)$ is proportional to $\varepsilon^m(\widetilde{x} - \widetilde{b})^m \exp[-(\widetilde{x} - \widetilde{b})]$. As a consequence, the leading tail at order ε^q in the large-x behavior $\overline{C}^{\mathrm{c}-\,\mathrm{as}}(x)$ of $\overline{C}^{\mathrm{c}-}(x)$ coincides with the leading tail $J^{(q)\,\mathrm{as}}_q(x)$ of $J^{(q)}_q(x)$, and the sum $\overline{C}^{\mathrm{c}-\,\mathrm{as}\,\star}(x)$ of the leading tails at every order ε^q in $\overline{C}^{\mathrm{c}-\,\mathrm{as}}(x)$ is $\overline{C}^{\mathrm{c}-\,\mathrm{as}\,\star}(x) = \sum_{q=1}^{+\infty} J^{(q)\,\mathrm{as}}_q(x)$. Similarly, for $D^{\mathrm{c}}_{\alpha}(x)$ defined in (D1)

$$D^{\mathrm{c\,as}\,\star}_{\alpha}(x) = \frac{e}{\sqrt{\epsilon_{\mathrm{solv}}}} Z_\alpha \left[\overline{D}^{(0)}_\phi(x) + \sum_{q=1}^{+\infty} J^{(q)\,\mathrm{as}}_q(x)\right] . \tag{D3}$$

The term $J^{(q)}_q(x)$ of order ε^q in the ε-expansion of $J_q(x)$ is obtained by replacing every bond F^{cc} by its zeroth-order expresssion $F^{\mathrm{c\,c}\,(0)}$, every I by its lowest-order value $[F^{\mathrm{c\,c}\,(0)}]^2/2$, and every weight $\rho_\alpha(x_n)$ by its bulk value $\rho^{\mathrm{B}}_{\alpha}$. Inspection of $J^{(q)}_q(x)$ for small values of q shows that only the part $\phi^{(0)}_{\mathrm{sing}} = \phi_{\mathrm{D}}$ of $\phi^{(0)}$ does contribute to the leading tail $J^{(q)\,\mathrm{as}}_q(x)$. Let us denote by $\widehat{J}^{(q)}_q(x)$ the corresponding part in $J^{(q)}_q(x)$. For the sake of simplicity, we relabel point pairs $\{p, p'\} \equiv \{(\mathbf{r}_p, \gamma_p), (\mathbf{r}'_p, \gamma'_p)\}$, with $p = 1, \ldots, q$, $x_q = x_{c'}$ and $x'_q = x''$, in the opposite sense and we set

$u_p \equiv \widetilde{x}_{q-(p-1)}$ and $u'_p \equiv \widetilde{x}'_{q-(p-1)}$. By using (7), (122) and the change of variable $t = 2\sqrt{1+q^2}$, we get

$$\widehat{J}^{(q)}_q(x) = -\frac{1}{\kappa_{\mathrm{D}}}\sqrt{\frac{2\epsilon_W}{\epsilon_{\mathrm{solv}}}}\left(-\varepsilon\frac{1}{4}\left(\frac{\Sigma_3}{\Sigma_2}\right)^2\right)^q \int_2^{+\infty}\frac{dt_q}{t_q}\int_{\widetilde{b}}^{+\infty} du_q\, e^{-|\widetilde{x}-u_q|}\int_{\widetilde{b}}^{+\infty} du'_q\, e^{-t_q|u_q-u'_q|} \cdots \int_2^{+\infty}\frac{dt_1}{t_1}\int_{\widetilde{b}}^{+\infty} du_1\, e^{-|u'_2-u_1|}\int_{\widetilde{b}}^{+\infty} du'_1\, e^{-t_1|u_1-u'_1|}e^{-(u'_1-\widetilde{b})}. \tag{D4}$$

Next steps of the calculations involve the following formulae,

$$I(u_1) \equiv \int_{\widetilde{b}}^{+\infty} du'_1\, e^{-t_1|u_1-u'_1|}e^{-(u'_1-\widetilde{b})} = \frac{2t_1}{t_1^2-1}e^{-(u_1-\widetilde{b})} - \frac{1}{t_1-1}e^{-t_1(u_1-\widetilde{b})} \tag{D5}$$

and

$$\int_{\widetilde{b}}^{+\infty} du_1\, e^{-|u'_2-u_1|}I(u_1) = \frac{2t_1}{t_1^2-1}(u'_2-\widetilde{b})e^{-(u'_2-\widetilde{b})} + R_0(u'_2-\widetilde{b}), \tag{D6}$$

where $R_p(u)$ denotes a function whose slowest exponential tail is equal to $\exp(-u)$ times a polynomial of rank p in the variable x. More generally, we find

$$\int_{\widetilde{b}}^{+\infty} du'_p\, e^{-t_p|u_p-u'_p|}(u'_p-\widetilde{b})^{p-1}e^{-(u'_p-\widetilde{b})} = \frac{2t_p}{t_p^2-1}(u_p-\widetilde{b})^{p-1}e^{-(u_p-\widetilde{b})} + R_{p-2}(u_p-\widetilde{b}) \tag{D7}$$

and

$$\int_{\widetilde{b}}^{+\infty} du_p\, e^{-|u'_{p+1}-u_p|}(u_p-\widetilde{b})^{p-1}e^{-(u_p-\widetilde{b})} = \frac{1}{p}(u'_{p+1}-\widetilde{b})^p e^{-(u'_{p+1}-\widetilde{b})} + R_{p-1}(u'_{p+1}-\widetilde{b}). \tag{D8}$$

Eventually, the multiple integral in (D4) is equal to

$$\left(\int_2^{+\infty} dt\frac{2}{t^2-1}\right)^q \frac{(\widetilde{x}-\widetilde{b})^q}{q!}e^{-(\widetilde{x}-\widetilde{b})} + R_{q-1}(\widetilde{x}-\widetilde{b}) \tag{D9}$$

where $\int_2^{+\infty} dt\, 2/(t^2-1) = \ln 3$, and

$$J^{(q)\,\mathrm{as}}_q(x) = -\frac{1}{\kappa_{\mathrm{D}}}\sqrt{\frac{2\epsilon_W}{\epsilon_{\mathrm{solv}}}}\left(-\varepsilon\frac{\ln 3}{4}\left(\frac{\Sigma_3}{\Sigma_2}\right)^2\right)^q \frac{(\widetilde{x}-\widetilde{b})^q}{q!}e^{-(\widetilde{x}-\widetilde{b})}. \tag{D10}$$

Therefore, $D^{\mathrm{c\,as}\,\star}_{\alpha}(x)$, given by (D3) with $\overline{D}^{(0)}_{\phi}(x)$ written in (7), proves to be the series of an exponential whose argument is proportional to $\varepsilon(\widetilde{x}-\widetilde{b})$,

$$D^{\mathrm{c\,as}\,\star}_{\alpha}(x) = -\frac{e}{\sqrt{\epsilon_{\mathrm{solv}}}}\,Z_{\alpha}\sqrt{\frac{2\epsilon_W}{\epsilon_{\mathrm{solv}}}}\,\frac{e^{-(\kappa_{\mathrm{D}}+\delta\kappa^{\star})(x-b)}}{\kappa_{\mathrm{D}}} \tag{D11}$$

with

$$\frac{\delta\kappa^{\star}}{\kappa_{\mathrm{D}}} = \varepsilon\frac{\ln 3}{4}\left(\frac{\Sigma_3}{\Sigma_2}\right)^2. \tag{D12}$$

By virtue of (86), $\delta\kappa^\star$ coincides with the first-order correction $\delta\kappa_{\mathrm{B}}^{(1)}$ to the screening length in the bulk. We notice that (D11) can be rewritten as

$$D_\alpha^{\mathrm{c\,as}\,\star}(x) = D_\alpha^{(0)}(x)\, e^{-\delta\kappa^\star (x-b)}. \tag{D13}$$

(D13) corresponds to the relation (94) in the bulk case.

---

[1] J.-N. Aqua and F. Cornu, Phys. Rev. E **68** (2003) 026133. This article is referred to as "Paper I" throughout the text.

[2] J.-N. Aqua and F. Cornu, J. Stat. Phys. **105**, 211 (2001).

[3] J.-N. Aqua and F. Cornu, J. Stat. Phys. **105**, 245 (2001).

[4] D.A. McQuarrie, *Statistical Mechanics* (Harper and Row, New York, 1973).

[5] J.P. Hansen and I.R. McDonald, *Theory of Simple Liquids* (Academic, London 1976).

[6] Ph.A. Martin, Rev. Mod. Phys. **60**, 1075 (1988).

[7] N.F. Mott, R. Parsons, and R.J. Watts-Tobin, Phil. Mag. **7**, 483 (1962); F.P. Buff and F.H. Stillinger, J. Chem. Phys. **39**, 1911 (1963).

[8] J.-N. Aqua and F. Cornu, J. Stat. Phys. **97**, 173 (1999).

[9] A.S. Usenko and I.P. Yakimenko, Sov. Tech. Phys. Lett. **5**, 549 (1979).

[10] B. Jancovici, J. Stat. Phys. **28**, 43 (1982).

[11] P. Debye and E. Hückel, Phys. Z. **9**, 185 (1923).

[12] D. J. Mitchell and B. W. Ninham, Phys. Rev **174**, 280 (1968).

[13] R. Kjellander and D.J. Mitchell, J. Chem. Phys. **101**, 603 (1994).

[14] J.D. Jackson, *Classical Electrodynamics* (Wiley, New York, 1962).

[15] E. Meeron, J. Chem. Phys. **28**, 630 (1958); *Plasma Physics* (MacGraw-Hill, New York, 1961).

[16] S. L. Carnie and D.Y.C. Chan, Chem. Phys. Lett. **77**, 437 (1981).

[17] F.H. Stillinger and R. Lovett, J. Chem. Phys. **48**, 3858 (1968); **49**, 1991 (1968).

[18] S. L. Carnie, J. Chem. Phys. **78**, 2742 (1983).

[19] B. Jancovici and L. Šamaj, J. Stat. Phys. **105**, 193 (2001).

[20] B. Jancovici, J. Stat. Phys. **29**, 263 (1982).

[21] F. Cornu, Phys. Rev. E **53**, 4595 (1996).

[22] A. Alastuey, F. Cornu and A. Perez, Phys. Rev. E **51**, 1725 (1995).

[23] E. Haga, J. Phys. Soc. Jap. **8**, 714 (1953).

[24] E.J.W. Verwey and J.Th.G. Overbeek, *Theory of the Stability of Lyophobic Colloids* (Dover, New York, 1999).

[25] M. Medina-Noyola and D.A. McQuarrie, J.Chem.Phys. **1980**, 6279 (1980).

[26] F. Cornu, Phys. Rev. E **58**, 5293 (1998).

[27] D.C.Brydges and P. Federbush, Commun. Math. Phys. **73**, 197 (1980).

[28] D.C. Brydges and Ph. A. Martin, J. Stat. Phys. **96**, 1163 (1999).

[29] B.P. Lee and M.E. Fisher, Europhys. Lett. **39**, 611 (1997).

[30] L.S. Brown and L.G. Yaffe, Physics Reports, **340**, 1-164 (2001).

[31] D. J. Mitchell and B. W. Ninham, Chem. Phys. Lett. **53**, 397 (1978).

[32] J.-N. Aqua and M.E. Fisher, Phys. Rev. Lett. **92**, 135702 (2004).

[33] S. Bekiranov and M.E. Fisher. Phys. Rev. E **59**, 492 (1999).

[34] B. Jancovici, J. Stat. Phys. **100**, 201 (2000).

[35] B. Jancovici, P. Kalinay, and L. Šamaj , Physica A **279**, 260 (2000).

[36] D. Zwillinger, *Handbook of Differential Equations* (Academic Press, 1989).

[37] I. M. Gel'fand and G.E. Shilov, *Generalized Functions*, Vol.1 (Academic, New York, 1964).

[38] L. Šamaj and B. Jancovici, J. Stat. Phys. **106**, 323 (2002).

[39] F. Cornu, in preparation.

[40] F. Cornu, Proceeding of the STATPHYS22 Conference in Bangalore 4-9 July 2004, to be published in Pramana-Journal of Physics.

FIGURE CAPTIONS

Fig.1 Representation of $h^{\mathrm{cc}}_{\alpha\alpha'}(\mathbf{r},\mathbf{r}')$ as the graph series defined in (51). A wavy line represents a bond F^{cc} and a grey disk stands for a bond I. A couple of variables $(\mathbf{r}_i,\gamma_i)$ is associated with every circle. For a white circle $a=(\mathbf{r},\alpha)$ [or $a'=(\mathbf{r}',\alpha')$], $\mathbf{r}$ and α are fixed, whereas, for a black circle $i=(\mathbf{r}_i,\gamma_i)$, $\mathbf{r}_i$ and γ_i are integrated over with the measure $\int d\mathbf{r}_i\sum_{\alpha_i}\rho_{\alpha_i}(\mathbf{r}_i)$.

Fig.2 Graphic representation of definition (52) for $h^{\mathrm{c}-}_{\alpha\alpha'}(\mathbf{r},\mathbf{r}')$.

Fig.3 Graphic representation of definition (53) for $h^{--}_{\alpha\alpha'}(\mathbf{r},\mathbf{r}')$.

Fig.4 Diagrams in $h^{\mathrm{cc}}_{\alpha\alpha'}(\mathbf{r},\mathbf{r}')$ that contribute to the correction of order ε in the screening length. A double wavy line denotes a bond $(1/2)\,[F^{\mathrm{cc}}]^2$.

Fig.5 Diagrams in $h^{\mathrm{c}-}_{\alpha\alpha'}(\mathbf{r},\mathbf{r}')$ that contribute to the correction of order ε in the screening length.

Fig.6 Diagrams in $h^{--}_{\alpha\alpha'}(\mathbf{r},\mathbf{r}')$ that contribute to the correction of order ε in the screening length.

Fig.7 Diagram $\widetilde{\Pi}_a$.

Fig.8 Diagrams $\widetilde{\Pi}_b$ (on the left) and $\widetilde{\Pi}_{b\star}$ (on the right).

Fig.9 Diagram $\widetilde{\Pi}_c$.

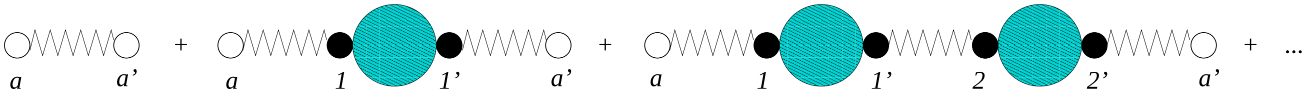

FIG. 1:

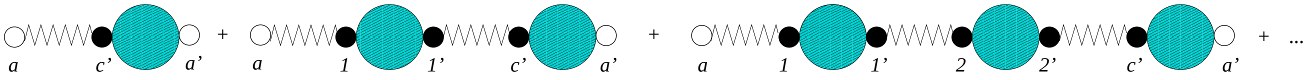

FIG. 2:

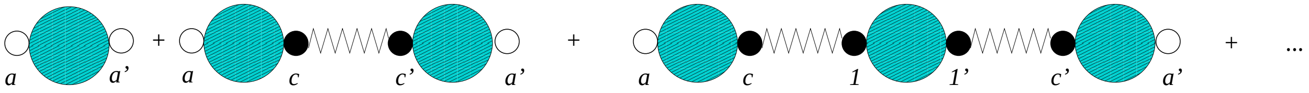

FIG. 3:

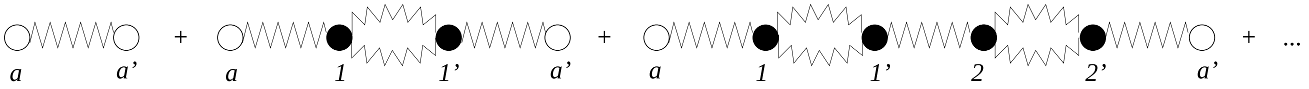

FIG. 4:

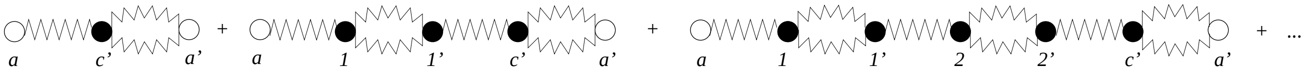

FIG. 5:

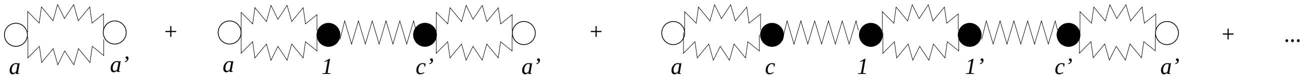

FIG. 6:

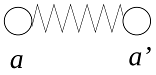

FIG. 7:

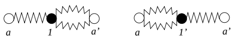

FIG. 8:

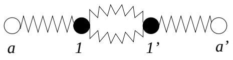

FIG. 9: